Gidiane Scaratti

Degradation of 1 ,4-dioxane from aqueous solution: Routes of decomposition using catalytic ozonation or peroxidation coupled to membrane filtration

Doctorate thesis for the degree of Doctor in Chemical Engineering presented to the Graduate Program in Chemical Engineering at Federal University of Santa Catarina.

Advisor: Prof. Dr. Regina de Fátima Peralta Muniz Moreira
Co-advisors: Prof. Dr. Pedro J. J. Alvarez and Prof. Dr. Humberto Jorge José

Florianopolis
2018

Ficha de identificação da obra elaborada pelo autor
através do Programa de Geração Automática da Biblioteca Universitária
da UFSC.

Degradation of 1,4-dioxane from Aqueous Solution: routes of decomposition using catalytic ozonation or peroxidation coupled to membrane filtration

por

Gidiane Scaratti

Tese julgada para obtenção do título de **Doutor em Engenharia Química**, na área de Concentração de **Desenvolvimento de Processos Químicos e Biotecnológicos** e aprovada em sua forma final pelo Programa de Pós-graduação em Engenharia Química da Universidade Federal de Santa Catarina.
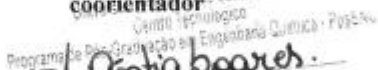
Prof.ª Dr.ª Regina de Fátima Peralta Muniz Moreira
orientadora

Prof. Dr. Humberto Jorge José
coorientador

Prof. Dr. Pedro J. J. Alvarez
coorientador

Prof.ª Dr.ª Cíntia Soares
coordenadora

Banca Examinadora:

Prof. Dr. Agenor De Noni Junior

Dr. Guilherme Zin

Dr.ª Vanessa Zanon Baldissarelli

Florianópolis, 14 de dezembro de 2018.

This doctorate thesis is dedicated to my best friends:
my parents, Dirceu and Gislaine
my little brother, Arthur
and to the love of my life, Kenji

Esta tese é dedicado aos meus melhores amigos:
meus pais, Dirceu e Gislaine
meu irmãozinho, Arthur
e ao amor da minha vida, Kenji

ACKNOWLEDGEMENTS

*"O correr da vida embrulha tudo,
a vida é assim: esquenta e esfria,
aperta e daí afrouxa,
sossega e depois desinquieta.
O que ela quer da gente, é coragem."*
(Guimarães Rosa)

ABSTRACT

Due to its carcinogen potential, 1,4-dioxane has been included as one of the priority pollutants by United States Environmental and Protection Agency, justifying the need to develop efficient and safe processes for its removal from water. This doctorate thesis will present the 1,4-dioxane degradation kinetics through catalytic oxidation combined with ceramic membrane filtration. 1,4-Dioxane degradation by heterogeneous catalytic processes was studied for the first time using FeOOH, CeO_2 and CuO as catalysts in aqueous suspension or immobilized on ceramic membrane surface. The selected catalysts were characterized by zeta potential, N_2 adsorption/desorption isotherm, XRD, FESEM, TEM, TGA and chemical composition. The catalytic activity of the solids was evaluated in their ability to decompose H_2O_2 or O_3 generating free radicals capable of destroying 1,4-dioxane in aqueous suspension. The results obtained showed that CuO is more active than FeOOH and CeO_2 to decompose H_2O_2 and O_3, this step is fundamental for application in catalytic advanced oxidation. However, CuO did not promote 1,4-dioxane mineralization by heterogeneous catalytic peroxidation, probably due to the low amount of free radicals produced, or even if the non-radical mechanism. For catalytic ozonation process, the addition of CuO increased the mineralization rate up to 82 times in relation to the non-catalyzed mineralization of 1,4-dioxane. Radical scavenging experiments demonstrated that superoxide radicals were the main species responsible for the degradation of 1,4-dioxane. The reaction mechanism proceeded through the formation of ethylene glycol diformate, which quickly hydrolyzed to ethylene glycol and formic acid as intermediate products. The stability of CuO indicated weak copper leaching and high catalytic activity upon five recycling cycles. The toxicity of the water, assessed by *Vibrio fischeri* bioluminescence assays, decreased after catalytic ozonation while it increased after treatment with ozonation alone. Finally, CuO catalyst was immobilized on a ceramic membrane, the catalyst loading affects 1,4-dioxane up to a limit. The deposition of CuO onto to a ceramic membrane contributed to the fouling reduction. Catalytic ceramic membrane is stable for four consecutive cycles. Therefore, the hybrid process, ultrafiltration coupled to catalytic ozonation proved to be a promising technology for the degradation of small and recalcitrant compounds and fouling removal.

Keywords: groundwater contamination; transition-metal oxides; heterogeneous catalysis.

RESUMO EXPANDIDO

Introdução
Devido ao seu potencial carcinogênico, o 1,4-dioxano foi incluído como um dos poluentes prioritários pela Agência de Proteção Ambiental dos Estados Unidos da América, justificando a necessidade de desenvolvimento de processos eficientes e seguros para sua remoção da água. A degradação do 1,4-dioxano por meio de processos catalíticos heterogêneos foi estudada pela primeira vez utilizando os catalisadores FeOOH, CeO_2 e CuO em suspensão aquosa ou imobilizados em membrana cerâmica. Os processos oxidativos avançados são conhecidos por mineralizar uma grande gama de compostos orgânicos através da geração de espécies reativas. Dentre estes processos, temos a ozonização e o Fenton que já estão sendo aplicados em escala industrial no tratamento de água e efluentes. Entretanto, estes processos possuem limitações, como a formação de subprodutos que não reagem com o ozônio e a estreita faixa de pH em que o sistema Fenton é ativo. Para transpor estas dificuldades, tem sido proposto pela literatura a aplicação de catalisadores sólidos que podem aumentar a eficiência do processo. Visando a aplicação em larga escala dessas tecnologias, é necessário desenvolver estratégias para reutilização do catalisador. Uma das alternativas é a imobilização do catalisador em membrana cerâmica. Acoplar processos catalíticos heterogêneos com membranas resolveria os problemas de recuperação do catalisador, da diminuição do fluxo durante o processo de filtração e do tratamento de compostos de baixo peso molecular e recalcitrantes que não são retidos pelo sistema de membranas e nem degradados nos sistemas convencionais de tratamento. Radicais livres seriam gerados durante as reações entre os catalisador heterogêneo impregnado na membrana e o oxidante dissolvido, degradando a matéria orgânica retida e, inclusive, os compostos pequenos e recalcitrantes.

Objetivo
O objetivo desta tese é investigar a degradação do 1,4-dioxano pelos processos de peroxidação catalítica heterogêna e ozonização catalítica heterogênea utilizando óxidos de metais de transição como catalisadores em suspensão ou impregnados em membrana cerâmica tubular.

Metodologia
Os catalisadores selecionados (FeOOH, CuO e CeO_2) foram caracterizados pela determinação do potencial zeta, área BET, DRX, FEG, MET, ATG e composição química. Em paralelo com as

caracterizações, a atividade catalítica dos sólidos foi avaliada em sua capacidade de decompor H_2O_2 ou O_3 gerando radicais livres capazes de destruir o 1,4 dioxano em suspensão aquosa. O catalisador que apresentou a maior atividade catalítica foi avaliado em detalhes (dosagem de catalisador e pH, radicais livres formados, produtos da reação, reuso e estabilidade e toxicidade). Após esse estudo detalhado, o catalisador foi imobilizado na superfície interna da membrana cerâmica tubular. A impregnação do catalisador na membrana foi realizada com o auxílio de uma bomba a vácuo, para isso, 10 mL de uma solução de 1000 ppm de catalisador foi filtrada e, o catalisador, retido na membrana. Por último, a membrana foi sinterizada a 550 °C por 30 min. Reações foram realizadas avaliando a quantidade de catalisador impregnada na membrana, toxicidade, recuperação do fluxo de permeado quando filtrado água proveniente da estação de tratamento de água municipal e, por último, estabilidade e reuso da membrana

Resultados e Discussão
Os resultados obtidos no processo de peroxidação catalítica mostraram que a atividade catalítica para decompor H_2O_2 decresce na ordem CuO > FeOOH ~ CeO_2. No entanto, nenhum dos catalisadores promoveu a mineralização do 1,4-dioxano nas condições experimentais avaliadas, devido à baixa quantidade de radicais livres produzidos. Dentre os catalisadores avaliados no processo de ozonização, o CuO apresentou as maiores constantes de velocidade tanto de decomposição do ozônio quanto de mineralização do 1,4-dioxano. Assim, um estudo detalhado do processo de degradação do 1,4-dioxano foi conduzido utilizando CuO como catalisador da ozonização. A adição desse catalisador no processo de ozonização proporcionou aumentos de até 82 vezes nas taxas de mineralização do 1,4-dioxano. Os experimentos com sequestrantes de radicais demonstraram que o radical superóxido é o principal responsável pela degradação do 1,4-dioxano. O mecanismo de reação, avaliado por meio de análise cromatográfica, ocorreu através da formação de diformiato de etilenoglicol, o qual foi rapidamente hidrolisado a etilenoglicol e ácido fórmico. Ao longo das reações o CuO apresentou baixa lixiviação e alta atividade catalítica após 5 ciclos de reuso. A toxicidade, avaliada através de ensaios bioluminescentes com *Vibrio fischeri*, diminuiu durante a ozonização catalítica, e aumentou durante a ozonização não catalítica. Finalmente, visando a ampliação de escala do processo proposto, o catalisador CuO foi imobilizado em membrana cerâmica. Os resultados obtidos mostram que a quantidade de catalisador impregnado na membrana afeta o tratamento do 1,4-dioxano. O processo

híbrido, membrana catalítica acoplado com ozonização reduziu o *fouling* causado pela água da estação de tratamento de água municipal. A atividade catalítica da membrana se manteve igual em quatro reusos. A maior constante de reação no tratamento do 1,4-dioxano foi obtida com a membrana impregnada com 0,9 mg cm^{-2} de catalisador, o que contribuiu para um aumento na toxicidade aguda, sendo necessário um maior tempo de reação quando comparado ao sistema com catalisador em suspensão.

Conclusão
Comparando as reações com o catalisador em suspensão e imobilizado na membrana cerâmica, temos que a ozonização catalítica em suspensão é mais eficiente em termos de taxas de reação e redução da toxicidade. No entanto, a imobilização do catalisador na superfície da membrana possui várias vantagens que superam a desvantagem da perda de superfície de contato, como por exemplo, a eliminação de etapa para recuperação do catalisador no final do processo e a oxidação da matéria orgânica causadora do *fouling* pelos radicais livres. Portanto, os resultados obtidos mostram que o óxido de cobre apresenta alta atividade catalítica na mineralização do 1,4-dioxano. O processo híbrido, ultrafiltração com membrana catalítica acoplada com ozônio, é uma tecnologia promissora para o tratamento de compostos pequenos e recalcitrantes e redução do *fouling*.

Palavras-chave: Contaminação de águas subterrâneas; óxidos de metais de transição; catálise heterogênea.

LIST OF FIGURES

LIST OF TABLES

LIST OF ABBREVIATIONS, SYMBOLS AND ACRONYMS

Symbol	Meaning	Unit
AAS	Atomic Absorption Spectroscopy	-
ABS	Absorbance	-
AOP	Advanced Oxidation Process	-
BET	Brunauer, Emmer e Teller	-
BJH	Barret, Joyner e Halenda	-
CCM	Catalytic ceramic membrane	-
C_e	Equilibrium concentration	ppm
CeO_2	Cerium oxide	-
CM	Ceramic membrane	-
C_{O3}	Aqueous ozone concentration	ppm
C_{sat}	Saturated ozone concentration	ppm
CuO	Copper oxide	-
DES	Dispersive energy spectroscopy	-
FeOOH	Goethite	-
FESEM	Field emission scanning electron microscopy	-
FTIR	Fourier transform infrared spectroscopy	-
GC-MS	Gas chromatography- mass spectroscopy	-
H_2O_2	Hydrogen peroxide	-
IEP	Isoeletric point	-
J	Permeate flux	$Lm^{-2}h^{-1}bar^{-1}$
k_d	Ozone self-decomposition constant	min^{-1}
k_{het}	Catalytic ozone decomposition constant	min^{-1}
k_{La}	Volumetric mass transfer coefficient	min^{-1}
k_T	Ozone decomposition rate constant	min^{-1}
NaF	Sodium fluoride	-
NOM	Natural Organic Matter	-
O_3	Ozone	-
$^{\cdot}OH$	Hydroxyl radical	-
PBQ	1,4-benzoquinone	-
PHOS	Phosphate	-
PVDF	Polyvinylidene fluoride	-
PZC	Point of zero charge	-
ROS	Reactive Oxygen Species	-
SA	Salicylic acid	-
TBA	*Tert*-butanol	-
TEM	Transmission Electron Microscopy	-

TGA	Thermogravimetric Analysis	-
TOC	Total Organic Carbon	ppm
UF	Ultrafiltration	-
UV	Ultraviolet	-
w	Catalyst dosage	ppm
WTP	Municipal Water Treatment Plant	-
XPS	X-ray photoelectron spectroscopy	-
XRD	X-ray diffraction	-
λ	Wavelength	nm
ξ	Zeta potential	mV
μ	Electrophoretic mobility	-
ε	Molar extinction coefficient	$Lcm^{-1}mg^{-1}$

1. INTRODUCTION

1,4-Dioxane is a synthetic ether, used as a stabilizer for chlorinated solvents, frequently detected in groundwater and in water contaminated with 1,1,1-trichloroethane and trichloroethylene. As a byproduct of chemical processes involving ethylene glycol, it is also present in industrial wastewater (USEPA, 2006; MOHR, 2010).

The interest in the impact caused by the presence of 1,4-dioxane in the environment has increased since it was classified as a priority pollutant with carcinogenic potential (USEPA, 2010; ECB, 2002). Due to its high solubility in water, low vapor pressure, boiling point near of the water and its bio-recalcitrant characteristic, its removal from the water by conventional treatment techniques is not effective (KIM et al., 2008; SO et al., 2009). Thus, it is necessary to develop innovative technologies capable of treating this kind of compound, for instance, advanced oxidation processes is a promising technology.

Advanced oxidation processes (AOPs) are capable to mineralize a wide range of organic compounds through the generation of highly reactive species, predominantly the hydroxyl radical ($\cdot$OH). Among these processes, ozonation and Fenton processes are already being applied in industrial scale in the treatment of water and wastewater, and may also be associated with biological processes (ASSÁLIN; DURÁN, 2007; MIRZAEI et al., 2017).

However, both ozonation and Fenton processes have limitations. In ozonation reactions, the mineralization rate constants are lower than those obtained when others AOPs are applied, due to the byproducts and the ozone selective reactions (LV et al., 2012). The Fenton process is limited by the narrow pH range in which the system is active, near to 3, and also by the formation of sludge in the catalyst separation and recovery process after the treatment (MA et al., 2015).

To overcome the difficulties aforementioned, the application of solid catalysts has been proposed in the literature. The addition of solids materials may increase the oxidation efficiency of a number of organic pollutants, reducing the ozone consumption in the case of ozonation and facilitate the separation and recovery of the catalyst after the reactions for both process (CRUZ et al., 2016). Several metallic oxides have been proposed, such as iron oxide (OPUTU et al., 2015; DU et al., 2016), manganese (NAWAZ et al., 2015; KIM et al., 2017), aluminum (ZHAO et al., 2015), copper (HU et al., 2017), among others.

Iron oxides have a wide natural availability, low toxicity and relatively low cost. Some studies have already shown that iron oxides can degrade a range of organic compounds when applied as catalysts in the ozonation and peroxidation processes (OPUTU et al., 2015; DU et al., 2016). However, its application in the degradation of 1,4-dioxane has not been studied.

Cooper oxide presents catalytic properties that favor a high density of adsorbed surface hydroxyl groups, which significantly increases the decomposition of ozone and organic pollutants (HU et al., 2016; VAKILABADI et al., 2017). In addition, CuO is inexpensive, chemically stable and has low toxicity (HU et al., 2016).

More recently, cerium oxide proved to be useful as catalyst in advanced oxidation process, since it could provide a higher oxygen storage due to its capacity of reversibly changing of oxidation states 3^+ and 4^+ (XU; WANG, 2012). It is a strong oxidizing agent and stable in aqueous solution, applied as catalyst in ozonation and peroxidation processes (BAI; YANG; WANG, 2016; XU; WANG, 2012).

However, there is no consensus in the literature about the reaction mechanisms involved in the catalytic ozonation and catalytic peroxidation processes using non-noble metal oxides as catalysts, as well as the optimum conditions. Some authors (SEHATI; ENTERAZI, 2017; WAN; WANG, 2017) have demonstrated that metal oxide catalysts are capable of producing oxidative free radicals from the decomposition of hydrogen peroxide and ozone, which will degrade the organic compounds dissolved in water. On the other hand, Ikhlaq et al., (2013) showed that free radicals' production does not occur from the reactions between ozone and solid catalysts. In this case, ozone would be accumulated on the surface of the solid, producing a local increase of ozone concentration and that would result in a greater rate of organic compounds degradation.

Although these metal oxides have proven catalytic activity in the treatment of organic compounds by peroxidation and ozonation, it is necessary to develop strategies to recover and reuse the catalyst. One alternative is immobilizing the catalyst on the surface of membranes (CHENG et al., 2017).

Coupling catalytic ozonation or catalytic peroxidation with membrane treatment technology may solve the problem of catalyst recovery since the membrane would be a single barrier to the catalyst and a selective barrier to the molecules to be degraded. Besides of that, fouling is an obstacle to be overcome in the application of membrane filtration system in treatment plants, which can be solved by integrating the use of membranes with AOPs. Positive results have already been demonstrated

in fouling reduction and organic matter removal using catalytic membranes coupled to ozonation (ALPATOVA; DAVIES; MASTEN, 2013; GELUWE; BRAEKEN; BRUGGEN, 2011) and peroxidation (ANGELIZ et al., 2016).

Moreover, small and recalcitrant compounds are not retained by the membranes in the water and wastewater treatment plants. These compounds could be completely or partially degraded in biodegradable ones into the catalytic membrane coupled to AOP. In this system, free oxidative radicals would be produced by the reactions between oxidant agent and the catalyst, destroying these compounds and eliminating one more step in the treatment plant (LI et al., 2018).

Therefore, this doctorate thesis aims to investigate the application of transition metal catalysts in suspension or immobilized on ceramic membrane in the treatment of 1,4-dioxane using ozone or hydrogen peroxide as oxidant.

1.1 AIM OF THIS STUDY

The aim of this doctorate thesis is to investigate the treatment of 1,4-dioxane by heterogeneous catalytic peroxidation and heterogeneous catalytic ozonation using transition metal oxides as catalyst in suspension or supported on ceramic membrane.

In order to achieve the aim of this study the following objectives were proposed:

1. Select and characterize transition metal oxide catalysts applicable to catalytic peroxidation and catalytic ozonation;
2. Determine the reaction kinetics of 1,4-dioxane mineralization through catalytic peroxidation and catalytic ozonation;
3. Investigate the optimum pH and catalyst dosage, reaction mechanism and catalyst stability of the catalyst that presents the highest mineralization rate, as well as 1,4-dioxane toxicity after and before treatment;
4. Determine the reaction kinetics of the best catalyst supported on ceramic membrane coupled to ozonation with different catalyst loading, as well as the toxicity of 1,4-dioxane before and after treatment.
5. Investigate fouling minimization during the filtration of a surface water from a municipal water treatment plant;
6. Evaluate the stability and reusability of the catalytic membrane using surface water.

1.2 STRUCTURE OF THIS DOCUMENT

This doctorate thesis is structured as follows:

- Chapter 1: the problem is contextualized, aim and objectives are presented.
- Chapter 2: a literature review addresses the most relevant topics for the present doctorate thesis. The first section of this chapter (2.1) concerns the target compound of the work, which is the 1,4-dioxane. Afterward in the next section (2.2), the advanced oxidation processes applied in this work will be explored, followed by the section (2.3), in which the state of the art concerning the 1,4-dioxane treatment by advanced oxidation processes will be presented. Ceramic membranes modified with catalyst and coupled to ozonation or peroxidation will be present in the section 2.4 of this chapter. Finally, the last section of this chapter (2.5) will focus on the relevant aspects from this literature review and the innovation of this doctorate thesis.
- Chapter 3: the methodology used to reach the aim of this doctorate thesis is summarized and explained.
- Chapter 4: the preliminary results will be provided. Firstly, methodology will be presented (4.1). Then, results will be presented and discussed as follows: catalysts characterization (4.2), adsorption kinetics of 1,4-dioxane over FeOOH, CeO_2 and CuO (4.3) and the evaluation of the catalysts in the treatment of 1,4-dioxane by catalytic peroxidation (4.4) and catalytic ozonation (4.5).
- Chapter 5: this chapter is based on the paper entitled "Treatment of Aqueous Solutions of 1,4-dioxane by Ozonation and Catalytic Ozonation with Copper Oxide (CuO)".
- Chapter 6: this chapter is based on the paper entitled "1,4-Dioxane removal from water and membrane fouling elimination by CuO-coated ceramic membrane coupled to ozonation".
- Chapter 7: conclusion are presented.

2. LITERATURE REVIEW

This literature review will address the most relevant topics for the present doctorate thesis. In the first section of this chapter (2.1), the advanced oxidation processes applied in this work will be explored. Afterward, the next section (2.2) concerns the target compound of the work, which is the 1,4-dioxane, followed by the section (2.3), in which the state of the art about 1,4-dioxane treatment by advanced oxidation processes will be presented. Ceramic membraned modified with catalyst and coupled to ozonation or peroxidation will be present in the section 2.4 of this chapter. Finally, the last section of this chapter (2.5) will focus on the relevant aspects from this literature review and the innovation of this doctorate thesis.

2.1 ADVANCED OXIDATION PROCESSES (AOPs)

Advanced Oxidation Processes (AOPs) are innovative technologies based on oxidant radicals' generation, which are highly reactive and not-selective oxidizing agents, mainly hydroxyl radical ($\cdot$OH). These oxidizing agents are capable to reduce the organic load and toxicity as well as increasing the biodegradability of the water and wastewater due to the oxidation of recalcitrant compounds into easily degradable substances, causing the mineralization in CO_2 and H_2O (KARCI, 2014).

Hydroxyl radicals are generated from different processes involving oxidants agents, such as ozone, hydrogen peroxide, irradiation UV and/or catalysts. These processes are classified into two groups: (i) homogeneous reactions, using O_3, H_2O_2 and/or UV and/or dissolved catalysts; (ii) heterogeneous reactions, in the presence of solid catalysts (DEZOTTI, 2008).

A great advantage in the treatment of organic compounds by AOPs against physicochemical processes is the mineralization of the pollutant. In physicochemical process, the pollutant is removed from the liquid phase but it persists on a solid material or in a gaseous emission (OLIVEIRA, 2012).

Researches involving the development of chemical processes capable of destroying refractory compounds in industrial wastewaters and waters are focused on heterogeneous AOPs, in which solid materials with active surface act as catalyst of the process. Examples are TiO_2, CuO, $FeOOH$, Al_2O_3 and MnO_2 (GHARBANI; MEHRIZAD, 2012; ANGI et al., 2014; ZBILJIC et al., 2015; HU et al., 2016).

So, the development of chemical processes capable to destroy refractory compounds in industrial wastewater and water are being more attractive. Among them, heterogeneous AOPs using solid catalysts (TiO_2, CuO, FeOOH, Al_2O_3 and MnO_2) have proved that it is possible to eliminate several classes of organic compounds (GHARBANI; MEHRIZAD, 2012; ANGI et al., 2014; ZBILJIC et al., 2015; HU et al., 2016). Despite this, there is no consensus about the best catalyst for catalytic peroxidation and catalytic ozonation (SABLE et al., 2017; VAKILABADI et al., 2017; WAN; WANG, 2017; KIM et al., 2017).

2.1.1 Heterogeneous catalytic peroxidation (Fenton-type)

Compared with AOPs, Fenton is considered the most attractive treatment process due to its high degradation efficiency of a wide range of organic compounds, low cost and easy application. The Fenton system consists of homogeneous reactions between Fe^{2+}/Fe^{3+} and H_2O_2, Equations 1 to 3 (NEYENS; BAEYENS, 2003).

$$Fe^{2+} + H_2O_2 \rightarrow Fe^{3+} + OH^- + {}^{\bullet}OH \tag{1}$$
$$Fe^{3+} + H_2O_2 \rightarrow Fe^{2+} + H^+ + HO_2{}^{\bullet} \tag{2}$$
$$HO_2{}^{\bullet} + H_2O_2 \rightarrow H_2O + {}^{\bullet}OH + O_2 \tag{3}$$
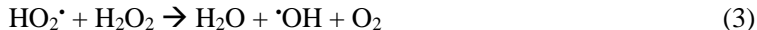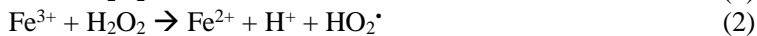
Fenton process is established in several industrial full-scale applications (BAE et al., 2015) despite its limitations, as the narrow pH range (pH $\approx$ 3) and separation/recovery of the catalyst after treatment (MA et al., 2015). To overcome some limitations for large scale application, it has been proposed the use of heterogeneous catalysts, based on the simple separation/recovery of the catalyst after the reactions (CRUZ et al., 2016). More recently, other catalysts have been also proposed (Table 1), such as composites (SEHATI; ENTERAZI, 2017; WAN; WANG, 2017; XU; WANG, 2012), supported, (ANEGGI; TROVARELLI; GOI, 2017) and unsupported metal oxides (KIM, et al., 2017; DU et al., 2016; LA PLATA; ALFANO; CASSANO, 2010), zeolites (BOLOVA; GUNDUZ; DUKKANCI, 2012) and activated carbon (MESQUITA et al., 2012).

Nevertheless, pH value has also been a limitation in the application of heterogeneous catalytic peroxidation. As displayed in Table 1, for most of the published articles, the optimum pH is acid (close to 3). However, it is recognized that sludge production and its separation after the Fenton treatment are the major drawbacks that can be overcome through the use of solid catalysts (ANEGGI; TROVARELLI; GOI, 2017). The development of an active heterogeneous catalyst capable of decomposing

hydrogen peroxide into free radicals throughout the pH range is one of the primary challenges in this field (SEHATI; ENTEZARI, 2017).

According to Table 1, it is noticeable that the most of studies investigated the effects of operational parameters on the degradation rate of several pollutants and using different catalysts. Some of them evaluated catalyst stability and reusability and free radicals involved in the reaction, while others only evaluated pH and catalyst dosage. Interactions among solid catalyst, H_2O_2, organic compounds, generated reactive oxygen species (ROS) and degradation byproducts are too complex. So, it is not surprising that different and controversial conclusions are achieved. Fundamental questions on the reaction mechanisms and the rate constants of elementary stages remain unanswered (VORONTSOV, 2018).

Lin and Gurol (1998) proposed the first mechanism of H_2O_2 decomposition on the surface of the iron oxide, Equations 4 to 9. In a simplified way, the reaction begins with the formation of a complex between H_2O_2 and the surface of the catalyst $-(H_2O_2)s$, Eq. 4. The complex on the surface undergoes a reversible electron transfer (Eq. 5), generating reduced Fe ion which will react with H_2O_2 according to Eq. 6 to form hydroxyl radicals. The peroxide and hydroxyl radicals produced during the reaction can still react with the Fe^{III} and Fe^{II} sites on the catalyst surface (Eq. 7-9). The rate of Fenton-type oxidation of organic compounds is limited by steps 4, 5 and 8, responsible for regeneration of Fe^{II}.

$$\equiv Fe^{III}\text{-}OH + H_2O_2 \xleftrightarrow{k_1} (H_2O_2)_S \tag{4}$$

$$(H_2O_2)_S \xleftrightarrow{k_2} \equiv Fe^{II} + H_2O_2 + HO_2^{\bullet} \tag{5}$$

$$\equiv Fe^{II} + H_2O_2 \xrightarrow{k_3} \equiv Fe^{III}\text{-}OH + {}^{\bullet}OH \tag{6}$$

$$HO_2^{\bullet} \leftrightarrow H^+ + O_2^{\bullet-} \tag{7}$$

$$\equiv Fe^{III}\text{-}OH + HO_2^{\bullet}/O_2^{\bullet-} \xrightarrow{k_5} \equiv Fe^{II} + H_2O/OH^- + O_2 \tag{8}$$

$${}^{\bullet}OH + \equiv Fe^{II} \xrightarrow{k_1} \equiv Fe^{III}\text{-}OH \tag{9}$$
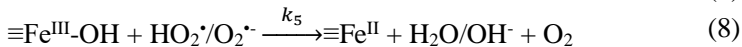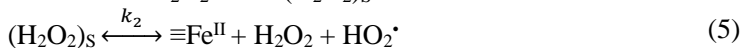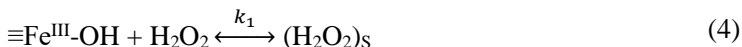
In this regard, to achieve an efficient electron transfer to H_2O_2, the ideal Fenton catalyst should exhibit multiple oxidation states and both the active and inactive redox states should be stable over a wide pH range to prevent the precipitation of the catalyst. Two examples are cerium oxide and copper oxide (BOKARE; CHOI, 2014). Among all the rare-earths, cerium is the only metal capable of activating H_2O_2 by Fenton-type

mechanism. Cerium oxide is the most common choice among all cerium compounds, due to the presence of oxygen vacancies on the oxide surface. The availability of Ce^{3+} at the surface sites is enhanced and induces high catalytic activity. In terms of its reactivity towards H_2O_2, copper shows similar redox properties as iron. However, copper complexes are soluble in neutral pH conditions, this means that Cu^{2+} based Fenton catalysts efficiently generate ·OH for the oxidation of pollutants in circumneutral aqueous solutions (MAMONTOV et al., 2000).

Table 1: State of the art regarding heterogenous catalytic peroxidation

Catalyst	Target compound	Optimum experimental conditions				Results	Reactive species	Reference
		pH	H_2O_2 dosage (ppm)	Catalyst dosage (ppm)	Reaction time/efficiency	Catalyst stability		
Ag/CeO_2	Phenol (C_0=100 ppm)	2	3300	Fixed in 100	2 h/100% of phenol	Stable in 5 reuses	It was not evaluated	Aneggi, Trovarelli e Goi, 2017
α-, β-, γ- e δ-MnO_2	Methylene blue (C_0 = 52 ppm)	6.1	986	100	20 min/100% of methylene blue. Best catalyst: γ-MnO_2	Stable in 4 reuses	•OH	Kim, et al., 2017
CuO/Ti_6O_{13} merosoporous	Orange G (C_0 = 30 ppm)	6	0,65 mL – 1 drop in each minute	40	15 min/100 % of orange G	Stable in 3 reuses	•OH ads and free	Sehati e Enterazi, 2017
Fe_3O_4-Mn_3O_4/graphene oxide	Sulfametazine (C_0 = 10 ppm)	3	205	1000	80 min/100% of the target	It was not evaluated	•OH on the catalyst surface	Wan e Wang, 2017
Iron oxide modified with sulfur	Bisphenol A (C_0 = 46 ppm)	3,5	136	500	20 min/100% of the target	57% and 30% of target removal in the second and third reuse, respectively	•OH	Du et al., 2016

Table 1 (Continued)

Catalyst	Target compound	Optimum experimental conditions			Results			Reference
		pH	H_2O_2 dosage (ppm)	Catalyst dosage (ppm)	Reaction time/efficiency	Catalyst stability	Reactive species	
Fe_3O_4/CeO_2	4-chlorophenol ($C_0 = 171$ ppm)	2	1020	2000	20 min/100% of the target	Stable in 5 reuses	˙OH ads and free	Xu e Wang, 2012
Goethite	2-chlorophenol ($C_0 = 52$ ppm)	3	2500	500	6 h/75% of TOC	It was not evaluated	It was not evaluated	La Plata, Alfano e Cassano, 2010
FeZSM-5	Orange II ($C_0 = 50$ ppm)	3,5	9070	2000	2 h / 60% of COD removal	Stable in 2 uses	It was not evaluated	Bolova, Gunduz, Dukkanci, 2012
Activated carbon impregnated with Fe	CSD dye ($C_0 = 12$ ppm)	3	77	7,5 g – packed bed reactor	2 h / 80% of TOC at 30 °C	Stable in 3 reuses	It was not evaluated	Mesquita et al., 2012
Goethite	2-Chlorophenol ($C_0 = 50$ ppm)	3	75	200	4 h / 40% of TOC	It was not evaluated	It was not evaluated	Lu, 2000

38

2.1.2 Heterogeneous catalytic ozonation of contaminants dissolved in water

Catalytic ozonation has been considered as a promising technology for the removal of organic pollutants in water and wastewater. Although ozone does not promote the complete oxidation of the recalcitrant compounds, catalytic ozonation easily mineralize them. It occurs because the catalyst increases the ozone decomposition rate into free radicals, which are non-selective, increasing the degradation and mineralization of the organic compounds (PARK; CHOI; CHO, 2004).

Besides of the high capacity to mineralize organic compounds, catalytic ozonation also reduces ozone consumption and it is easier to remove the catalyst in the end of the process when compared to the homogeneous catalytic ozonation, resulting in less waste in the treatment systems (ZHUANG et al., 2014).

The presence of metals oxides in aqueous suspension containing dissolved organic compounds and ozone can trigger a series of phenomena according to Nawrocki (2013):

1. Adsorption and subsequent ozone decomposition into free radicals (hydroxyl and hydroperoxyl):
2. Adsorption of the organic compounds present in the solid, followed by surface reaction with the dissolved ozone;
3. Simultaneous adsorption of dissolved organic compounds and ozone, followed by surface reaction;
4. Homogeneous reaction between the dissolved organic compounds and the molecular ozone dissolved in water.

The catalytic activity discussed by Nawrocki (2013) is based on the promotion of the catalytic ozone decomposition and the increase of hydroxyl radicals' production. At pH values above the isoelectric point (IEP), the predominant specie on the surface of the catalyst is M-O$^-$ and at pH values below the IEP, M-OH$_2^+$ is the predominant specie. These species act as initiators of the reactions involving ozone decomposition, leading to the formation of $^{\bullet}$OH (ZHANG et al., 2008).

Ma et al., (2014) proposed a mechanism for the degradation of 4-nitrophenol by ozonation using Mn-Co-Fe as catalyst (Figure 1). The catalyst surface is deprotonated in solutions with pH below to the IEP. Ozone molecules are adsorbed on the negatively charged surface of the catalyst, and some molecules are transformed into $^{\bullet}$OH. 4-nitrophenol is

degraded in the solution by ozone. Then the carboxylic acid generated from the degradation of the target compound by ozone is adsorbed onto the surface of the catalyst. Finally, adsorbed organic molecules are oxidized to CO_2 by adsorbed ozone and $\cdot OH$ generated from ozone decomposition.

Figure 1: Catalytic ozonation mechanism for 4-nitrophenol treatment using Mn-Co-Fe as catalyst proposed by Ma et al. (2014).
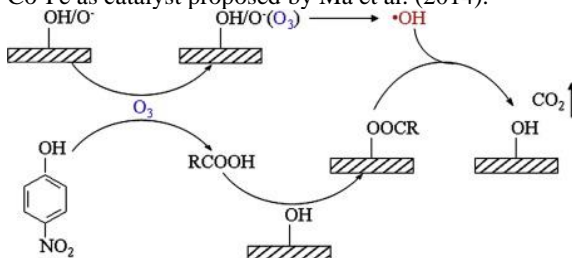
Source: Ma et al., 2014.

However, studies carried out in different research groups suggest different catalytic ozonation mechanisms, as the formation of groups between the carboxyl groups of the pollutants and their components on the surface of the catalyst (BELTRAN; RIVAS; MONTERO-DE-ESPINOSA, 2003).

The generation of ROS involved in the heterogeneous catalytic ozonation process are also not defined and explained. Some studies suggest the formation of different ROS that do not include $\cdot OH$, such as superoxide radical and the peroxide through redox reaction on the surface of the metal oxide. In the Lewis weak sites, hydrogen bonds with OH groups on the surface are observed, while in reactions with Lewis strong sites the interaction with ozone results in the formation of oxygen atoms (BULANIN; LAVALLEY; TSYGNENKO, 1995).

Ikhlaq et al. (2013) investigated the mechanisms involved in the catalytic ozonation process using alumina and zeolite (ZSM-5) as catalysts. Alumina produced $\cdot OH$, H_2O_2 and superoxide radical by the decomposition of ozone on its surface. On the other hand, no free radicals were performed on the ZSM-5 surface, and the solid acted only as an adsorbent of the organic compound and the ozone, leading to the degradation of the organic compounds by direct reaction on the solid surface.

The state of art shows that several catalysts have been proven effective in the enhancement of ozonation efficiency but the mechanism is still not understood (Table 2). There is still no consensus about the most

suitable catalyst and the operational conditions (pH value, catalyst dosage, for instance) to large applications. Moreover, even the formation of ROS and catalyst stability are still controversial. Frequently, the same catalyst studied by different research groups, lead to contradictory results, especially considering the amount of impurities on the solid surface (NAWROCKI; KASPRZYK-HORDERN, 2010).

There are at least two important questions that need answering when heterogeneous catalytic ozonation is applied in the treatment of organic compounds: (i) whether the catalyst decomposes aqueous ozone into ROS or if the direct attack on the surface of the catalyst is responsible by the degradation of organic compounds and (ii) what is the long-term activity of catalysts? (IKHLAQ et al., 2013; NAWROCKI; KASPRZYK-HORDERN, 2010).

Table 2: State of the art regarding heterogeneous catalytic ozonation

Catalyst	Target compound	Optimum experimental conditions			Results			Reference
		pH	O_3 dosage (g h^{-1})	Catalyst dosage (ppm)	Reaction time/efficiency	Catalyst stability	Reactive species	
Cu-Al	Clofibric acid (C_0=100 ppm)	7	1.2	500	2 h – 85% of TOC	Stable in 3 reuses	It was not evaluated	Sable et al., 2017
CuO supported in mesoporous carbon aerogel	Synthetic textile wastewater (C_0=800 ppm)	10.6	0.48	3000	1 h – 60% of CDO	It was not evaluated	It was not evaluated	Hu et al., 2017
Carbon impregnated with $Fe^{II}Fe^{III}O_4$	Petrochemical wastewater (CDO_0=362 ppm)	7	0.3	450	2 h – 75% of CDO	Stable in 5 reuses	·OH	Ahmadi et al., 2017
Activated carbon/MnO_x	Oxalic acid (C_0=80 ppm)	3.5	5 ppm	100	1 h – 80% of TOC	It was not evaluated	·OH	Huang et al., 2017
MgO	Paracetamol (C_0=50 ppm)	5.4	0.11	100	30 min – 90% of TOC	Stable in 3 reuses	·OH	Mashayekh-Salehi et al., 2017
$Ce_{0,1}Fe_{0,9}OOH$	Sulfamethazine (C_0=10 ppm)	7	20 ppm	400	2 h – 45% of TOC	It was not evaluated	It was not evaluated	Bai, Yang e Wang, 2016

Table 2 (Continued)

Catalyst	Target compound	Optimum experimental conditions			Results			Reference
		pH	O_3 dosage (g h^{-1})	Catalyst dosage (ppm)	Reaction time/efficiency	Catalyst stability	Reactive species	
β-FeOOH	4-Chlorophenol (C_0=257 ppm)	3.5	0.036	100	40 min – 100% of 4-chlorophenol	Catalyst stability was not evaluated, but Fe ions were leached	It was not evaluated	Oputu et al., 2015
$ZnAl_2O_4$	Phenol (C_0=300 ppm)	6.4	0.045	1000	1 h– 70% of phenol	Stable in 5 reuses	$^\bullet OH$	Zhao et al., 2015
$α-MnO_2$	4-nitrophenol (C_0=50 ppm)	3.5	0.3	100	9 min – 80.5% of TOC	0.05 ppm was leached after 90 min	$O_2^{\bullet-}$	Nawaz et al., 2015
$CuFe_2O_4$	Phenacetin (C_0=36 ppm)	7.2	0.36 ppm	3000	30 h – 95% of phenacetin	It was not evaluated	$^\bullet OH$	Qi, Chu e Xu, 2015
Mn-Co-Fe	4-nitrophenol (C_0=10 ppm)	6.5	0.12	200	60 min – 90% of TOC	Stable in 5 reuses	$^\bullet OH$	Ma et al., 2014
Ni/TiO_2	2,4-Dichlorophenoxyacetic acid (C_0=80 ppm)	3.1	0.75	100	30 min – 100% of the target	It was not evaluated	It was not evaluated	Rodríguez et al., 2013

2.2 1,4-DIOXANE

1,4-dioxane (Figure 2) is a synthetic cyclic diether compound, used as a solvent in the manufacture of chemicals. It has historically been used as a stabilizer in chlorinated solvents. According to the Agency of Toxic Substances and Disease Registry, 1,4-dioxane is manufactured by dehydration and ring closure of diethylene glycol in a closed system. 1,4-Dioxane can also be prepared by dehydrohalogenation of 2-chloro-2'-hydroxydiethyl ether, by reacting ethylene glycol with 1,2-dibromoethane (ULLMANN'S, 2000).

1,4-Dioxane is a by-product of chemical processes, for instance, in the production of surfactants that are used for food and personal care products (ZENKER; BORDEN; BARLAZ, 2003). It can also be found in paint, adhesives, pesticides and household cleaners (MOHR, 2010).

Figure 2 : 1,4-Dioxane chemical structure
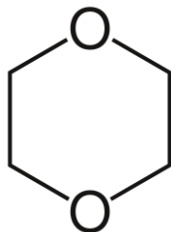
1,4-Dioxane gets into water from industrial uses and landfill leachate as a result of the disposal of waste products containing it. Due to its presence in consumer products, it can leach into groundwater from septic systems or be released into the environment after wastewater treatment. Once released into the environment, it enters into ground or surface water used as drinking water (ECB, 2002; USEPA 2010).

Exposure to 1,4-dioxane occurs by drinking or using water that is contaminated with it, which can happen during the preparation of beverages, such as tea and coffee, and when cooking foods that retain water. There is no significant absorption during showering or bathing because 1,4-dioxane is not absorbed through the skin and does not vaporize into the air when solubilized in water (ATSDR, 2012).

The International Agency for Research on Cancer classifies 1,4-dioxane as carcinogenic to animals and probable human carcinogen. It causes irritation to the eyes and respiratory tract, it is suspected of causing

damages to the central nervous system, liver and kidneys when the person is expose to very high levels (ECB, 2002; USEPA, 2010).

The World Health Organization suggests a maximum 1,4-dioxane concentration of 50 µg L^{-1} in drinking water, while USEPA established 3 µg L^{-1} (MOHR, 2010). In Japan the tolerable concentration is up to 50 µg L^{-1} for tap water (Ministry of Health of Japan). Germany's federal environmental agency has set 0.1 µg L^{-1} as a caution limit (STEPIEN; DIEHL; HELM, 2014). Brazil has not yet set a limit for releasing 1,4-dioxane into aqueous environment.

In addition of its negative health effects, this substance is relatively bio-recalcitrant and resilient to treatment by conventional processes, mainly due to its high solubility in water (4.3×10^5 mg L^{-1}), low vapor pressure (37 mmHg at 25 ºC) and the absence of the reactive O-H bond (ZENKER; BORDEN; BARLAZ, 2003). The use of chlorination as a conventional technology produces good results in 1,4-dioxane degradation. However, chlorine oxidation produces intermediates more toxic than 1,4-dioxane (SUH; MOHSENI, 2004). The removal efficiency using other conventional technologies, such as activated sludge, coagulation, biodegradation and sand filtration are also unsatisfactory (16.2%, 7.7%, 10% and 1,1%, respectively) (LEE et al., 2011).

Therefore, due to the difficulty to treat 1,4-dioxane by the conventional processes, other technologies have to be studied and applied, such as Advanced Oxidation Processes (AOPs).

2.3 1,4-DIOXANE TREATMENT BY ADVANCED OXIDATION PROCESSES

The state of the art concerning the 1,4-dioxane treatment by AOPs are presented in Table 3. Among them, O_3/H_2O_2 (KWON et al., 2012), Fenton (MERAYO et al. (2014)), photocatalysis (VESCOVI; COLEMAN; AMAL, 2010; COLEMAN et al., 2007), photo-Fenton (CHITRA et al., 2012; BARNDÕK et al., 2016) and electrocatalysis (PARK et al., 2018) have already been applied in the treatment of 1,4-dioxane.

From our best knowledgement, only one study was reported about the heterogeneous catalytic ozonation of 1,4-dioxane, and the catalyst used by Tian et al. (2016) was activated carbon. There is only one study about UV photo-Fenton using zero-valent iron, but the author neglected the results in the absence of UV light (BARNDÕK et al., 2016). Furthermore, no report was found dealing with the heterogeneous catalytic peroxidation of 1,4-dioxane.

The non-catalytic ozonation of 1,4-dioxane is ineffective ($k(O_3)$ = 0.32 $M^{-1} s^{-1}$), as previously reported by Bardnõk et al. (2014) and Kwon et al. (2012). Hence, 1,4-dioxane would be decomposed only at high pH values or in the presence of H_2O_2 to promote O_3 decomposition into hydroxyl radicals, that will react quickly with 1,4-dioxame $k(^\bullet OH)$ = (1.1-2.35) $\times 10^9 M^{-1} s^{-1}$ (THOMAS, 1965).

Consequently, for ozone and Fenton processes being effective in the treatment of 1,4-dioxane should occur in a basic and acidic pH range, respectively. Therefore, to work in neutral pH values, it is necessary to use solid catalysts that will cause the decomposition of the O_3 and H_2O_2 into free radicals that can degrade 1,4-dioxane. In this work, three metal oxides were investigated for the treatment of 1,4-dioxane by ozonation and peroxidation: iron oxide (goethite), cerium oxide and copper oxide.

Table 3: State of the art concerning 1,4-dioxane treatment by advanced oxidation processes.

Process	[1,4-dioxane] (ppm)	Optimum experimental conditions	Results	Reference
Electrocatalysis RuO_2-TiO_2	Textile wastewater + 1,4-dioxane	Ru:Ti=0.6:0.4–0.9:0.1 pH 7.4 ± 0.2 3.4 ± 0.3 mS/cm	$^{\cdot}$OH is not the main radical produced. 1,4-dioxane degradation occurs by chlorine reactive species.	Park et al. (2018)
Sodium persulfate + Fe^0	500	$[Na_2S_2O_8]$ = 63 mM; Fe^0 = 67 mM	It is necessary to add Fe^0 slowly until reach 100% of 1,4-dioxane removal, because the excess of Fe^{2+} scavenge the sulfate ions.	Kambhu et al. (2017)
Catalytic oxidation Clays impregnated with Fe(II)	0.4	pH = 6.4 [Nontronite]=5 g L^{-1}	The best clay tested were nontronite, due to its slowly $^{\cdot}$OH production, which were the main radical. The main byprodutcs were formic acid and methoxyacetic acid.	Zeng et al. (2017)
O_3/ultrasound	0.02	pH 7; Ultrasound: 20kHz; $[O_3]$: 16 mg L^{-1}	1,4-dioxane removal depends of ozone consumption, which increase with ultrasound and in basic pH.	Dietrich et al. (2017)
O_3/activated carbon	50	pH 7; [cat]=3g L^{-1} O_3 flow=1.62g h^{-1}	CDO and 1,4-dioxane removal were 40% and 65% in 3 h, respectively. Author confirmed $^{\cdot}$OH using t-butanol as scavenger.	Tian et al. (2016)
UV/H_2O_2/Fe^0	248	Lamp = 450W; pH 7; H_2O_2/DQO=2.625 H_2O_2/Fe^0=60	100% of CDO removed in 20 min.	Barndõk et al. (2016)

Table 3 (Continued)

Process	[1,4-dioxane] (ppm)	Optimum experimental conditions	Results	Reference
Pt-CeO$_2$-ZrO$_2$-Bi$_2$O$_3$/SBA-16 Aqueous oxidation	100	Air atmosphere; T=80 °C; [cat]=1000 ppm	62% of 1,4-dioxane removed in 6h.	Choi et al. (2015)
O$_3$	248	pH 10, buffer solution. O$_3$ flow= 4 L min^{-1}	Best results at pH basic, in the presence of bicarbonate the process efficiency increased, due to the buffer effect, keeping the pH basic. 90% of the CDO was removed.	Barndōk et al. (2014)
Fenton	248	pH 2.8; H$_2$O$_2$/DQO = 4.250	Experiments were performed in ambient temperature, 65% of CDO removal in 45 min.	Merayo et al. (2014)
O$_3$/H$_2$O$_2$/UV	100	pH 10; H$_2$O$_2$/O$_3$ = 0.5; Irradiation: 254 nm	94% of CDO was removed in 90 min.	Kwon et al. (2012)
Sun light/Fe(II)/H$_2$O$_2$ UV(15W)/Fe(II)/ H$_2$O$_2$ Ultrasound/Fe(II)/ H$_2$O$_2$ Fe(II)/H$_2$O$_2$ UV(15W)/H$_2$O$_2$	8811	pH 3; [cat]=223 ppm [H$_2$O$_2$]=1M	100% 1,4-dioxane removal: Sun light/Fe(II)/H$_2$O$_2$ = 1,75h UV(15W)/Fe(II)/H$_2$O$_2$ = 2,25h Ultrasound/Fe(II)/H$_2$O$_2$ = 8h Fe(II)/H$_2$O$_2$ = 4h UV(15W)/H$_2$O$_2$ = 5,5h Therefore, the best result obtained was for the system Sun light/Fe(II)/H$_2$O$_2$	Chitra et al. (2012)

Table 3 (Continued)

Process	[1,4-dioxane] (ppm)	Optimum experimental conditions	Results	Reference
UVA/TiO$_2$, TiO$_2$ = P25, sol–gel and P25 immobilized	36	pH 7 [cat]=1000 ppm	The best result obtained was for p25 in suspension, constants obtained were: kP25 (min^{-1}) = 1.48 ksol-gel(min^{-1}) = 0.11 kP25 imobilizado = 0.55	Vescovi, Coleman and Amal (2010)
UVC/H$_2$O$_2$ P25/UVA/H$_2$O$_2$ P25/UVA TiO$_2$ = P25	0.36	pH 3 Lamp 20W [H$_2$O$_2$]=30 ppm [cat]=100 ppm	The addition of H$_2$O$_2$ decreased the constant rate in the system P25/UVA/H$_2$O$_2$ 100% of 1,4-dioxane was removed in 10 min in the system P25/UVA.	Coleman et al. (2007)
O$_3$/H$_2$O$_2$	160	pH 9	H$_2$O$_2$:O$_3$ above of 0.45 mol decreased 1,4-dioxane removal. Author confirmed the production of $^{\bullet}$OH	Suh e Mohseni (2004)

2.4 CATALYTIC MEMBRANES

Ultrafiltration is one of the most promising technologies for water treatment aiming to produce high quality drinking water (GUO; XU; QI, 2016). However, fouling is an obstacle to be overcome for the application of this technology in water and wastewater treatment plants (KARNIK et al., 2005).

In order to prevent the membrane fouling, researchers are coupling the separation process using ceramic membranes (CMs) with AOPs. For the purpose of increasing the efficiency of this process, catalytic ceramic membrane (CCMs) are being investigated. Besides of promoting a higher anti-fouling property and increasing the removal efficiency of organic pollutants, it also solves the catalyst recovery issue in the AOPs (GUO; XU; QI, 2016).

To date, there is one paper published in the literature regarding permeate flux recovery using the hybrid system ultrafiltration-catalytic peroxidation. Angelis et al. (2016) modified CM with iron oxide and obtained $97\pm2\%$ of flux recovery using 10 ppm of humic acid and 5 mM of H_2O_2. The authors concluded that Fenton-like treatment was effective in 4 reuse cycles of ultrafiltration cleaning.

For the ultrafiltration-ozonation system using CCM, several studies were reported in the last thirteen years, Table 4. The first studies were focused on the treatment of waters from lakes and rivers (KARNIK et al., 2005; CORNEAL et al., 2011; BYUN et al., 2011). Chen et al. (2015), published the first study on the degradation of industrial wastewater using this technology.

Catalyst impregnation method on the CM surface is an important factor to be discussed. As can be seen in Table 4, most of the authors modified the CM following the layer-by-layer method developed by Lvov et al. (2000) and they did not specify the mass of the catalyst contained on the CCM. Some authors characterized the CCM by FESEM with the objective of ascertaining the homogeneity of the catalyst layer on the surface of the CM. Therefore, it is not possible to compare the catalytic activity of the CM modified with metal oxide between the studies already published. Most of the researches modified the CM with MnO_2 (CHENG et al. (2017); CORNEAL et al. (2011); BYUN et al. (2011)), but there are also some works that used Fe_2O_3 (KARNIK et al. (2005); BYUN et al. (2011)) and composites with Mn (GUO et al. (2018); ZHANG et al. (2016); GUO, XU E QI (2016); CHEN et al. (2015)).

According to Table 4, positive results in terms of organic pollutant removal and fouling reduction were obtained by hybrid process ultrafiltration coupled to catalytic ozonation. Nevertheless, none of them focused on the treatment of small and recalcitrant compounds that are not retained into the filtration processes, including reverse osmosis.

1,4-Dioxane is an example of small and recalcitrant compound that is not retained by reverse osmosis process (LI et al., (2018)). The complete or partial oxidation of these compounds in biodegradable ones in a single step is an ideal to be achieved. In addition to solving the aforementioned problems, catalyst recovery and fouling reduction, it would reduce the area and maintenance required for the treatment plant.

A sequential combination of membrane treatment and UV-based AOP is presented in Figure 3. This process can be considered as a standard system applied in the industry for potable water reuse. The secondary wastewater is composed of 1,4-dioxane and ammonia, chloramines are added as membrane antifouling agents. The wastewater is then carried throw to the microfiltration process, followed by reverse osmosis and for last into the UV reactor. Coupling AOP with the membrane technology would reduce one step in the treatment plant (UV reactor), besides of increasing the process efficiency as a whole, as it would reduce the fouling in the membrane system and no addition of chemicals, in this case HOCl, would be necessary.

Figure 3: Example of a secondary wastewater treatment plant.
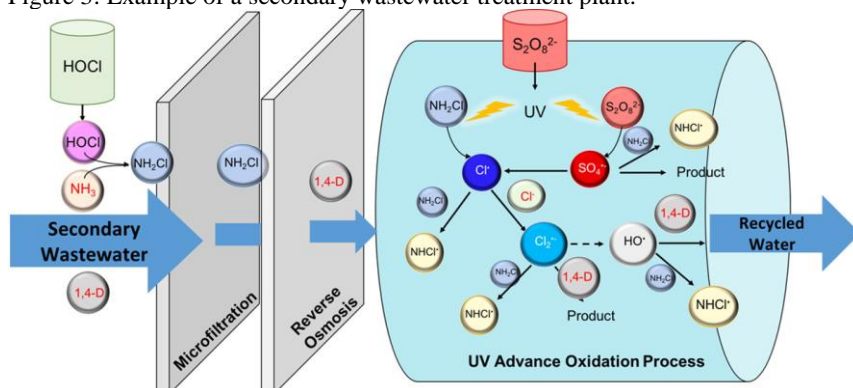
Table 4: State of the art regarding catalytic membranes coupled to ozonation

Catalyst immobilized on the CM	CM composition	Molecular weight cut-off (kDa)	CM pore diameter (nm)	CM geometry	Catalyst impregnation method	Aiming	Results	Reference
$CuMn_2O_4$	Al_2O_3 e ZrO_2	-	50	Tubular	Immersed in $CuMn_2O_4$ sol for 60 min and sintered at 753 °C for 4h (3x).	Treatment of UV light absorbers	The CCM increased the catalytic activity for degradation of the target compounds and reduced the fouling.	Guo et al. (2018)
$C-MnO_2$ $M-MnO_2$ $S-MnO_2$	ZrO_2 e TiO_2	50	-	Plane	Deposition of 20 mg on the surface, dried under vacuum at 100 °C for 30 min and sintered at 500 °C for 60 min.	Fouling control and p-chloronitrobenzene degradation	$S-MnO_2$ modified CM showed the best target compound removal efficiency and fouling reduction	Cheng et al. (2017)
Ti-Mn	Al_2O_3	-	2000	Tubular	Imersed in Ti-Mn sol, dried at 50 °C for 12 h and sintered at 550 °C for 2 h	Tertiary treatment of dyestuff wastewater in a pilot-scale plant	Permeate flux was constant for 30 days and 90% of CDO was removed	Zhang et al. (2016)

Table 4 (continued)

Catalyst immobilized on the CM	CM composition	Molecular weight cut-off (kDa)	CM pore diameter (nm)	CM geometry	Catalyst impregnation method	Aiming	Results	Reference
MnO$_2$-Co$_3$O$_4$	Al$_2$O$_3$ e ZrO$_2$	-	20-50	Tubular	Layer-by-layer 80 layers of catalyst	Benzophenone degradation	CCM increased benzophenone and toxicity removal, ·OH was the main radicalo.	Guo, Xu e Qi (2016)
Ti-Mn	Al$_2$O$_3$	-	2000	Tubular	Imerssed in Ti-Mn sol for 2 min, extracted at 200 μm s^{-1} (2x). Sintered at 500 °C for 1 h.	A pilot-scale for aquaculture water treatment	Fouling and organic matter removal	Chen et al. (2015)
MnO$_2$	ZrO$_2$ e TiO$_2$	5	-	Tubular	Layer-by-layer	Permeate flux evaluation and natural water treatment from a lake in the USA.	CCM restored the permeated flux and removed the organic matter. Best result was obtained with 20 layers of catalyst.	Corneal et al. (2011)

Table 4 (continued)

Catalyst immobilized on the CM	CM composition	Molecular weight cut-off (kDa)	CM pore diameter (nm)	CM geometry	Catalyst impregnation method	Aiming	Results	Reference
MnO_2 e Fe_2O_3	ZrO_2 e TiO_2	5	-	Tubular	Layer-by-layer	To compare CM modified with MnO_2 and Fe_2O_3 with a commercial TiO_2 CM in the treatment of water from a Canadian lake	The MnO_2 CCM showed the best result in terms of TOC and fouling removal. CCM efficiency is dependent of the number of catalyst layers impregnated on the surface. The increase of catalyst layers from 20 to 40 layers did not increase CCM recovery permeate flux efficiency.	Byun et al. (2011)
Fe_2O_3	Al_2O_3, ZrO_2 e TiO_2	15	-	Tubular	Layer-by-layer	Water disinfection		Karnik et al. (2005)

2.5 IMPORTANT ASPECTS FROM THE LITERATURE REVIEW AND THE NOVELTY OF THIS DOCTORATE THESIS

According to the literature review, heterogeneous catalytic peroxidation and heterogeneous catalytic ozonation processes reveal some contradictory results. The reactive species, reaction mechanism involved, optimum pH and catalyst dosage are not stablished. Unfortunately, the same catalyst studied by different research groups leads to distinct conclusions. The development of a catalyst capable of promoting the degradation of a wide range of organic compounds and decomposing hydrogen peroxide and ozone throughout the pH range is the biggest challenge of these two technologies.

Another important issue of these technologies concerns the catalyst recovery. Although catalyst recovery is easier when compared to the homogeneous process, it still requires an additional step in the treatment plant. In other to overcome this matter, the immobilization of solid catalyst on the surface of ceramic membranes is a promising approach, which will also promote anti-fouling property and increase the removal efficiency of organic compounds.

Therefore, this doctorate thesis proposes the application of heterogeneous catalytic peroxidation and heterogeneous catalytic ozonation processes for the treatment of 1,4-dioxane. Thus, three commercial metal oxides widely used as catalysts of these processes were selected: iron oxide, copper oxide and cerium oxide. These catalysts were selected due to their high catalytic activity and stability in the degradation of several organic compounds.

The best catalyst in terms of catalytic activity in the degradation and mineralization of 1,4-dioxane and decomposition of the oxidant into free radicals was investigated in detail. Finally, the catalyst was impregnated on the surface of an ultrafiltration ceramic membrane and the hybrid process ultrafiltration coupled to catalytic oxidation was studied.

In this way, the development of this doctorate thesis intends to elucidate several open questions:

(i)   which ROS were involved in the heterogeneous catalytic ozonation and heterogeneous catalytic peroxidation reactions?

(ii)   what is the optimum pH and catalyst dosage for the catalyst that presented the best catalytic activity?

(iii)   what is the long-term activity of it?
(iv)   what is the effect of catalyst loading impregnated on the ceramic membrane surface?
(v)   when immobilized on the ceramic membrane surface, is the catalytic activity the same when compared in suspension?
(vi)   does the proposed hybrid system reduce membrane fouling when municipal water is filtrated?
(vii)   are the proposed treatments safe in terms of byproducts toxicity?

2.5.1 Simplified methodology applied to elucidate the questions

To elucidate the questions presented above the methodology applied is summarized in Figure 4. The catalysts selected to be employed in the treatment of 1,4-dioxane by ozonation and peroxidation are presented in Table 5.

Experiments were carried out with a solution of 200 ppm of 1,4-dioxane dissolved in deionized water, which correspond to a theoretical concentration of TOC equals to 108.96 ppm. The initial 1,4-dioxane concentration was chosen based on the studies conducted by the research group from the Universidad Complutense of Madrid. The authors worked with real wastewater from a chemical industry, 1,4-dioxane concentration varied between 135-300 ppm (BARNDÕK et al., 2016a; BARNDÕK et al., 2016b; BARNDÕK et al., 2014).

First of all, adsorption kinetics were performed with 250 ppm of catalyst. Catalysts were characterized by zeta potential to obtain the point of zero charge (PZC), X-ray diffraction (XRD), morphology and size of the particles by field emission scanning electron microscopy (FESEM) and transmission electron microscopy (TEM), specific surface area calculated by the Brunauer, Emmett e Teller (BET) method, thermogravimetry analysis (TGA) and elemental composition using atomic absorption spectroscopy (AAS).

Afterward, catalytic peroxidation and catalytic ozonation reactions were performed following the steps presented in the flowchart, Figure 4. The characterization of the catalysts, adsorption kinetics, catalytic peroxidation kinetics and catalytic ozonation kinetics using the three catalysts are presented in the chapter 4 entitled as "Preliminary results".

A detailed investigation was carried out using CuO as catalyst for ozonation process. This part is presented in the Chapter 5, entitled as

"Treatment of 1,4-dioxane by ozonation and catalytic ozonation with copper oxide".

Catalytic ceramic membranes experiments were performed after the selection of the process (catalytic peroxidation or catalytic ozonation) and the catalyst (FeOOH, CeO_2 and CuO). Ceramic membrane was modified with CuO and coupled to ozonation in the treatment of 1,4-dioxane, it is presented in the chapter 6, entitled as "1,4-Dioxane removal from water and membrane fouling elimination by CuO-coated ceramic membrane coupled to ozone".

Table 5: Catalysts selected to be used in this work

Catalyst	Chemical formula	Origin
Iron oxide	FeOOH	Carbonífera Criciúma S.A.
Cerium oxide	CeO_2	SkySprings Nanomaterials (USA)
Copper oxide	CuO	Nanostructured and Amorphous Materials Inc. (USA)

Figure 4: Flowchart of the applied methodologies
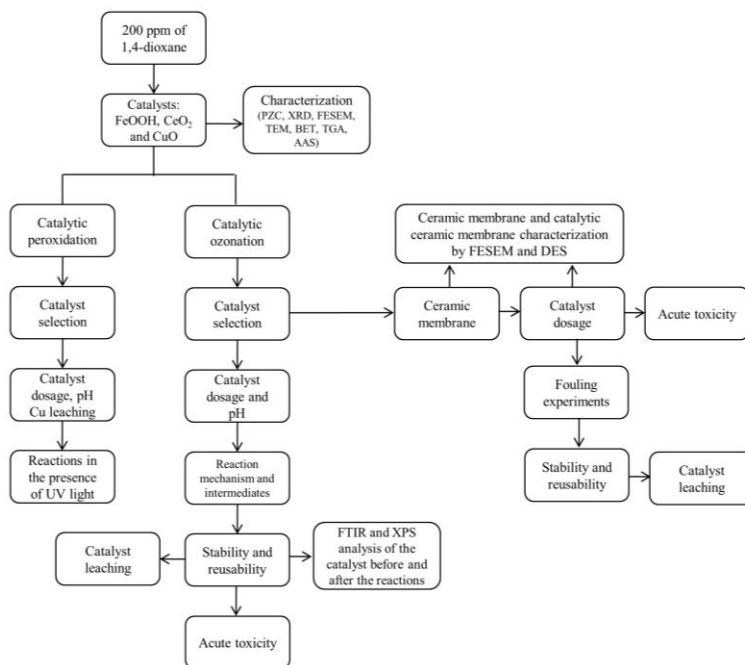
Source: Author's own elaboration

3. PRELIMINARY RESULTS

In this chapter the preliminary results will be provided. Firstly, methodology will be presented (3.1). Then, results will be presented and discussed as follows: catalysts characterization (3.2), adsorption kinetics of 1,4-dioxane over FeOOH, CeO_2 and CuO (3.3) and the evaluation of the catalysts in the treatment of 1,4-dioxane by catalytic peroxidation (3.4) and catalytic ozonation (3.5).

3.1 METHOLOGY

This section of the chapter 3 describes the methodology performed to obtain the results presented, catalyst characterization and catalyst evaluation by peroxidation and ozonation processes in the treatment of 1,4-dioxane.

3.1.1 CHARACTERIZATION OF THE CATALYSTS

The catalysts selected to the present investigation were characterized as BET surface area, TGA, zeta potential, FESEM, TEM, XRD and elemental composition using AAS.

3.1.1.1 Thermogravimetric Analysis (TGA)

Thermogravimetric analysis was performed to check if physical and chemical properties occur when the catalysts selected for this study are heated from ambient temperature to 950 °C, under inert gas atmosphere conditions (N_2) with a flow of 100 mL min^{-1} and heating rate of 10 °C min^{-1} using a Shimadzu equipment, model DTG60/60H, available at the Laboratory of Energy and Environment of the Department of Chemical and Food Engineering from UFSC.

3.1.1.2 Zeta potential

Zeta potential analyses were performed to obtain the pH value at which catalyst are stable in suspension. For that, a Stabino/Nano-flex 180 ° DLS equipment was used, available at the Laboratory of Process Control of the Department of Chemical and Food Engineering from UFSC. Catalysts solutions were prepared in deionized water at the concentration of 250 ppm for CuO and CeO_2 and 70 ppm for FeOOH,

sonicated for 60 min (Unique – 25 kHz) and the analyses were performed varying the pH from 3 to 10.

3.1.1.3 Specific surface area (BET) and porosity

The BET surface area, pore diameter distribution and total pore volume were obtained by adsorption and desorption isotherms at 77 K, using a Quantachorme equipment, model Autosorb-1, at the Analysis Center of the Department of Chemical and Food Engineering from UFSC. Degassing process was carried out under vacuum at 140 °C for 12 h. The specific surface area was calculated by the Brunauer, Emmett e Teller (BET) method with relative pressure varying from 0.05 to 0.30 and the pore size distribution was calculated by the Barret, Emmett e Teller (BJH) method.

3.1.1.4 Morphology and size of the particles – Electron Microscopy (FESEM and MET)

For the evaluation of the morphology and size of each catalyst, field emission scanning electron microscopy (FESEM) and transmission electron microscopy (TEM) analyses were performed at the Central Laboratory of Electron Microscopy from UFSC, using the scanning electron microscope JEOL JSM-6701F and the transmission electron microscope JEM-1011.

For that, powder samples were adhered to the metal stub with carbon tape to avoid interferences and covered with gold for the FESEM analysis. For the TEM analysis, catalysts suspension in ethanol were prepared and one drop was placed into the carbon-coated copper grids and dried at room temperature.

3.1.1.5 X-ray diffraction (XRD)

In order to know the crystalline structure and the composition of the catalysts used in this work, XRD analyses were performed using a Philips X'Pert Diffractometer, available at the Analysis Center of the Department of Chemistry from UFSC. Copper radiation ($\lambda = 1.542$ Å), potential difference of 40 kV, current of 30 mA and scanning in the range from 10 to 70° (2θ) (geometry θ - 2θ e $\lambda = 1.54056$ Å). Samples did not require any previous preparation for analysis.

3.1.1.6 Elemental composition

Copper and iron concentration present in the CuO and FeOOH catalysts, respectively, were determined by atomic absorption spectrophotometry using an Agilent 240 FSAA spectrophotometer, available at the Laboratory of Energy and Environment of the Department of Chemical and Food Engineering from UFSC. CeO_2 was not evaluated due to the difficulty of atomization of the cerium metal by the flame atomic absorption technique. Therefore, the data was obtained by the manufacture supplier.

Samples were digested according to APHA (1995). A desired sample concentration was placed in a beaker with a solution of HNO_3 and HCl. Then, the beaker was placed on a hot plate and cautiously evaporated to less than 5 mL, making sure to not boil and dry. Additional acid was added until complete digestion, observed by the clear color of the solution. After measurements, the purity was determined by stoichiometric calculations.

3.1.2 1,4-DIOXANE TREATMENT BY ADVANCED OXIDATION PROCESSES

3.1.2.1 Catalytic peroxidation and catalytic photo peroxidation

For heterogeneous catalytic peroxidation experiments in the presence or absence of UV light, 800 mL of 1,4-dioxane (200 ppm) and the desired concentration of catalyst were placed into a 1000 mL double-jacket cylindrical reactor ($20 \pm 0.5°C$), Figure 5. The pH of the 1,4-dioxane solution was adjusted with NaOH 0,5 M and H_2SO_4 0,5 M solutions. Hydrogen peroxide (500 ppm) was immediately added and the suspension was stirred. For $UV/H_2O_2/CuO$ process, UV lamp (Osram - 80 W; nominal level of emission intensity 365-550 nm) was then switched on. Samples withdrawn at regular intervals were filtered through a PVDF membrane (Millipore; 0.22 μm pore size) for the analytical determination of the TOC, H_2O_2 concentration and Cu leached by atomic absorption technique. The molar ratio H_2O_2/TOC used in the experiments was 2.15, that is slightly higher than the stoichiometric value (2.0) (Melero et al., 2009).

Figure 5: Experimental apparatus for heterogeneous catalytic peroxidation reactions without UV light (1 – magnetic stirrer; 2- UV lamp; 3 – sample collector).
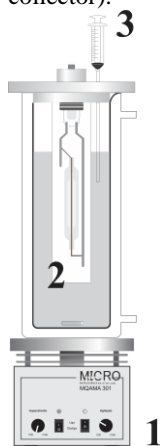
Source: Modified from Scaratti, 2014.

3.1.2.2 Catalytic ozonation

Ozonation experiments were carried out at 25 ± 1 °C in a 1.5 L glass-jacketed vessel (21 cm height and 8 cm diameter) continuously stirred (~500 rpm) with a magnetic stirrer (Dist – model DI-03) as shown in Figure 6. In a typical procedure, 1.5 L of a 200 ppm 1,4-dioxane aqueous solution was transferred into the reactor, the pH was adjusted to the desired value (10.0, 7.0, 5.5 or 3.0) using 0.5 M H_2SO_4 or 0.5 M NaOH solutions, and a specific catalyst dose (0, 100, 250, 500, 1000 or 3000 ppm) was added. Ozone was then continuously bubbled into the vessel through two air diffusers at a rate of 0.063 m^3 h^{-1}. Ozone was generated from the ambient air using an ozone generator (O_3R Philozon – model ID-5) coupled to an oxygen concentrator, available at the Laboratory of Energy and Environment of the Department of Chemical and Food Engineering from UFSC, with capacity for continuous generation of up to 0.5 kg h^{-1}. The reactor was operated in semi-batch mode for 6 h. Samples withdrawn at regular intervals (15 mL) were filtered through a PVDF membrane (Millipore; 0.22 μm pore size) for the analytical determination of the TOC, 1,4-dioxane concentration, aqueous ozone concentration $[O_3]$ and pH.

Figure 6: Experimental apparatus for catalytic and non-catalytic reactions (1 – oxygen concentrator; 2 – Ozone generator; 3 – Magnetic stirrer; 4 – air diffusers; 5 – Borosilicate glass reactor; 6 – Sample collector).
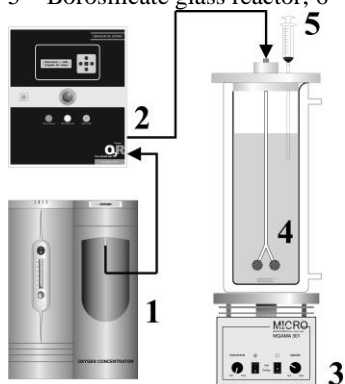
Source: Modified from Scaratti, 2014.

3.1.3 ANALYTICAL DETERMINATIONS

The analytical determinations performed in this work were: pH, total organic carbon (TOC), 1,4-dioxane concentration and intermediates identification. All the procedures were realized according to the methodologies described at Standard Methods (APHA, 1995).

3.1.3.1 pH

The pH values of the samples were determined by the potentiometric method using a pHmetro Q 400A (Quimis), previously calibrated with pH 4.0 and 7.0 buffer solutions.

3.1.3.2 Hydrogen peroxide concentration

Hydrogen peroxide concentration was quantified by titration method with Titanium (IV) oxysulfate solution (Sigma Aldrich) using UV-Vis measurements at 407 nm (POBINER, 1961).

3.1.3.3 Aqueous ozone concentration

Aqueous ozone concentration was evaluated in a spectrophotometer (HACH DR 500) by quantifying the absorbance at 258 nm by the Lambert-Beer law (Equation 10):

$$ABS = \varepsilon LC \hspace{4cm} (10)$$

where ε is the molar extinction coefficient equal to 2950 M^{-1} cm^{-1} at 258 nm (APHA, 1995), L is the optical path and C is the ozone concentration in the aqueous phase.

3.1.3.4 Total Organic Carbon

Total Organic Carbon (TOC) measurements were realized using a TOC-V_{CPH} analyzer (Shimadzu), equipped with an ASI-V automatic sampler, available at the Laboratory of Energy and Environment of the Department of Chemical and Food Engineering from UFSC. The analysis is done by the combustion catalytic oxidation method at 680 °C with a non-dispersive infrared detector.

3.1.3.5 1,4-Dioxane quantification and intermediates identification

Samples were collected and analyzed by gaseous chromatography with mass spectrometry detection (CG-MS) using a Shimadzu QP2010 plus, equipped with a Supel-Q PLOT column, available at the Laboratory of Energy and Environment of the Department of Chemical and Food Engineering from UFSC. 1,4-Dioxane was extracted according to the methodology proposed by Li et al., (2011). The column temperature was maintained at 150 °C during the analysis (total time was 4 min) and the injector and interface temperature was 200 °C. Samples (1 μL) were injected in split mode (1:18). Helium was used as the carrier gas. The quantification and confirmation ions were m/z 88 and m/z 58, respectively.

3.1.3.6 Acute toxicity

Acute toxicity tests were performed using a Microtox® equipment. *Vibrio fischeri* was purchased from BIOLUX® (Brazil). The methodology used was proposed by ISO 11348-3.

The lyophilized bacteria were rehydrated using reactivation buffer supplied by BIOLUX® and maintained at 4 ± 5 °C throughout the experiments. First reading of bacteria luminescence (I_0) was performed before add the samples to the cuvettes. After initial reading, each sample

was transferred to the cuvettes containing the bacteria and 30 min later the second luminescence reading was done (I_{30}).

Osmotic adjustment was performed with 22% of NaCl solution, for each 10 mL of samples, 100 μL of it was added. The method used consists of eight dilutions: 80%, 50%, 33.33%, 25%, 16.67%, 12.5%, 8.33% and 6.25%, which were performed with 2% of NaCl solution.

The pH of the samples was adjusted to 6-7 using solutions of NaOH and HCl, it is necessary because *Vibrio fischeri* does not support acidic and basic conditions.

3.2 CATALYST CHARACTERIZATION

Characterization of the catalysts are summarized in the Table 6 and shown in details below.

Table 6: Characterization of the catalysts used in this work.

	FeOOH	CeO$_2$	CuO
Point of zero charge	3,1	5,9	7,4
BET surface area (m^2 g^{-1})	58,6	19,0	12,6
Total pore volume (cm^3 g^{-1})	0,41	0,22	0,04
Average pore diameter (BJH) (nm)	16,0	2,3	3,6
Purity % (m m^{-1})	95,4%	99,9%*	100%
Crystallography analysis	Orthorhombic goethite structure	CeO$_2$ cubic phase with fluorite structure	CuO monoclinic phase
Particles size (nm)	12-84	20-30*	77-200
Particles morphology	Acicular	Irregular spherical	Irregular spherical

*Supplier data: CeO$_2$ purity and particle size were not measured due to the difficulty of cerium metal atomization by flame atomic absorption spectroscopy and because cerium oxide particles are agglomerate, making it impossible to measure isolated particles.

3.2.1 Zeta potential

Catalyst surface charge is very important in the degradation of organic pollutants by heterogeneous catalysts reactions. In solutions with pH value below to the pH of zero charge (pH_{pcz}), the surface of the particle is positively charged and above the pH_{pcz} is negatively charged (ILLÉS; TOMBÁCZ, 2006). Zeta potential values as a function of the solution pH are presented in Figure 7 for the three catalysts evaluated in this work.

The pH_{pcz} of synthetic goethite is approximately 9.0 (GABORIAUD; EHRHARDT, 2003; ZHANG; STANFORTH; PEHKONEN, 2007), while natural iron oxide has pH_{pcz} much lower, due to the adsorption of the anionic species such as CO_2 on the surface causing a reduction of the surface load (CORNELL; SCHWERTMANN, 2003). The pH_{pcz} obtained for the goethite selected for this research agrees with the literature, $pH_{pcz} = 3.1$, since it is a residue from acid mine drainage.

In general, the pH_{pcz} of cerium oxide can range from 5.8 to 7.6, depending on the synthesis method (BUETTNER, RINCIOG; MYLON, 2010). During the synthesis, it occurs the adsorption of cationic and/or anionic species on the surface that modify the net charge (NABAVI; SPALLA; CABANE, 1993). The pH_{pcz} value obtained for cerium oxide was 5.9.

The pH_{pcz} value obtained for CuO (7.9) agrees with Kosmulski (2004) and for Guedes et al., (2009), but it is more acid when compared with the pH_{pcz} value equal to 9.9 obtained by Li e Chang (2004).

Figure 7: Zeta potential values as a function of solution pH for FeOOH, CeO_2 and CuO.

Catalyst	pH_{pcz}
FeOOH	3,1
CeO_2	5,9
CuO	7,4
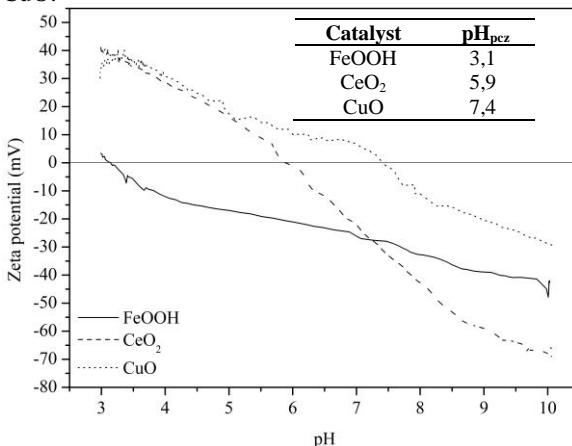
Source: Author's own elaboration

3.2.2 Specific surface area (BET) and porosity

The nitrogen adsorption/desorption isotherms of FeOOH, CeO_2 and CuO are shown in Figure 8. The isotherms for the three catalysts presented small significant hysteresis of type II, which correspond to non-porous surface (THOMMES et al., 2015), and they are typical for nanosized particles.

Figure 8: Nitrogen adsorption/desorption isotherms for FeOOH, CeO2 and CuO.
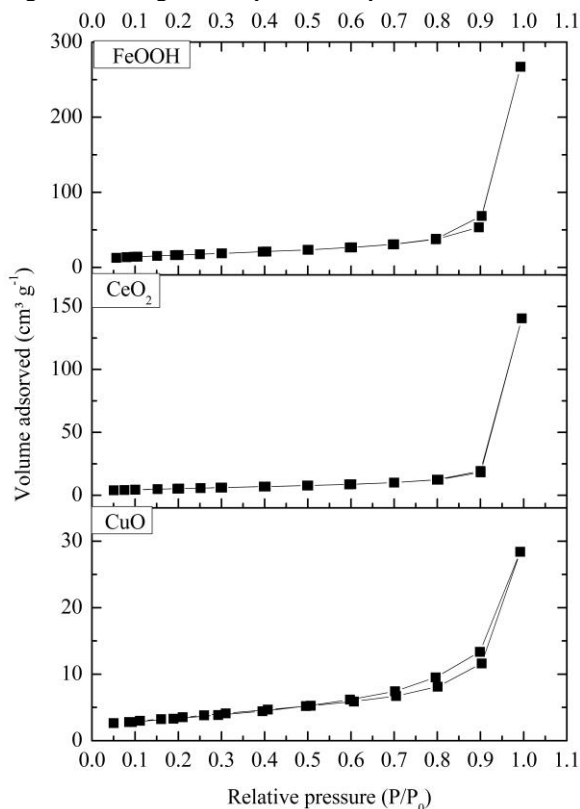
Source: Author's own elaboration

Specific surface area, total pore volume and average pore diameter obtained from the isotherms are presented in Table 6. BJH method was used to determine the average pore diameter, since this method is more suitable for pores distribution of microporous and mesoporous materials

with pore up to 50 nm (BARRET; JOYNER; HALENDA, 1951). As can be seen in table 6, the average of pore diameters of the catalysts is between 2 and 16 nm.

For specific surface area determinations, the BET method was used. FeOOH presented surface area 3 and 5 folds higher than CeO_2 and CuO, respectively. FeOOH also presented higher total pore volume, being 2 and 10 folds higher than CeO_2 and CuO, respectively.

3.2.3 Thermogravimetric analysis

In the Figure 9 are presented the graphs of the thermogravimetric analysis for CuO, CeO_2 and FeOOH.

Figure 9: Thermogravimetric analysis of FeOOH, CeO_2 e CuO.
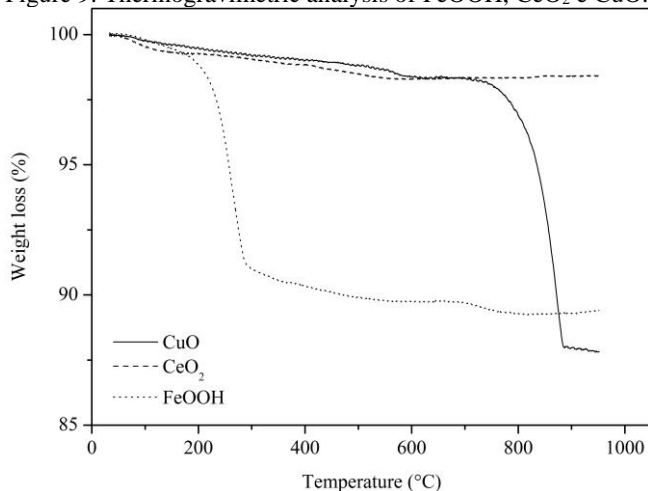
Source: Author's own elaboration

For FeOOH, the first mass loss of approximately 0.7% is observed from the ambient temperature up to 164.0 °C, resulted from the desorption of water bonded by hydrogen bonds (LIU et al., 2013). The second mass loss occurred between 214.2 °C and 295.0 °C, corresponding to 8.5%, associated to the structural loss of hydroxyl groups and transformation of goethite into hematite that occurs from 200 °C to 300 °C (CORNELL; SCHWERTMANN, 2003). The third weight loss (2.2%) was between 295 °C and 950 °C due to the decomposition of remaining structural hydroxyl groups and also by non-stoichiometric hydroxyl units (LIU et al., 2013). The theoretical mass loss during the transformation of the

goethite in hematite is 10.1%. The total weight loss in the last two stages corresponding to its transformation was 10.7%.

CeO_2 presented a mass loss of 1.67% over the entire temperature range, due to the loss of water on the surface of the catalyst and the decomposition of remaining hydroxyl groups. CuO showed an initial mass loss of 0.41% corresponding to water loss and a second mass loss equal to 10.34% due to the conversion of copper (II) oxide to copper (I) oxide at temperatures above 800 °C, which agrees with the theoretical mass loss of the thermal decomposition of CuO (Equation 11) (PATNAIK, 2003; CAO; CASENAS; PAN, 2006).

$$2CuO \xrightarrow{>800\ °C} Cu_2O + 1/2O_2 \hspace{3cm} (11)$$
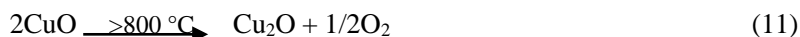
3.2.4 Morphology and size of the particles

The FESEM and TEM images for CuO, CeO_2 and FeOOH are presented in Figure 10. As can be observed, FeOOH (Figure 10a) presented acicular geometry with different diameters and lengths (ROUT et al., 2014), CeO_2 (Figure 10b) is an aggregate of nanoparticles and CuO (Figure 10c) predominates crystallites of irregular spherical shape (XU et al., 2017; RAJ; BIDU, 2017).

3.2.5 X-ray diffraction

X-ray diffractograms of FeOOH, CeO_2 and CuO are shown in Figure 11. FeOOH showed only peaks of FeOOH, $2\theta = 17.80°$, $21.22°$, $33.24°$, $34.70°$, $36.65°$, $39.98°$, $41.17°$, $50.61°$, $53.24°$ e $59.20°$, similar to those reported in the database (JCPDS 29-0713), characteristic of the crystalline phase of α-FeOOH with orthorhombic structure. CeO_2 diffractograms showed peaks at $28.60°$, $33.20°$, $47.6°$, $56.42°$ e $59.26°$ (JCPDS 34−0394), characteristic of the cubic phase of $CeO2$ with fluorite structure. The CuO diffractogram showed a series of peaks related to the monoclinic phase of copper (II) oxide $2\theta = 32.4°$, $35.6°$, $38.8°$, $48.9°$, $53.3°$, $58.2°$, $61.6°$, $66.3°$ e $67.9°$ (JCPDS 48-1548).

Figure 10: FESEM (left) and TEM (right) images: (a) FeOOH; (b) CeO_2; (c) CuO.
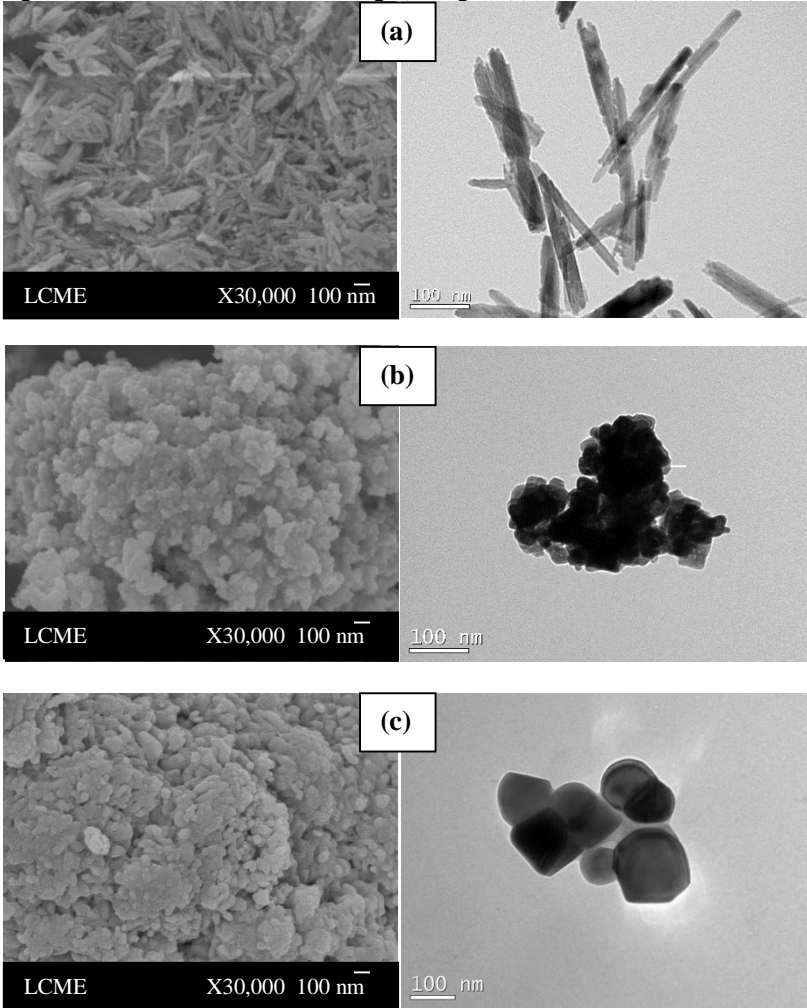
Source: Author's own elaboration

Figure 11: X-Ray diffractograms of FeOOH, CeO$_2$ and CuO.
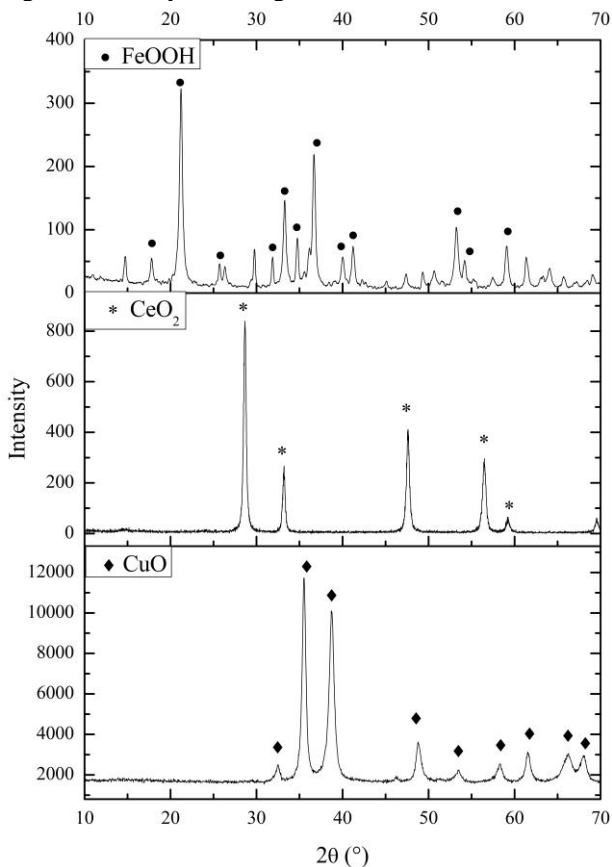
Source: Author's own elaboration

3.3 ADSORPTION KINETICS OF 1,4-DIOXANE OVER FeOOH, CeO$_2$ AND CuO

As can be seen in Figure 12, the catalysts selected for this work did not adsorb 1,4-dioxane at pH 7. The low adsorption capacity of 1,4-dioxane is due to the high solubility of this compound in water and low vapor pressure, which makes its adsorption treatment unfeasible (BARNDÕK et al., 2014). The pH values remained neutral during the six hours of adsorption in the presence of the catalysts.

Figure 12: Adsorption kinetics of 1,4-dioxane in the presence of CuO, CeO$_2$ and FeOOH (pH = 7.0 ± 0.5; T = 25.0 ± 1 °C; [catalyst] = 250 ppm; [1,4-dioxane] = 200 ppm).
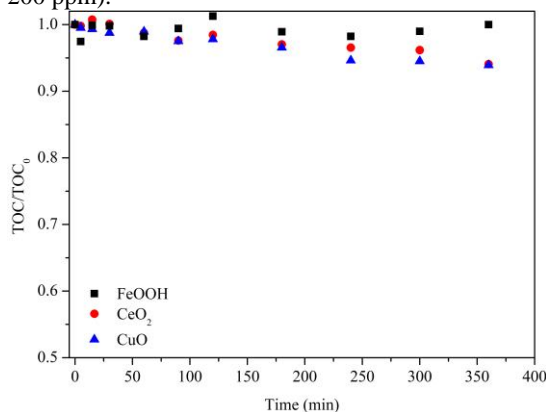
Source: Author's own elaboration

3.4 HETEROGENEOUS CATALYTIC PEROXIDATION

Catalytic peroxidation reactions using FeOOH, CeO$_2$ and CuO were analyzed in terms of TOC and H$_2$O$_2$ concentration, as we can see in Figure 13. FeOOH showed a negligible H$_2$O$_2$ decomposition rate. CeO$_2$ presented a pseudo-first order constant for H$_2$O$_2$ decomposition equal to 0.4×10^{-3} min^{-3} ($R^2 = 0.86$), however, TOC removal was similar to the adsorption kinetic and it is within the experimental standard deviation (item 4.3). Among the selected catalysts, CuO showed the higher pseudo-first order constant in terms of H$_2$O$_2$ decomposition, 2.0×10^{-3} min^{-1} ($R^2 = 0.92$). Although no 1,4-dioxane mineralization occurred in its presence, it was selected to proceed the study due to the higher catalytic activity at pH 7.

Figure 13: Kinetics of TOC removal (a) and H_2O_2 decomposition (b) during catalytic peroxidation reactions in the presence of CuO, CeO_2 and FeOOH. (pH = 7.0 ± 0.5; T = 25.0 ± 1 °C; [catalyst] = 250 ppm; [H_2O_2] = 500 ppm; [1,4-dioxane] = 200 ppm).
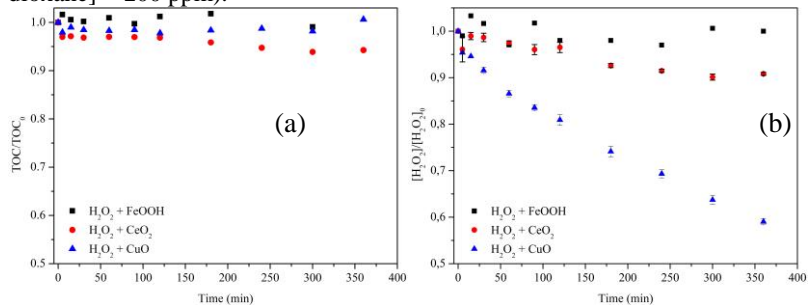
Source: Author's own elaboration

The effect of the pH on the reaction rate using CuO as catalyst was evaluated in the range 3<pH<9, at a constant solid dosage (2000 ppm) and 1,4-dioxane initial concentration (100 ppm) (Figure 14).

The amount of copper leached to the aqueous solution is neglected (Table 7) at different pH, so homogeneous reactions can be neglected. The H_2O_2 decomposition obeyed the pseudo-first order kinetic model and the kinetic parameter are shown in Table 7. The behavior shown in Figure 14b is in good agreement with the classical Haber-Weiss mechanism for H_2O_2 decomposition (WEISS, 1969). In solution with high acidity, H_2O_2 molecules dissociate on ·OH species via cleavage of the O-O bond on the catalytic surface and then take part in the chain reaction leading to the formation of water and oxygen. In neutral and basic solutions, however, H_2O_2 molecules can decompose directly to water and oxygen in accordance with Equation 12.

$$2H_2O_2 \rightarrow 2H_2O + O_2 \tag{12}$$

Despite the presence of CuO in the reaction has promoted the H_2O_2 decomposition, no 1,4-dioxane removal occurred, probably due to the low adsorption capacity for 1,4-dioxane and/or fast H_2O_2 decomposition.

On the other hand, under UV irradiation (Figure 15) and pH 7.0, the production of ·OH was initiated and 80% of mineralization was obtained in 6 h of reaction.

The kinetics of TOC removal and H_2O_2 decomposition are identical in the presence and absence of CuO, under UV light. This behavior indicates that the photochemical decomposition of H_2O_2 could

be the main responsible for the generation of ·OH and, therefore, mineralization of 1,4-dioxane. It is already known in the literature that 1,4-dioxane reacts rapidly with ·OH (k = 1.1 - 2.35x10^9 M^{-1} s^{-1}) (THOMAS, 1965; BARNDÕK et al., 2014). The presence of metals oxides besides promoting H_2O_2 decomposition in free radicals could also promote the non-radical mechanism, forming non-reactive species such as H_2O, O_2 (MCKEE, 1969) or H_2O, O_2 and OH^- (KANUNGO, 1979).

Figure 14: Kinetics of TOC removal (a) and H_2O_2 decomposition (b) during catalytic peroxidation reactions in the presence of CuO at different pH values (T = 25.0 ± 1 °C; [catalyst] = 2000 ppm; [H_2O_2] = 500 ppm; [1,4-dioxane] = 100 ppm).
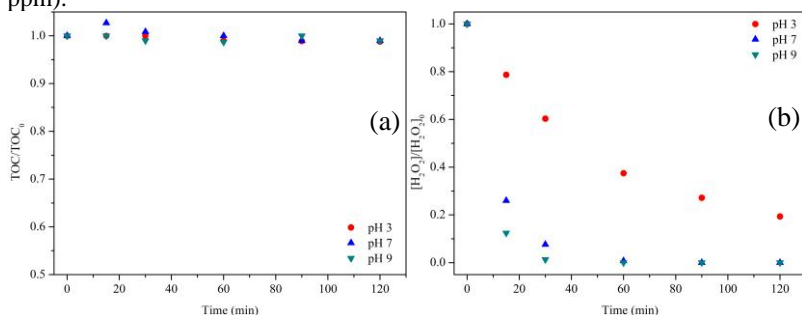
Source: Author's own elaboration

Table 7: Pseudo-first order rate constants in terms of H_2O_2 decomposition (k_{H2O2}) and copper ions leached after 120 min of reaction at different pH values in the presence of CuO.

pH	k_{H2O2} (min^{-1})	R^2	Cu leached (%)
3	16.4x10^{-3}	0.99	0.084±0.039
7	82.8x10^{-3}	0.99	0.034±0.005
9	143.4x10^{-3}	0.99	0.033±0.004

Based on the results presented above, it was demonstrated that the 1,4-dioxane mineralization occurs by radical mechanism under UV irradiation. In the presence of UV light, H_2O_2 is decomposed into ·OH, which reacts rapidly with 1,4-dioxane (COLEMAN et al., 2007), according to Equations 13-14. When radical production is low or catalytic activity follows the non-radical mechanism, the mineralization of 1,4-dioxane is negligible.

$$H_2O_2 + hv \rightarrow 2HO^· \tag{13}$$
$$C_4H_8O_2 + HO^· \rightarrow CO_2 + H_2O \tag{14}$$

Figure 15: Kinetics of TOC removal (a) and H_2O_2 decomposition (b) in the presence and absence of UV light (pH = 7.0 ± 0.5; T = 25.0 ± 1 °C; [catalyst] = 250 ppm; [H_2O_2] = 500 ppm; [1,4-dioxane] = 200 ppm).
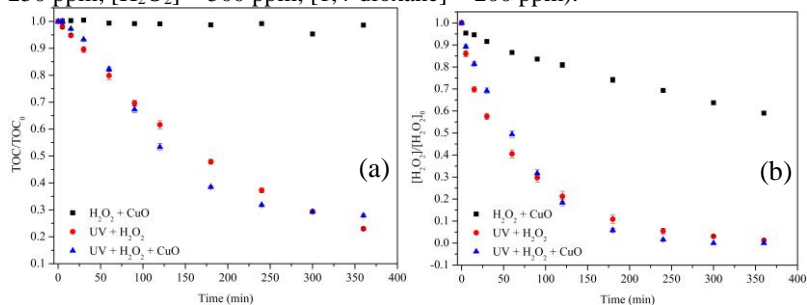
Source: Author's own elaboration

3.5 HETEROGENEOUS CATALYTIC OZONATION

Catalytic ozonation experiments were performed with the purpose of selecting the best catalyst in terms of TOC removal and aqueous O_3 concentration. As we can see in Figure 16, catalysts showed the same behavior for TOC removal and ozone decomposition, following an order of $CuO>CeO_2>FeOOH$.

Results presented in the item 4.3 showed that the interaction between the catalysts and 1,4-dioxane is negligible. Therefore, the process efficiency will be determined by the interaction between ozone and the catalyst. In the presence of catalyst, aqueous ozone concentration (Figure 16(b)) is lower than in the absence, indicating that catalyst addition increases aqueous ozone decomposition into free radicals that reacts with 1,4-dioxane faster than ozone molecules.

The rigorous control of pH is very important for ozonation reactions (Figure 16(c)), because at basic and acid pH values, the indirect reactions and direct reaction are predominant, respectively (NAWROCKI, 2013). In addition, the pH of the solution directly influences the formation of hydroxyl groups on the surface of the catalyst. When pH > pH_{pzc}, the surface of the catalyst is negatively charged and the Lewis acid sites are responsible for ozone decomposition. At pH < $pH_{pzc,}$ the surface is positively charged, and the Bronsted acid sites may be responsible for ozone decomposition and hydroxyl radical formation (IKHLAQ; BROWN; KASPRZYK-HORDERN, 2012).

In this work, CuO showed the highest ozone decomposition and 1,4-dioxane mineralization at pH 7. The pH values during catalytic ozonation in the presence of CuO was kept between 6-7, probably the pH

values of the formed byproducts are in this range, different from the reactions in the presence of FeOOH, CeO₂ and in the absence of the catalyst. According to Huang et al., (2015), neutral surfaces followed by protonated surfaces are more active than deprotonated surfaces in the decomposition of ozone in free radicals, justifying the catalytic activity of the catalysts tested, since CuO and CeO₂ presented neutral and protonated surfaces during the 6 hours of reaction, while FeOOH remained deprotonated (Figure 16(c)).

Figure 16: Kinetic of 1,4-dioxane mineralization (a) aqueous ozone concentration (b) pH values during the catalytic ozonation reactions in the presence of FeOOH, CuO and CeO₂ (pH = 7.0 ± 0.5; T = 25.0 ± 1 °C; ozone flow=0.063 m³ h⁻¹; [catalyst] = 250 ppm; [1,4-dioxane] = 200 ppm).
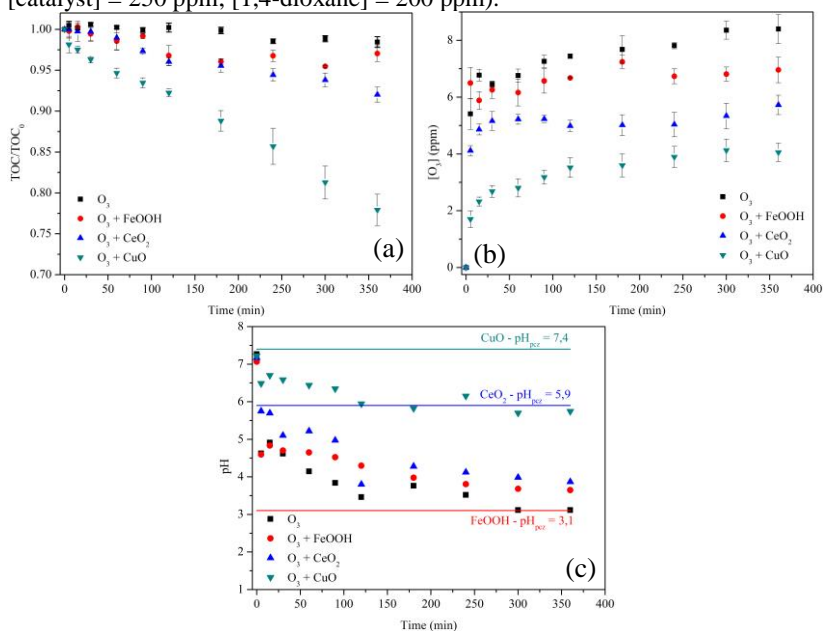
Source: Author's own elaboration

It has been demonstrated by Zhao et al., (2009) that the reactions of catalytic ozonation obey the models of kinetics of pseudo-first order or second order. In this work, 1,4-dioxane mineralization by catalytic ozonation in the presence of FeOOH, CeO₂ or CuO were adjusted by pseudo-first order model (Figure 17), data is presented in Table 8.

The pseudo-first order constants obtained were 3.52, 6.11 and 17.87 times highest than the reaction without catalyst for FeOOH, CeO₂

or CuO, respectively. Analyzing BET surface area values obtained for the catalysts evaluated (Table 6), it is concluded that the increase of the reaction rate k is not related to the BET area. The highest catalytic activity for 1,4-dioxane mineralization was obtained using CuO, of the three catalysts studied, which has the lowest BET area.

As mentioned before, CuO showed the best results. According to Hu et al., (2016) and Raj et al., (2017), copper oxide has been used as catalyst in the catalytic ozonation due to its high stability and high density of hydroxyl groups on its surface, increasing the rate of organic pollutants degradation in the bulk when compared to the non-catalytic ozonation.

Figure 17: Pseudo-first order adjustments for 1,4-dioxane mineralization kinetics using FeOOH, CeO_2 and CuO as catalysts (pH = 7.0 ± 0.5; T = 25.0 ± 1 °C; Ozone flow = 0.063 m³ h⁻¹; [catalyst] = 250 ppm; [1,4-dioxane] = 200 ppm).
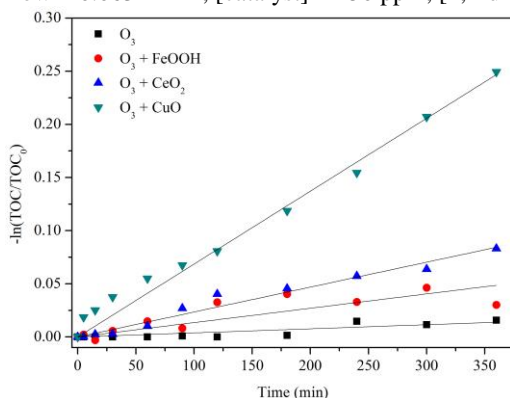
Source: Author's own elaboration

Table 8: Pseudo-first order constants (k_m) of 14-dioxane mineralization for catalytic ozonation and non-catalytic ozonation.

	k_m x 10^5 (min⁻¹)	Standard error x 10^5	R^2
O_3	3,84	0,54	0,82
O_3 + FeOOH	13,51	1,71	0,85
O_3 + CeO_2	23,45	0,91	0,98
O_3 + CuO	68,56	1,81	0,99

A detailed study using CuO as catalyst was performed and the results were published and are presented in the chapter 5 of this doctorate thesis.

TREATMENT OF 1,4-DIOXANE BY OZONATION AND CATALYTIC OZONATION WITH COPPER OXIDE

This chapter is based on the paper entitled "Treatment of Aqueous Solutions of 1,4-dioxane by Ozonation and Catalytic Ozonation with Copper Oxide (CuO)" (Environmental Technology), by Gidiane Scaratti, Alex Basso, Richard Landers, Pedro J. J. Alvarez, Gianluca Li Puma and Regina de Fátima Peralta Muniz Moreira. Abstract, keywords, introduction, acknowledgments and references were omitted, some minor amendments were performed, but the procedures, results and conclusions reported in the original paper were not modified.

4.1 MATERIALS AND METHODS

4.1.1 Chemicals and materials

All reagents used were analytical grade and solutions were prepared with deionized water. 1,4-Dioxane (99.99%) was supplied by Neon (Brazil). Commercial copper oxide (99% of purity) was purchased from Amorphous and Nanostructures Materials Inc. (Houston, TX, USA). Sodium dihydrogen phosphate (NaH_2PO_4) was purchased from Vetec (Brazil), 1,4-benzoquinone ($C_6H_4O_2$) from Sigma Aldrich (USA), salicylic acid ($C_7H_6O_3$) from Reagen (Brazil) and sodium fluoride (NaF) from Synth (Brazil).

4.1.2 Characterization of the catalyst

The morphology of the CuO particles was determined by transmission electron microscopy (TEM) (JEOL, JEM-1011). The crystalline phases in the samples were determined by X-ray diffraction (XRD) on a Bruker D2-Phaser diffractometer with CuKα radiation (λ=1.54056 Å), from 10º to 70º.

The specific surface area (S_{BET}) and pore diameter distribution of the CuO, according to the Barret-Joyner-Halenda (BJH) method, were determined by N_2 adsorption-desorption experiments. Analysis was carried out by means of isotherms obtained on an Autosorb 1C (Quantachrome, USA) adsorptometer. Prior to the analysis, the samples were degassed for 12 h at 140 ºC under vacuum.

The zeta potential (ξ) of aqueous suspensions of CuO (0.5 g of CuO in 50 mL of deionized water) as a function of pH (from 3 to 10) was

measured using a Stabino NANO-flex particle. The zeta potential was determined from the electrophoretic mobility (μ) based on the Smoluchowski equation. NaOH and HCl (0.01 N solutions) were used as titration media to automatically adjust the pH values.

The Cu content of the catalysts was determined using atomic absorption spectroscopy (AAS). In this procedure, 1.0 mg of the catalyst was solubilized in 20 mL of concentrated HNO_3 and HCl solution and evaporated to less than 5 mL (APHA, 1995). After solubilization, the samples were transferred to volumetric flasks. The volume was adjusted to 50 mL with distilled water and analyzed via AAS with an Agilent 240FSAA spectrometer.

Fourier transform infrared (FTIR) spectra of CuO before use and after 5 treatment cycles were recorded between 400 and 4000 cm^{-1} using an FTIR spectrometer (Agilent Technologies – Cary 600 Series).

The X-ray photoelectron spectroscopy (XPS) spectra were obtained with a VSW HA-100 spherical analyzer and MgKα radiation (hν = 1253.6 eV). The high-resolution spectra were measured with constant analyzer pass energies of 44eV. The pressure during the measurements was always less than 2×10^{-8} mbar. The sample was fixed to a stainless steel sample holder with double-faced conducting tape and analyzed without further preparation. Surface charge was corrected, shifting all spectra so that the C1s line associated with adventitious carbon was at 284.6 eV. Curve fitting was performed using Gaussian line shapes and a Shirley background was subtracted from the data.

4.1.3 Ozonation and catalytic ozonation experiments

Ozonation experiments were carried out isothermally at 25 °C in a 1.5 L glass-jacketed vessel (21 cm height and 8 cm diameter) continuously stirred (~500 rpm) with a magnetic stirrer (Dist – model DI-03). In a typical procedure, 1.5 L of a 200 ppm 1,4-dioxane aqueous solution was transferred into the reactor, the pH was adjusted to the desired level using 0.5 M H_2SO_4 or 0.5 M NaOH solutions, and a specific catalyst dose (when used) was added. Ozone was then continuously bubbled into the vessel through two air diffusers at a rate of 0.063 m^3 h^{-1}. The reactor was operated in semi-batch mode for 6 h. Samples withdrawn at regular intervals were filtered through a PVDF membrane (Millipore; 0.22 μm pore size) for the analytical determination of the TOC, 1,4-dioxane concentration [1,4-dioxane], aqueous ozone concentration [O_3], pH and acute toxicity.

In previous tests performed to select a suitable catalyst, involving a comparison of the TOC removal and ozone decomposition rate obtained using different non-noble metals (goethite, cerium oxide or copper oxide), copper oxide resulted in the highest catalytic activity (CENTURIÃO et al., 2018; SCARATTI, 2017).

4.1.4 Ozone decomposition experiments

The same reactor described above was used to determine the rate of ozone decomposition. The experiments were carried out using 1.5 L of deionized water in the absence of catalyst and in the presence of the CuO catalyst at 0.1 ppm, 0.25 ppm or 0.5 ppm. Ozone was then continuously bubbled into the reactor at a rate of 0.063 $m^3 h^{-1}$, at 25 ± 1 °C and at pH 10, 7.0, 5.5 or 3.0. Samples collected at appropriate intervals over a period of 40 min were rapidly filtered through a PVDF membrane (Millipore; 0.22 μm pore size). The residual aqueous ozone concentration (C) was evaluated in a spectrophotometer (HACH DR 5000) by quantifying the absorbance at 258 nm by the Lambert-Beer law (Eq. 15).

$$ABS = \varepsilon LC \tag{15}$$

where ε is the molar extinction coefficient equal to 2950 $M^{-1} cm^{-1}$ at 258 nm (APHA, 1995), L is the optical path and C is the ozone concentration in the aqueous phase.

The theoretical aqueous ozone concentration was calculated through the liquid phase mass balance (Eq. 16):

$$\frac{dC_{O_3}}{dt} = k_{L_a}\left(C_{sat} - C_{O_3}\right) - k_T C_{O_3} \tag{16}$$

$$k_T = k_d + w k_{het} \tag{17}$$

where C_{sat} is the saturated ozone concentration, C_{O3} the aqueous ozone concentration, k_L the volumetric mass transfer coefficient, k_T the ozone decomposition rate constant, k_d the ozone self-decomposition constant, w the catalyst dosage and k_{het} the catalytic ozone decomposition constant. The right-hand side of Eq. 2 reduces to a pseudo-first-order rate law under an excess of ozone in the reactor.

The ozone self-decomposition constant (k_d) was obtained through the correlation proposed by Sullivan and Roth (1979) (Eq. 18).

$$k_d = 9.811 \cdot 10^7 [OH^-]^{0.123} \exp\left(\frac{-5606}{T}\right) \tag{18}$$

where $[OH^-]$ is the OH^- concentration and T is the temperature in Kelvin.

4.1.5 Catalyst reuse

The catalyst was reused in selected experiments to assess its stability over multiple cycles. At the end of each cycle, the catalyst was separated by membrane filtration (Millipore; 0.22 µm pore size). The solids were dried at 60 ± 1 °C for 15 h and reused for the subsequent cycle without any further purification.

4.1.6 Analytical methods

The pH was determined by the potentiometric method using a pH meter (Quimis, Model Q400A), previously calibrated with pH 4.0 and 7.0 buffer solutions. The concentration of leached copper ion in the liquid phase after the heterogeneous catalytic ozonation reactions was measured using AAS.

The aqueous ozone concentration during the experiments was analyzed as described in section 2.4 and the TOC was determined on a TOC-V$_{CPH}$ analyzer (Shimadzu).

The 1,4-dioxane was extracted according to the methodology proposed by Li and collaborators (LI et al., 2011) and quantified using a CG-MS instrument (Shimadzu QP2010 plus) equipped with a Supel-Q PLOT column. The column temperature was maintained at 150 °C during the analysis (total time was 4 min) and the injector and interface temperature was 200 °C. Samples (1 µL) were injected in split mode (1:18). Helium was used as the carrier gas. The quantification and confirmation ions were m/z 88 and m/z 58, respectively.

The 1,4-dioxane and TOC degradation rate constants (k_1) were obtained according to the pseudo-first-order rate laws (Eq. 19) together with the material balance of the batch reactor, which was operated under an excess of ozone (continuous bubbling).

$$-\ln\left(\frac{C}{C_0}\right) = k_1 t \tag{19}$$

where C_0 and C are the initial concentration and the concentration after the catalytic ozonation process at various time intervals, respectively, k_1 is either the 1,4-dioxane or TOC degradation pseudo-first-order rate constant (min^{-1}) and t is the reaction time. The first-order rate constant (k_1) was determined by the slope of the straight line fitting of $-ln(C/C_0)$ versus time.

The acute toxicity test with the bioluminescent bacteria *Vibrio fischeri* (lyophilized) was performed according to the methodology proposed by ISO 11348-3.

4.2 RESULTS AND DISCUSSION

4.2.1 Catalyst characterization

The morphology of the CuO powder is shown in the TEM images in Figure 18. The CuO particles had irregular spherical shapes with different diameters and were well distributed without aggregation (XU et al., 2017; RAJ; BIJU, 2017). The XRD pattern for CuO, with lattice planes of vibration, can be seen in Figure 18b (JCPDS 48-1548). The XRD analysis showed a series of diffraction peaks at $2\theta = 32.4°$, $35.6°$, $38.8°$, $48.9°$, $53.3°$, $58.2°$, $61.6°$, $66.3°$ and $67.9°$ characteristic of the monoclinic phase of copper (II) oxide (ANANTH et al., 2015).

Figure 18: (a) TEM images of CuO and (b) XRD of CuO.
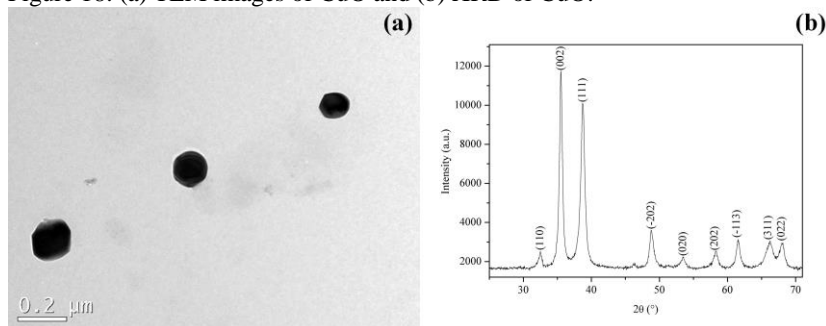
Source: Author's own elaboration

The results for the main parameters used to characterize the CuO particles are shown in Table 9. High purity and low surface area are notable features of the catalyst used in this study.

Table 9: Characterization of CuO particles.

Particle Size, nm	77 - 200.
Purity, %	100%
Point of zero charge	7.41
BET surface area, m^2/g	12.61
Pore size diameter, nm	3.6 nm
Total pore volume, cm^{3}g^{-1}	0.044

The oxidation state of the CuO before and after the catalytic ozonation of 1,4-dioxane was investigated by XPS (Figure 19). The O1s spectra for the CuO after and before catalytic ozonation can be seen in Figures 19a and 19b, respectively. The peaks at 528.97-529.21 eV were attributed to lattice oxygen and the peaks at 530.76-531.10 eV were assigned to O-C, as well as to the oxygen adsorbed at the surface (LUPAN et al., 2016; ZHOU et al., 2013). The smallest peak, observed only for the sample before catalytic ozonation at 533.17 eV, was assigned to O-H and/or to oxygen adsorbed at the surface (LUPAN et al., 2016; SHEN et al., 2015).

Figures 19c and 19d show the two doublets Cu-2p$_{3/2}$ and Cu-2p$_{1/2}$, presenting energetic differences of 20 eV, in good agreement with data published in the literature (SHEN et al., 2015). In general, copper oxide can exist in two phases, cupric oxide (CuO) and cuprous oxide (Cu$_2$O). The peaks at 934.2 eV and 954.2 eV are attributed to CuO (Cu^{2+}). However, the peaks at 932.2 eV and 952.2 eV are attributed to Cu$_2$O (Cu$^+$), indicating the presence of Cu$_2$O on the solid surface of the sample caused by redox reactions on the solid surface (HUANG et al., 2018). The satellite peaks in the spectra (941.7 eV, 943.05 eV and 961.7 eV) are associated with the presence of Cu(II) (CuO) (ZHOU et al., 2013; SHEN et al., 2015). Since no Cu$_2$O diffractions peaks were detected in the XRD pattern (Fig. 18b), this is restricted to the surface.

For the CuO sample after catalytic ozonation the peaks at 934.2 eV and 954.2 eV shifted to lower binding energy when compared to the sample before the reaction, which means that more Cu$^+$ was present on the CuO surface after ozonation.

Figure 19: XPS spectra: (a, c) CuO before catalytic ozonation and (b, d) CuO after catalytic ozonation (ozone flow = 0.064 m³ h⁻¹; T = 25 ± 1 °C).
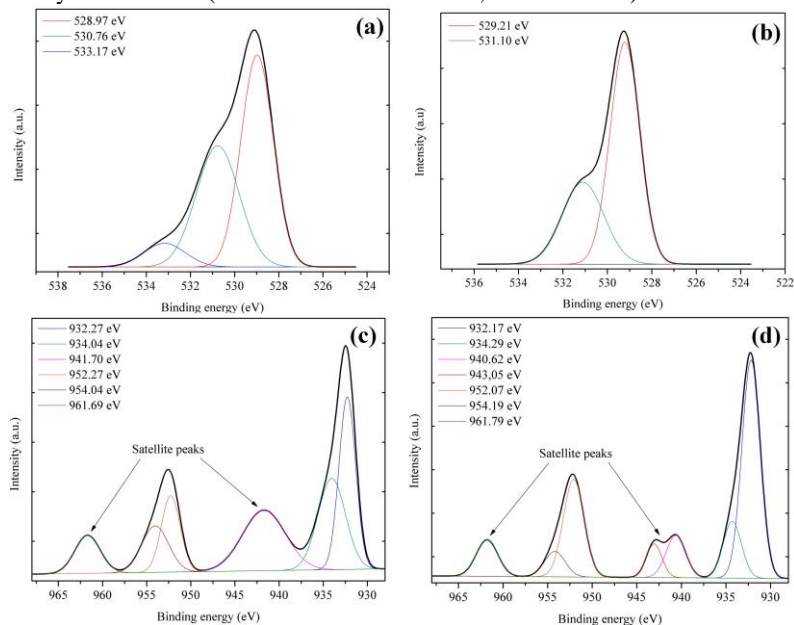
Source: Author's own elaboration

4.2.2 Catalytic decomposition of ozone

The impact of CuO on the absorption and decomposition of ozone was determined at different pH values and using different catalyst dosages at pH 5.5 (Figure 20). Table 10 shows the k_d, C_e and k_{het} values, determined by fitting Eq. 16 to the experimental results. The values of k_{La} (0.475±0.036 min⁻¹) and C_{sat} (10.264±1.063 ppm) were constant and dependent only on the reaction temperature (25 °C) and the mixing conditions in the reactor. The residual concentration of ozone at equilibrium (C_e) showed a small decrease as the pH increased, in the absence of catalyst, since ozone was continuously supplied into the system. In contrast, the ozone decomposition constant (k_d) rapidly increased above pH 7 due to the decomposition of O_3 molecules to ˙OH radicals (BELTRÁN, 2004). The catalytic ozone decomposition constant (k_{het}) decreased slightly as the catalyst dose was increased, remaining close to the average value of 1.268±0.018. The mechanism of heterogeneous catalytic ozone decomposition, as proposed by Beltrán et al. (2004), is described in Eqs. 20-23.

$$OH^- + S \leftrightarrow OH \cdot S \tag{20}$$
$$O_3 + OH \cdot S \leftrightarrow O_3 \cdot S + HO \tag{21}$$
$$O_3 \cdot S \leftrightarrow O \cdot S + O_2 \tag{22}$$
$$O_3 + O \cdot S \leftrightarrow O_2 + S + O_2 \tag{23}$$

where S is the catalyst surface. The above reactions are the steps involved in the surface chemical reaction involving adsorption, surface reaction and desorption processes.

Figure 20: Effect of (a) pH and (b) catalyst dosage at pH 5.5 on the ozone absorption and catalytic ozone decomposition (pH = 5.5; ozone flow = 0.064 m³ h⁻¹; T = 25 ± 1 °C).
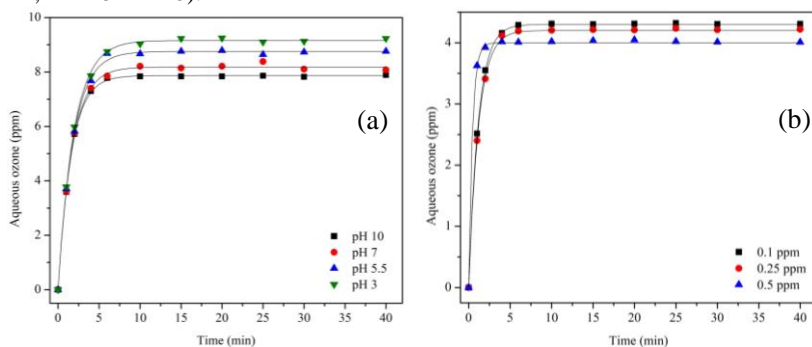
Source: Author's own elaboration

Table 10: The k_d, Ce and k_{het} values for deionized water ozonation at different pH values and catalyst dosages ($k_La = 0.475\pm0.036$ min⁻¹ and $C_{sat} = 10.264\pm1.063$ ppm) (ozone flow rate = 0.064 m³ h⁻¹; T = 25 ± 1 °C).

CuO dosage/pH	k_d (min⁻¹)	C_e (ppm)	k_{het} (min⁻¹)
0 ppm/10.0	0.21	7.87±0.03	-
0 ppm/7.0	0.09	8.18±0.16	-
0 ppm/5.5	0.06	8.75±0.06	-
0 ppm/3.0	0.03	9.16±0.17	-
0.1 ppm/5.5	0.06	4.31±0.01	1.34±0.01
0.25 ppm/5.5	0.06	4.21±0.01	1.26±0.02
0.5 ppm/5.5	0.06	4.02±0.01	1.20±0.02

4.2.3 Degradation and mineralization of 1,4-dioxane by ozone in the absence of catalyst

The chromatographic analysis showed that 1,4-dioxane could be efficiently removed from the water with ozone alone under alkaline

conditions (Figure 21). In contrast, at pH ≤ 7 the rate of degradation was very low. No mineralization was observed under acidic or basic pH, since the pH rapidly decreased during the reaction (Figure 22).

Lower pH values do not favor the decomposition of O_3 to ˙OH, which has a much greater reactivity with 1,4-dioxane than O_3 (KWON et al., 2012; SUH; MOHSENI, 2004). This chain mechanism of ˙OH production is initiated by hydroxide anions at higher pH values, where the reaction proceeds through the conversion of ˙O_3^- to ˙OH (BARNDÕK et al., 2014). The lower reactivity of 1,4-dioxane with molecular O_3 at pH ≤ 7 results from the absence of significantly electron-rich sites in the molecular structure of 1,4-dioxane.

Figure 21: Kinetics of 1,4-dioxane removal at different pH values ([1,4-dioxane] = 200 ppm; ozone flow = 0.064 m³ h⁻¹; T = 25 ± 1 °C).
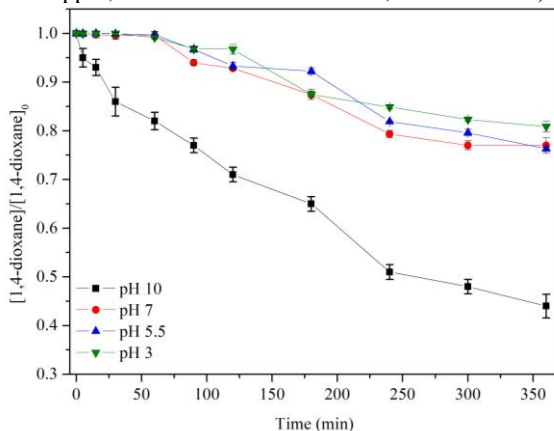
Source: Author's own elaboration

The pseudo-first-order kinetics constant was obtained from Eq. 19, since the reactor was operated under an excess of ozone. The rate constants of 1,4-dioxane removal (k_1) at pH 3.0, 5.5 and 7.0 were quite similar (0.00061 ± 0.00007 min⁻¹, 0.00071 ± 0.00007 min⁻¹, 0.00065 ± 0.00004 min⁻¹ respectively). In contrast, at pH 10 a significantly higher value was reached (0.00249 ± 0.00008 min⁻¹). Barndõk and collaborators (2014) determined significantly higher pseudo-first-order rate constants for 1,4-dioxane degradation, under an excess of ozone, at pH 7.0 and 10.0 (1.2 min⁻¹ and 30 min⁻¹, respectively). The faster kinetics may have resulted from the use of constant pH throughout the experiment and a significantly higher ozone flow rate (0.24 m³ h⁻¹).

However, the rate constants for the decomposition of ozone over the CuO catalyst (k_{het}, Table 10) were at least 3 orders of magnitude higher than that for the reaction of ozone with 1,4-dioxane at pH 5.5 (0.00071 ± 0.00007 min^{-1}). As a consequence, in the presence of CuO, the degradation of 1,4-dioxane by direct ozonation alone is slow in comparison to the reaction between 1,4-dioxane and the free radicals produced by the ozone decomposition on the solid surface at pH 5.5.

4.2.4 Catalyzed ozonation of 1,4-dioxane with CuO

In heterogeneous catalytic ozonation, the role of the pH involves multiple aspects, including the decomposition of the ozone molecules, the surface properties of the catalyst and the charge of ionizable organic molecules, which in turn affects the production of ROS and the degradation rate of water contaminants (CHEN et al., 2016; HUANG et al., 2015). The effect of the initial pH on 1,4-dioxane degradation and mineralization under catalytic ozonation was investigated using 250 ppm of CuO. The results in Figures 22a and 22b show that the rate of TOC and 1,4-dioxane removal increased slightly as the pH increased and the rate of degradation was considerably higher at pH 10. The relatively small impact of the initial pH observed in these unbuffered experiments can be attributed to the relatively fast decrease in the pH, which reached a plateau at similar pH values (around 5 to 6) (Figure 22c).

Figure 22: (a) TOC removal, (b) 1,4-dioxane removal and (c) pH values during 1,4-dioxane treatment by catalytic ozonation at different initial pH values ([1,4-dioxane] = 200 ppm; ozone flow = 0.064 m³ h^{-1}; T = 25 ± 1 °C; [catalyst] = 250 ppm).
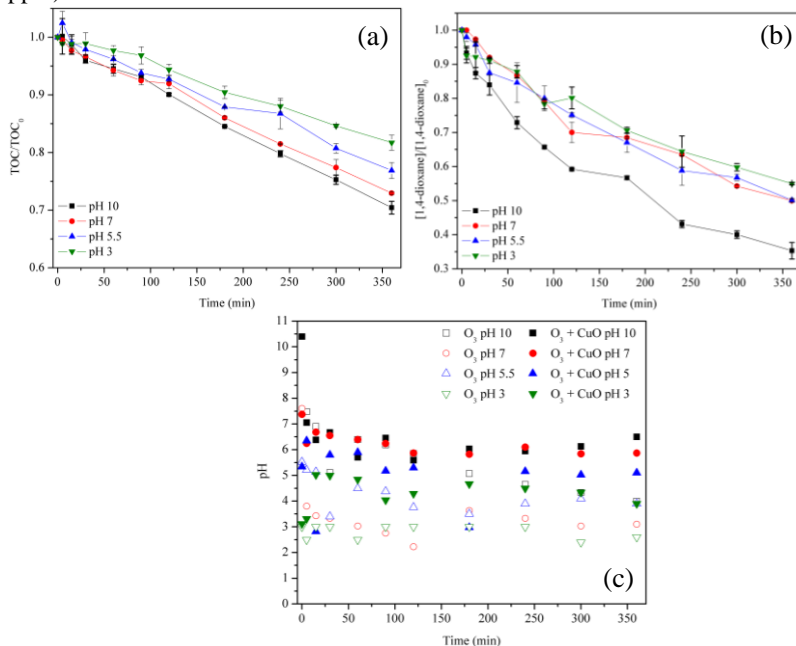
Source: Author's own elaboration

The concentration profiles for ozone in the aqueous phase observed during the experimental runs can be seen in Figure 23a. The concentration of ozone in the absence and in the presence of CuO rapidly increased during the initial stage of the reaction, reaching equilibrium concentrations (C_e) approaching the saturation values, observed in the absence of 1,4-dioxane at the temperature of the experiments (Table 10). These results demonstrate that the gas-liquid ozonation reactions occurred through a relatively slow kinetic regime (small Hatta numbers) (LAN; NIGMATULLIN; LI PUMA, 2008).

Figure 23: (a) Aqueous ozone concentration in the absence and presence of CuO, (b) pseudo-first order constants for 1,4-dioxane and (c) pseudo-first-order constants for TOC at different initial pH values during 1,4-dioxane catalytic ozonation ([CuO] = 250 ppm; [1,4-dioxane] = 200 ppm; ozone flow = 0.064 m³ h⁻¹; T = 25 ± 1 °C; t = 360 min).
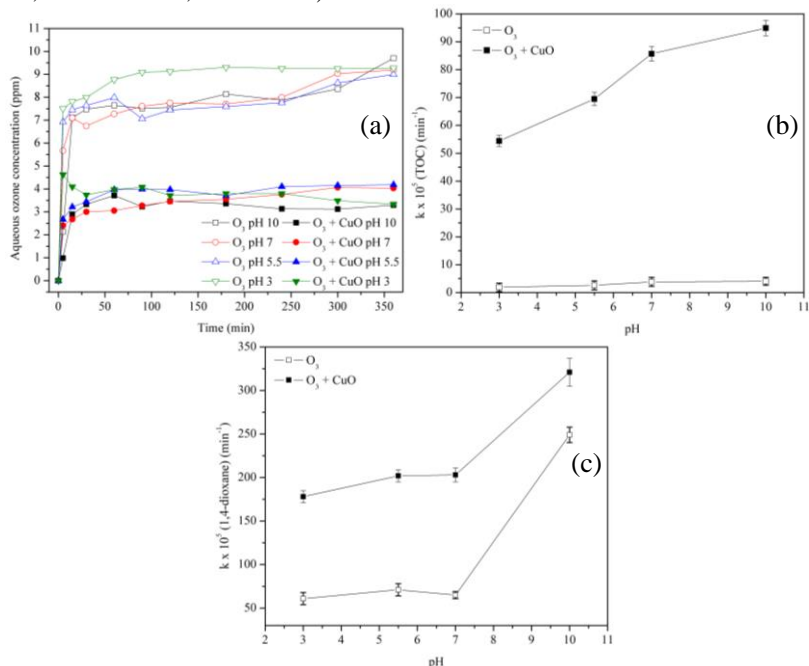
Source: Author's own elaboration

The pseudo-first-order rate constants of ozonation and CuO catalytic ozonation of 1,4-dioxane as a function of pH are shown in Figures 23b (mineralization) and 23c (degradation). The k_1 value for catalytic ozonation at pH 7, with 250 ppm of CuO, increased by factors of 22.3 and 3.12 for TOC and 1,4-dioxane removal, respectively, in comparison to ozonation. The increase in the TOC removal with an initial pH of 10 is not significant, especially in the absence of CuO, due to the decrease in the pH during the reactions. It is known that the ozone decomposition with the formation of hydroxyl radicals is greatly enhanced under highly alkaline conditions (ZHANG; LI; CROUÉ, 2012). However, the pH decreased during the reaction and reached a value of 4 after 6 h. The k_1 value at pH 3 increased by factors of 28.63 and 2.91 for TOC and 1,4-dioxane removal, respectively in comparison to ozonation.

It is expected that homogeneous catalytic ozonation also could occur due to leaching of copper ions, that increased from 0.1%, 0.3% to 4.9% at the initial pH of 7.0, 5.5 and 3.0, respectively. Although the homogeneous catalytic ozonation cannot be neglected at the initial pH 3 due to copper leaching as Cu^{2+} ions, at pH circumneutral the main reactions responsible to 1,4-dioxane degradation occur as a heterogeneous catalytic process. Conversely, a significant impact on the rate of TOC and 1,4-dioxane removal (Figure 24) was observed as the concentration of CuO was increased from 100 to 3000 ppm, at neutral pH.

Figure 24: (a) TOC removal and (b) 1,4-dioxane removal at different catalyst dosages ([1,4-dioxane] = 200 ppm; pH = 7.0±0.5; ozone flow = 0.064 m³ h⁻¹; T = 25 ± 1 °C).
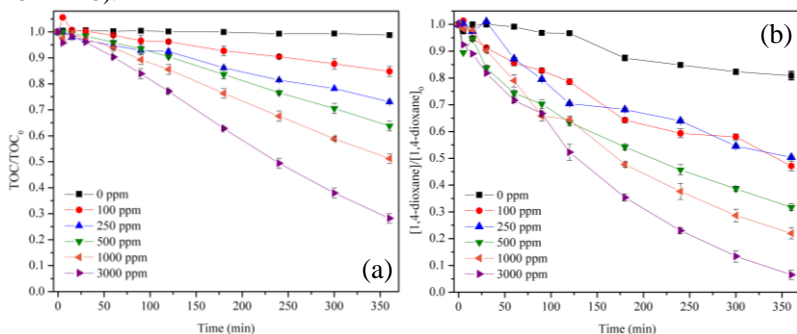
Source: Author's own elaboration

The pseudo-first-order kinetics constants at different catalyst concentrations are reported in Figure 26b. It can be observed that the rate constants (k_1) increased by factors of 81.25 and 10.35 for TOC and 1,4-dioxane removal, respectively, at pH 7 with 3000 ppm of CuO. These values suggest that 1,4-dioxane and TOC removal are strongly dependent on the amount of catalyst used, in agreement with results reported in the literature for other target water contaminants (AHMADI et al., 2017; HUANG et al., 2017; CHEN et al., 2014).

An increase in the catalyst surface area and the amount of active sites available favored the decomposition of ozone, as shown by the lower equilibrium concentrations of ozone in solution (Figure 26a). The subsequent enhanced production of ROS and the reaction with 1,4-dioxane and its breakdown products led to higher rates of mineralization (AHMADI et al., 2017; HUANG et al., 2017).

In the absence of ozone, 1,4-dioxane would be removed by adsorption onto the solid surface, because the formation of free radicals

at room temperature is negligible (JI; LI; DENG, 2011). In fact, CuO is an effective catalyst for the degradation of organic compounds by wet catalytic oxidation via a radical reaction mechanism (SADANA; KATZER, 1974), but these reactions only occur at high temperature (200 – 325°C) and pressure (5 – 15 MPa) in the presence of oxygen/air (SUSHMA; KUMARI; SAROHA, 2018).

The impact of the adsorption of 1,4-dioxane by CuO can be considered negligible, since only 4% of the TOC and 8% of the 1,4-dioxane was adsorbed by 3000 ppm of CuO after 6 h (Figure 25). The low adsorption capacity of CuO is due to its low specific area (Table 9), the high solubility of 1,4-dioxane in water and low pressure, which also results in insignificant removal by adsorption on activated carbon (BARNDÕK et al., 2014).

Figure 25: Kinetics of 1,4-dioxane adsorption onto CuO as a function of TOC and 1,4-dioxane removal ([1,4-dioxane] = 200 ppm; T = 25 ± 1 °C; [catalyst] = 3000 ppm; pH = 7.0±0.5).
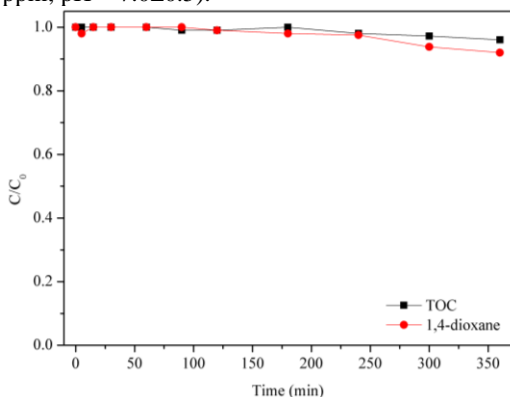
Source: Author's own elaboration

The results collectively show that the effect of catalytic ozonation in the presence of CuO was higher than the combined effect of adsorption onto the catalyst surface and ozonation in the absence of catalyst, demonstrating that CuO is a highly active ozonation catalyst for the mineralization of 1,4-dioxane.

Figure 26: (a) Aqueous ozone concentrations with different catalyst dosages; (b) Pseudo-first-order constants for 1,4-dioxane and TOC removal after 6 h of reaction at different dosages of CuO ([1,4-dioxane] = 200 ppm; pH = 7.0±0.5; ozone flow = 0.064 m³ h^{-1}; T = 25 ± 1 °C).
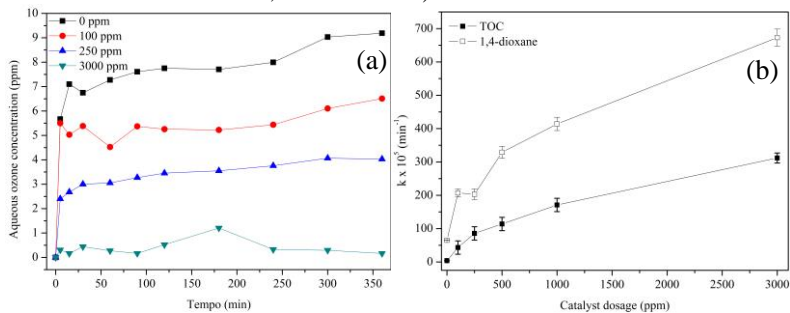
Source: Author's own elaboration

4.2.5 Radical species and reaction mechanism

The nature of the ROS produced during the CuO catalytic ozonation reaction was investigated in the presence of selected radical scavengers: salicylic acid (SA), sodium fluoride (NaF), 1,4-benzoquinone (PBQ) and phosphate (PHOS). The results in Figure 27 show the pseudo-first-order rate constant for the 1,4-dioxane and TOC removal. The TOC was evaluated for reactions with NaF and PHOS because these scavengers had no influence on the TOC detection.

SA and NaF were used to determine the role of $^{\bullet}OH_{free}$ and $^{\bullet}OH_{ads}$, respectively, in the degradation of 1,4-dioxane (BELTRÁN, 2004; KWON et al., 2012). Although *tert*-butanol (TBA) is generally used as an $^{\bullet}OH$ scavenger this was not employed in this study since the second-order reaction rate of TBA with $^{\bullet}OH$ (5.0 x 10^8 M^{-1} s^{-1}, (HOIGNÉ; BADER, 1983)) was slower than the reaction rate of 1,4-dioxane with $^{\bullet}OH$ ((1.1 to 2.35) x 10^9 M^{-1} s^{-1}, (THOMAS, 1965)). On the other hand, SA reacts faster with $^{\bullet}OH$, with a reaction rate of 2.2 x 10^{10} M^{-1} s^{-1} (CRITTENDEN et al., 2012).

The reaction rate in the presence of SA decreased only slightly (by a factor of 1.2), indicating that $^{\bullet}OH_{free}$ had a negligible effect on the 1,4-dioxane degradation. In the presence of NaF, the reaction rate decreased by factors of 1.4 and 1.7 for 1,4-dioxane and TOC, respectively, suggesting that $^{\bullet}OH_{ads}$ had a stronger influence in the degradation of the intermediate products. In contrast, in the presence of PBQ, a superoxide radical ($O_2^{-\bullet}$) scavenger (NAWAZ et al., 2015; YANG et al., 2013), the

reaction rate decreased by a factor of 2.7, indicating that 1,4-dioxane was mainly degraded by $O_2^{-\bullet}$.

Lewis acid sites are considered to be catalytic centers on the catalyst surface for ozone decomposition reactions (KASPRZYK-HORDERN; ZIÓLEK; NAWROCKI, 2003; MASHAYEKH-SAEHI; MOUSSAVI; YAGHMAEIAN, 2017). On the other hand, PHOS has high affinity toward the Lewis acids and thus can fill the active sites on the surface of catalysts, leading to a loss of catalytic activity. Figure 27 shows that in the presence of PHOS the reaction rate decreased by factors of 7.52 and 1.32 for TOC and 1,4-dioxane removal, respectively, suggesting that the adsorption of ozone on the catalyst surface was prevented. This effect was more significant for the degradation of the intermediate products compared with the removal of 1,4-dioxane.

Figure 27: Pseudo-first-order constants for 1,4-dioxane and TOC removal after 6 h of reaction in the presence of selected radical scavengers ([1,4-dioxane] = 200 ppm; [CuO] = 250 ppm; pH = 7.0±0.5; ozone flow = 0.064 m³ h⁻¹; T = 25 ± 1 °C; [SA] and [PBQ] = 10 mM; [NaF] = 60 mM; [PHOS] = 40 mM).
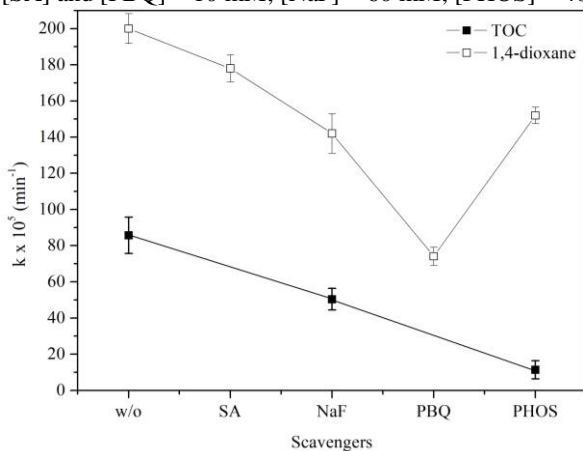
Source: Author's own elaboration

The reaction intermediates detected by GC-MS in the experiment using 3000 ppm of CuO at pH 7 were investigated to elucidate further the degradation of 1,4-dioxane by ozone alone and by catalytic ozonation. Similar intermediates were detected in the two cases; however, the appearance of the primary intermediates was faster and more pronounced in the presence of CuO. Ethylene glycol, formic acid and succinic acid were identified as the major reaction intermediates and the evolution of their concentrations in the presence of CuO can be seen in Fig. 28.

Figure 28: Evolution of the concentrations of the intermediates.
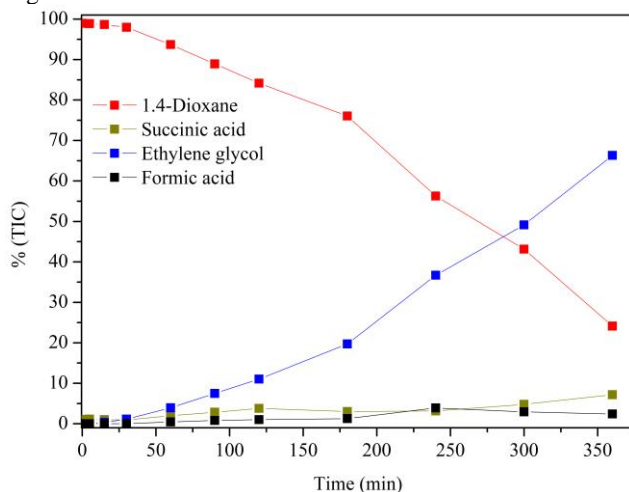
A simplified reaction scheme for 1,4-dioxane decomposition by catalytic ozonation with CuO is given in Figure 29. The presence of ethylene glycol (EG) and formic acid (FA) as reaction intermediates, suggested that the degradation pathway mainly progressed through the formation of ethylene glycol diformate (EGDF) (BARNDÕK et al., 2016; MERAYO et al., 2014), although this compound was not detected by GC-MS as it quickly hydrolyzes to EG (BARNDÕK et al., 2014) and FA (VOLLHARDT; SCHORE, 2011). It should be noted that EG has previously been reported as the main intermediate of 1,4-dioxane during ozonation (BARNDÕK et al., 2014), electrolysis/O_3 (KISHIMOTO, 2015), Fenton (MERAYO et al., 2014) and UV/H_2O_2/Fe^0 (BARNDÕK et al., 2016) treatments.

Figure 29: Simplified schematic of 1,4-dioxane decomposition by catalytic ozonation with CuO ([1,4-dioxane] = 200 ppm, [CuO] = 3000 ppm, pH = 7.0±0.5, ozone flow = 0.064 m³ h⁻¹ and T = 25 ± 1 °C).
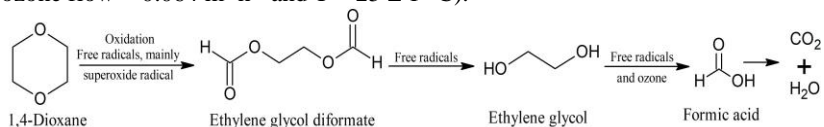
4.2.6 Catalyst stability and reusability

The recyclability and stability of the catalyst are critical factors for the large-scale application of heterogeneous catalytic ozonation systems for water and wastewater treatment. In this study, the recyclability and stability of the CuO used in the treatment of 1,4-dioxane by catalyst ozonation were assessed during five consecutive reuse cycles.

The catalytic activity of CuO during each cycle decreased slightly (Figure 30a) but remained at acceptable values. The TOC and 1,4-dioxane removal efficiencies decreased from 49% to 30% and from 78% to 56%, respectively, but were still significantly higher than the removals achieved with ozonation alone (20% for 1,4-dioxane and negligible for TOC). The apparent loss of activity could result from the poisoning of the active sites, fouling of the catalyst surface by the reaction products, the loss of catalyst mass during each reusing cycle and copper leaching (AHMADI et al., 2017; VAKILABADI et al., 2017).

The FTIR spectra for the CuO before and after five cycles of catalytic ozonation (Figure 30b) show no alterations, suggesting good stability and structural composition of the catalyst. A strong absorption band peak was observed at 539 cm^{-1} due to the vibrational stretching of CuO (MERAYO et al., 2014). The peaks observed in the range of 1107 cm^{-1} and 1637 cm^{-1} may be attributed to O-H bending vibrations combined with copper atoms. The presence of humid air and hydrated CuO samples was responsible for the formation of peaks in the range of 2900 and 3500 cm^{-1} (DUBAL et al., 2010).

Copper leaching from the catalyst to the solution during catalytic ozonation at pH 7 was quantified after each cycle by AAS. Copper leaching was 0.28 ppm, 0.26 ppm, 0.2 ppm, 0.12 ppm and 0.7 ppm for cycles 1, 2, 3 ,4 and 5, respectively. The sum of the amount of copper dissolved in the aqueous media during all cycles was less than 0.1%, indicating that the CuO catalyst has a high degree of stability.

Figure 30: (a) The stability and reusability of CuO in the catalytic ozonation of 1,4-dioxane over 5 cycles and (b) FTIR spectra of CuO before and after 5 cycles of catalytic ozonation ([1,4-dioxane] = 200 ppm; pH = 7.0; ozone flow = 0.064 $m^3 h^{-1}$; T = 25 ± 1 °C; [catalyst] = 1000 ppm; reaction time: 360 min).
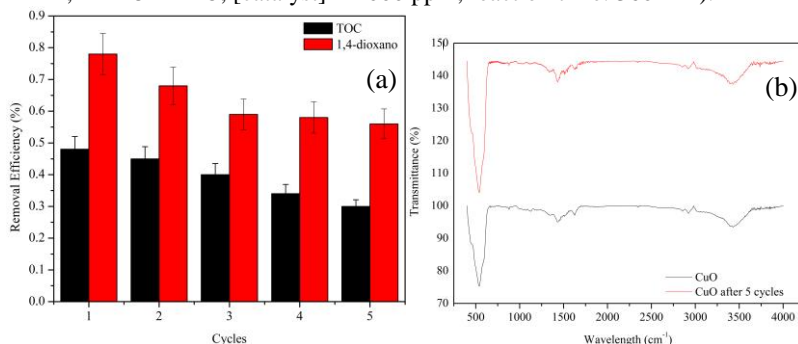
Source: Author's own elaboration

4.2.7 Acute toxicity test with *Vibrio fischeri*

The toxicity results for the water containing 1,4-dioxane, before and after treatment in the absence and presence of CuO (3000 ppm), after 0, 30, 60 and 360 min, are shown in Fig. 31. The acute toxicity observed after the treatment in the presence of CuO was significantly lower than that observed after the treatment in the absence of the catalysis. Catalytic oxidation with CuO increased the mineralization rate of the toxic intermediates formed during the 1,4-dioxane oxidation treatment, as also observed in the case of treatment by the photoelectron-peroxone process (SHEN et al., 2017). Notably, the toxicity of the samples treated by ozonation alone increased significantly during the treatment process, presumably due to the insignificant rate of mineralization observed, suggesting a gradual accumulation of toxic intermediates in solution, in agreement with the results obtained using the electro-peroxone process (WANG et al., 2015). This observation indicates that detailed toxicity studies need to be performed before implementing advanced water treatment processes.

Figure 31: Acute toxicity of 1,4-dioxane and byproducts after ozonation or catalytic ozonation for 0, 30, 60 and 360 min ([1,4-dioxane] = 200 ppm; pH = 7.0; ozone flow = 0.064 m³ h⁻¹; T = 25 ± 1 °C; [catalyst] = 3000 ppm; reaction time: 360 min).
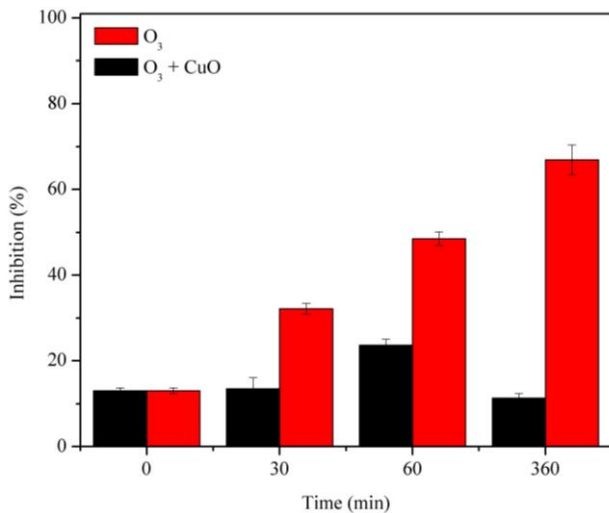
Source: Author's own elaboration

4.3 CONCLUSIONS

This study demonstrated the effective treatment of 1,4-dioxane by catalytic ozonation using CuO. It was found that the mechanism of reaction involves primarily superoxide radicals, rather than hydroxyl radicals. These in turn react with 1,4-dioxane to form ethylene glycol, which was further decomposed to formic acid with a higher rate of mineralization when compared with ozonation alone. This further contributed to reducing the acute toxicity of the treated water. In contrast, in the absence of catalyst the toxicity of the water increased after treatment by ozonation at circumneutral pH.

5. 1,4-DIOXANE REMOVAL FROM WATER AND MEMBRANE FOULING ELIMINATION BY CuO-COATED CERAMIC MEMBRANE COUPLED TO OZONATION

This chapter is based on the paper entitled "1,4-Dioxane removal from water and membrane fouling elimination by CuO-coated ceramic membrane coupled to ozonation" (submitted to Chemical Engineering Journal), by Gidiane Scaratti, Agenor de Noni Junior, Humberto Jorge José and Regina de Fátima Peralta Muniz Moreira. Abstract, keywords, introduction, acknowledgments and references were omitted, some minor amendments were performed, but the procedures, results and conclusions reported in the original paper were not modified.

5.1 MATERIALS AND METHODS

5.1.1 Chemicals, Materials, and Feed Water

1,4-Dioxane (99.99%) was supplied by Neon (Brazil). Commercial copper oxide (99% of purity) was purchased from Amorphous and Nanostructures Materials Inc. (Houston, TX, USA) and it was well characterized previously: particle size: 77-200 nm; point of zero charge: 7.41; BET surface area: 12.61 m^2 g^{-1}; pore size diameter: 3.6 nm; total pore volume: 0.044 cm^3 g^{-1} (SCARATTI et al., 2019). CuO density is equal to 6.4 g cm^{-3}.

All others reagents were analytical grade, and solutions were prepared by dissolution in deionized water or spiked into a surface water. The surface water used in this study was collected from the Municipal Water Treatment Plant (WTP) (Palhoça, Brazil), after fast sand filtration and before the chlorination step. In that WTP, the surface water from Cubatão River is collected and treated by the conventional coagulation/flocculation process using aluminum sulfate, followed by sand filtration. The general quality parameters of this water are provided in Table 11.

Tubular ultrafiltration ceramic membranes (CM) used in this study are one channel (Pall Ceramics) (Figure 33) consisting of an α-Al_2O_3 supporter and a mixed filtration layer of Al_2O_3 and ZrO_2. The basic CM specifications are as follows: length of 25 cm, diameter of 1 cm, internal diameter of 0.6 cm, pore diameter of 50 nm, permeation area of 47.12 cm^2 and molecular weight cut off was 20 kDa.

Figure 32: Tubular ceramic membrane used in this work.
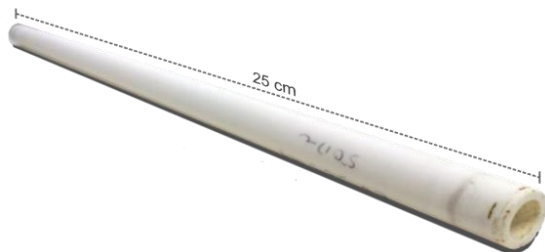
Source: Author's own elaboration

Table 11: Main physicochemical characteristics of water of Cubatão River (Brazil) used in this work.

Parameters	Value
pH	~ 7.0
Conductivity	50.71 μS cm^{-1}
TOC	2.92 mg L^{-1}
Turbidity, NTU	≤ 5
1,4-Dioxane, mg/L	not detected

5.1.2 Coating procedure

First, 250 mg of CuO was suspended in 250 mL of deionized water and pH was adjusted to 3.5 to assure the stability of the particles. Then, CuO suspension was sonicated for 60 min to guarantee the homogeneity of the suspension (Unique – Model USC – 1650A - 25 kHz). The deposition of CuO layer was performed by suction of 10 mL of CuO dispersion (pH 3.5) inside the CM with a vacuum pump. To promote the attachment of CuO particles to the CM surface, the CuO-coated CM were thermally treated in a furnace under air atmosphere, at 550 °C for 30 min. After sintering, membranes were cooled until atmosphere temperature inside the furnace. This procedure was sequentially repeated until the desired amount of CuO was deposited inside the CM. Before the impregnation process, CM was weighed as W_0. After sintering, CuO-coated CM was weighed as W_1. The final catalyst loading amount was calculated by the weight difference $W=W_1-W_0$. Three different catalyst loadings were deposited on the CM surface (7.9±0.4 mg; 22.8±1.1 mg; 42.4±2.3 mg) to produce different catalyst cover density (0.17 mg cm^{-2}; 0.48 mg cm^{-2}; 0.90 mg cm^{-2}) and catalyst thickness (0.3 μm; 0.8 μm; 1.4 μm). Finally, the CuO-coated CM were washed by filtering deionized water for 30 min and, then, they were ready to use.

5.1.3 Ceramic membrane characterization

The topography of the CuO-coated CM and CM surfaces were evaluated by field emission scanning electron microscopy (FESEM) in a JEOL JSM-6701F. At the same time, dispersive energy spectroscopy (DES) analysis were performed using an X-ray microanalysis probe coupled to the scanning electron microscope to identify the composition on the surface of the CM and 0.90 mg cm^{-2} CuO-coated CM.

5.1.4 Filtration experiments of the coated and uncoated membranes

The coated and uncoated membranes were evaluated for permeate flux and rejection using the experimental module without ozone addition (Figure 34a). The apparatus consisted of a stainless-steel membrane module, gear pump (Cole-Parmer, Model 75211-15) and pressure manometer. The experiments were conducted at an operational pressure of 0.25 bar at (20 ± 3 °C), using a solution of 1,4-dioxane (200 ppm) diluted in water from the WTP. Permeate flux was monitored manually at regular time intervals and the Total Organic Carbon (TOC) and 1,4-dioxane concentrations were measured.

5.1.5 Hybrid treatment of catalytic ozonation and membrane filtration

Figure 34b presents the experimental apparatus used for the hybrid treatment (catalytic ceramic membrane coupled to ozonation) tests in a closed system. The apparatus consisted of an ozone generator (Philozon O$_3$R - Model ID-05), ozone contact tank, a stainless-steel membrane module, gear pump (Cole-Parmer, Model 75211-15) and pressure manometer. Ozone was continuously bubbled into the 1,4-dioxane solution at a rate of 0.063 m^3 L^{-1} inside the ozone contact tank and then pumped to the membrane module. Similar experiments were performed using 1,4- dioxane (200 ppm) diluted in the water from the WTP or in deionized water. The operate pressure was 0.25 bar. The permeate was recirculated using a peristaltic pump keeping the same volume at the ozone contactor tank. Permeate flux was monitored at regular time intervals and a sample (12 mL) was withdrawn at the outlet of membrane module at regular intervals for the analytical determination of TOC concentration, 1,4-dioxane concentration, the aqueous ozone concentration [O$_3$], permeate flux and the acute toxicity. For the hybrid

experiments with 0.90 mg cm^{-2} CuO-coated CM coupled to ozonation, Cu ion leached in the aqueous phase was quantified using Atomic Absorption Spectroscopy (AAS).

After each experiment, the fouled membranes were cleaned by filtration of deionized water continuously bubbled with ozone for 0.5-1 h until the initial clean water flux was restored, except for the reusability tests. Before each experiment, the initial flux was measured using deionized water to ensure that the permeability of the membrane was at its initial value.

Figure 33: Experimental apparatus used to evaluate the filtration (a) and hybrid process (b) (1 – Oxygen concentrator; 2 – Ozone generator; 3 – Magnetic stirrer; 4 – Stones diffusers; 5 – Ozone contact tank; 6 – Gear pump; 7 – Pressure manometer; 8 – Membrane module; 9 – Permeate; 10 – Peristaltic pump).
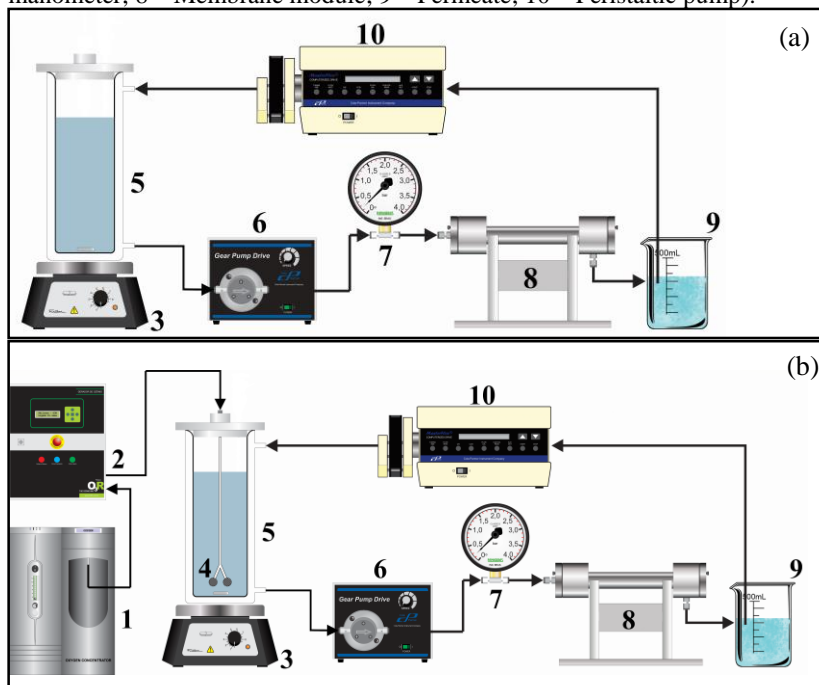
Source: Author's own elaboration

5.1.6 Continuous treatment and reusability

Ozone was continuously bubbled into the solution consisting in 1,4-dioxane diluted in water from WTP (200 ppm). This mixture was feed into the experimental apparatus at 20 ± 3 °C, and the flow rate of the permeate was monitored continuously. The TOC concentration and 1,4-dioxane concentration on the permeate were measured at regular time intervals.

5.1.7 Analytical Methods

The pH was determined by potentiometric method using pHmeter Quimis (Model Q400A), previously calibrated with pH 4.0 and 7.0 buffer solution. The TOC concentration was determined on a TOC-VCPH analyzer (Shimadzu). The concentration of leached copper ion in the liquid phase after the hybrid process 0.90 mg cm^{-2} CuO-coated CM coupled to ozonation was measured via AAS with an Agilent 240FSAA spectrometer.

The residual aqueous ozone concentration (C) of ozone was evaluated in a spectrophotometer (HACH DR 5000) by quantifying the absorbance at 258 nm by the Lambert-Beer law (Eq. 24), since no absorption is due to the 1,4-dioxane.

$$ABS = \varepsilon LC \tag{24}$$

where ε is the molar extinction coefficient equal to 2950 M^{-1} cm^{-1} at 258 nm (APHA, 1995), L is the optical path and C is the ozone concentration in the aqueous phase.

1,4-Dioxane was extracted according to the methodology proposed by Li and collaborators (LI et al., 2011) and quantified using a CG-MS (Shimadzu QP2010 plus) equipped with a Supel-Q PLOT column. The column temperature was maintained at 150 °C during the analysis (total time was 4 min) and injector and interface temperature were both 200 °C. Samples (1 μL) were injected in split mode (1:18). Helium was used as the carrier gas. The quantification and confirmation ions were m/z 88 and m/z 58, respectively.

The 1,4-dioxane and TOC degradation rate constants (k_1) were obtained according to the pseudo first-order rate laws (Eq. 25) coupled to the material balance of the closed system reactor, which was operated under an excess of ozone (continuous bubbling).

$$-\ln\left(\frac{C}{C_0}\right)=k_1 t \tag{25}$$

where C_0 and C are the initial concentration and the concentration after the catalytic ozonation process at various time intervals, respectively, k_1 is either the 1,4-dioxane or TOC, degradation pseudo-first-order rate constant (min^{-1}) and t is the reaction time. The first-order rate constant (k_1) was determined by the slope of the straight-line fitting of $-\ln(C/C_0)$ versus time.

The acute toxicity test with the bioluminescent bacteria Vibrio fischeri (lyophilized) was performed according to the methodology proposed by ISO 11348-3.

5.2 RESULTS AND DISCUSSION

5.2.1 Ceramic membrane characterization

Fig. 35 shows FESEM images of the CM, fresh CuO-coated CM and four reused CuO-coated CM surfaces. The membrane surface morphology changes significantly after the nanoparticles deposition (Fig 35a and 35b). After being coated with CuO particles, the CuO-coated CM appeared to be rougher and the surface coated by a large number of CuO particles (Fig. 35(b) and 35(c)) compared to the uncoated one (Fig. 35(a)). The four reused 0.90 mg cm^{-2} CuO-coated CM surface became smoother when compared to the fresh CuO-coated CM, it is noticeable fouling on the membrane surface. In the table 12 are presented the apparent concentration of the elements on the surface of the CM and 0.90 mg cm^{-2} CuO-coated CM. the analyses confirm that the CM is composed of Zr and Al and a higher concentration of Cu is presented on the surface of the 0.90 mg cm^{-2} CuO-coated CM after four reused times.

Figure 34: FESEM surface images of a) virgin CM; b) 0.90 mg cm^{-2} fresh CuO-coated CM; c) four times reused 0.90 mg cm^{-2} CuO-coated CM.
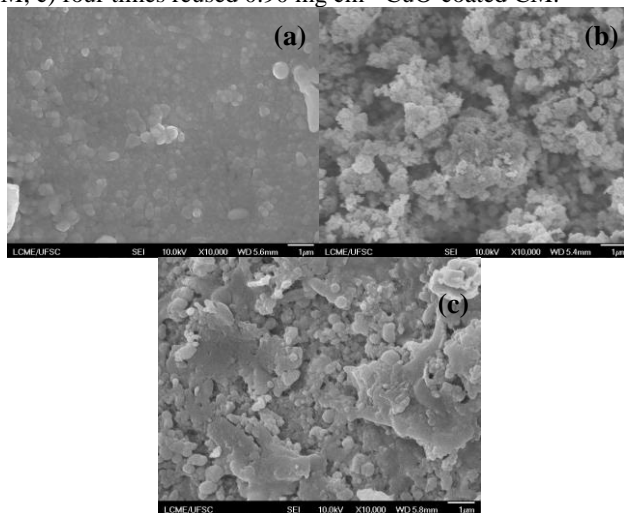
Source: Author's own elaboration

Table 12: Apparent elements concentration obtained by EDS

Element	Wt%	
	Uncoated	Four reused times 0.90 mg cm^{-2} CuO-coated CM
C	26.84	24.35
O	24.53	25.57
Al	0.27	1.82
Si	0.06	2.32
Cl	0.30	0.25
Fe	-	3.35
Cu	-	22.77
K	0.20	-
Zr	47.81	19.58

5.2.2 Comparison of permeate flux and resistance fouling in presence and absence of ozone

Figure 36 displays the effect of ozone on permeate flux for the hybrid system using the uncoated CM and CuO-coated CM. In absence

of ozone (Fig 36a), the permeability declined rapidly during the first 180 minutes for the uncoated and 0.9 mg cm^{-2} CuO-coated CM. In this stage, the fouling cake begins to form on the membrane surface. Modifying CM with CuO did not change CM permeability, as reported on the literature (GUO; XU; QI, 2016; CHENG et al., 2017).

Figure 36b displays the effect of the ozone flow rate, 0.064 m³ h^{-1}, on the permeate flow. Initially the permeate flux decreases due to the fouling effect, but it is completely reestablished after 60 minutes, in the case of filtration using 0.9 mg cm^{-2} CuO-coated CM. Using the uncoated CM, the permeate flow also increases in a higher time than when using it without ozone addition. When the permeate flux reached steady state condition, the rate of formation of the fouling cake due to the deposition of natural organic matter (NOM) on the surface of the membrane is presumed to be similar to the rate of reaction of the accumulated foulants with ozone and free radicals. The free radicals were formed as the result of the catalytic decomposition of ozone by CuO. These results confirmed that the fouling caused by NOM in the municipal water is efficiently removed by ozone dissolved in the water.

Figure 35: Permeate flux for the uncoated and 0.9 mg cm^{-2} CuO-coated CM during filtration of municipal water containing 1,4-dioxane a) absence of ozone; b) ozone flow 0.064 m³ h^{-1} ([1,4-dioxane] = 200 ppm; T = 25 ± 1 °C; TMP = 0.25 bar).
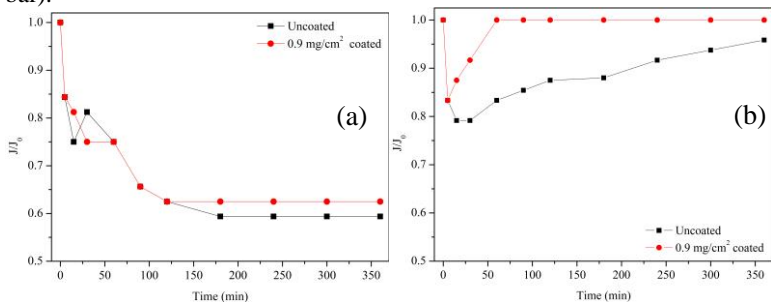
Source: Author's own elaboration

Previous tests showed that no mineralization or 1,4-dioxane removal is found by filtration on the coated or uncoated membrane, since the pore size of the membrane (50 nm) is much bigger than the 1,4-dioxane molecular diameter (0.65 nm) (PIERA et al., 1999).

In the presence of ozone, the TOC and 1,4-dioxane removal using 0.90 mg cm^{-2} CuO-coated CM or CM is presented in Figure 37. As expected, the CuO coating improves both mineralization and 1,4-dioxane

removal since the non-catalytic ozonation of this organic compound is slow (KWON et al., 2011; SHEN et al., 2017).

Figure 36: Kinetics of TOC and 1,4-dioxane degradation by the hybrid process with the coated or uncoated CM ([1,4-dioxane] = 200 ppm; ozone flow = 0.064 $m^3 h^{-1}$; T = 25 ± 1 °C; TMP = 0.25 bar).
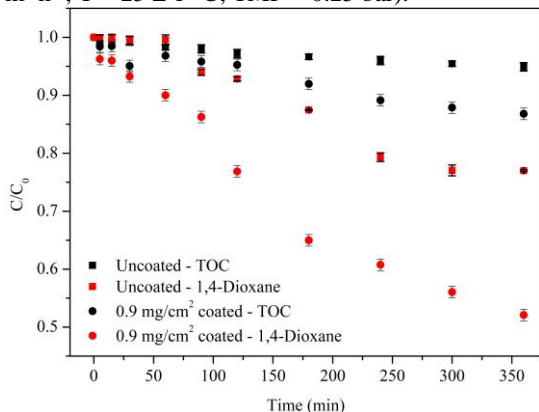
Source: Author's own elaboration

5.2.3 CuO-coated CM loading effects performance in 1,4-dioxane degradation using ozone

Figure 38 shows the effect of catalyst loading on 1,4-dioxane degradation and mineralization. The catalyst loading influences the performance significantly and CM coated with 0.9 mg cm^{-2} of CuO exhibits the highest performance, due to the increase of active component content. The 0.9 mg cm^{-2} coated-CM increased by 11.4% and 45% the mineralization and 1,4-dioxane degradation efficiency in comparison to the CM, respectively. 1,4-Dioxane adsorption over CuO-coated CM can be considered negligible due to the high solubility of 1,4-dioxane in water and low pressure, which results in low removal rate constants by adsorption also on activated carbon (BARNDÕK, 2014).

The pseudo-first order kinetics constants were determined from Eq. 25, since the reactor was operated under an excess of ozone, Figure 39a. The pseudo-first order kinetics constants for 1,4-dioxane degradation and mineralization increased 4.21 and 2.98 times when compared to the uncoated-hybrid process, respectively.

The reactions follow the second order kinetics constants when ozone concentration reached steady state, Table 13. The second order

kinetic constants for 1,4-dioxane removal and TOC removal increased 8.19 and 5.78 times in comparison to the uncoated-hybrid process, respectively.

Figure 37: Effect of catalyst loading on 1,4-dioxane degradation kinetics (a) and 1,4-dioxane mineralization kinetics (b) ([1,4-dioxane] = 200 ppm; ozone flow = 0.064 m^3 h^{-1}; T = 25 $\pm$ 1 °C; TMP = 0.25 bar)
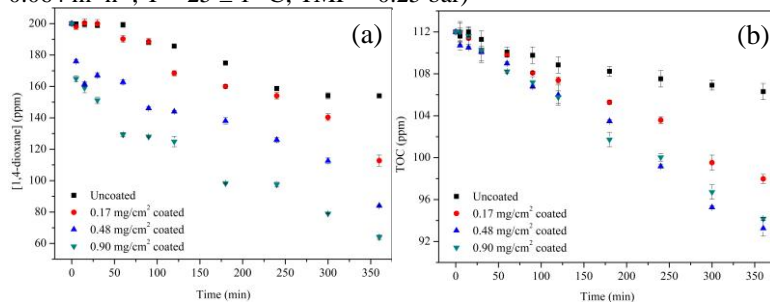
Source: Author's own elaboration

The increment in catalyst load on CM surface favored the decomposition of ozone as shown by the lower equilibrium concentration of ozone in the system, Figure 39b. The enhanced production of free radicals increased the 1,4-dioxane removal and its products in CO_2 and water. No change in permeate flux was observed for all conditions tested, since 1,4-dioxane molecule is smaller than CM pore size. The pH was between 4 – 5.5 during all the reactions time.

No significant improvement in 1,4-dioxane mineralization and decomposition of ozone was observed by increasing the catalyst loading from 0.484 mg cm^{-2} to 0.9 mg cm^{-2} was observed. This is mainly due to because the CuO particles coating probably covered almost the entire CM surface or the amount of coated CuO particles were sufficient for catalytic ozonation process (BYUN et al., 2011).

Figure 38: (a) Aqueous ozone concentration (b) Pseudo-first order constants for 1,4-dioxane and TOC removal after 6 hours of reaction at different loadings of catalyst impregnated ([1,4-dioxane] = 200 ppm; pH = 7.0±0.5; ozone flow = 0.064 m³ h⁻¹; T = 25 ± 1 °C; TMP = 0.25 bar).
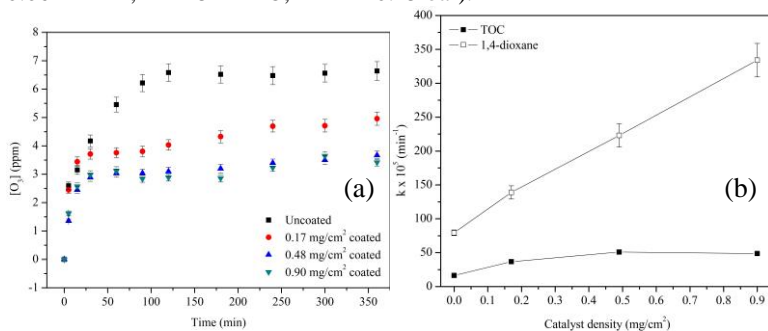
Source: Author's own elaboration

Table 13: Second order kinetics constants for TOC and 1,4-dioxane removal at different catalyst cover density ([1,4-dioxane] = 200 ppm; ozone flow = 0.064 m³ h⁻¹; T = 25 ± 1 °C; TMP = 0.25 bar)

Catalyst cover density (mg cm⁻²)	k TOC (L mg⁻¹ min⁻¹)	k 1,4-dioxane (L mg⁻¹ min⁻¹)
0	2.47	11.94
0.17	7.39	28.03
0.48	13.86	60.76
0.9	14.27	97.75

5.2.4 Reusability tests

Considering the industrial application of the CuO-coated CM, it is essential to maintain the high catalytic activity. The 0.9 mg cm⁻² CuO-coated CM for the treatment of 1,4-dioxane dissolved in a municipal water coupled to ozone were assessed during four consecutive reusing cycles, Fig. 40. As expected, no remarkable change was observed on the catalytic activity of the 0.9 mg cm⁻² CuO-coated CM, even with 2.3 ppm of Cu leached into the aqueous phase, approximately 6.8% of the total Cu impregnated on the CM surface. Flux recovery took 30 more min in the last reuse, Fig. 41. The apparent loss of activity could result from the poisoning of the active sites, fouling of the catalyst surface by the reaction products, the loss of catalyst mass during each reusing cycle and copper leaching (AHMADI et al., 2017; VAKILABADI et al., 2017).

Figure 39: Reusability of the 0.9 mg cm^{-2} CuO-coated CM on 1,4-dioxane degradation and mineralization in for consecutive reusing cycles ([1,4-dioxane] = 200 ppm; ozone flow = 0.064 m³ h^{-1}; T = 25 ± 1 °C; TMP = 0.25 bar).
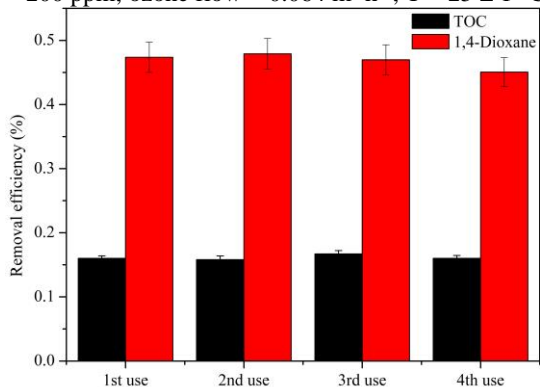
Source: Author's own elaboration

Figure 40: Permeate flux recovery of the 0.9 mg cm^{-2} CuO-coated CM on municipal water containing 1,4-dioxane treatment by hybrid process during four consecutive reusing cycles ([1,4-dioxane] = 200 ppm; ozone flow = 0.064 m³ h^{-1}; T = 25 ± 1 °C; TMP = 0.25 bar).
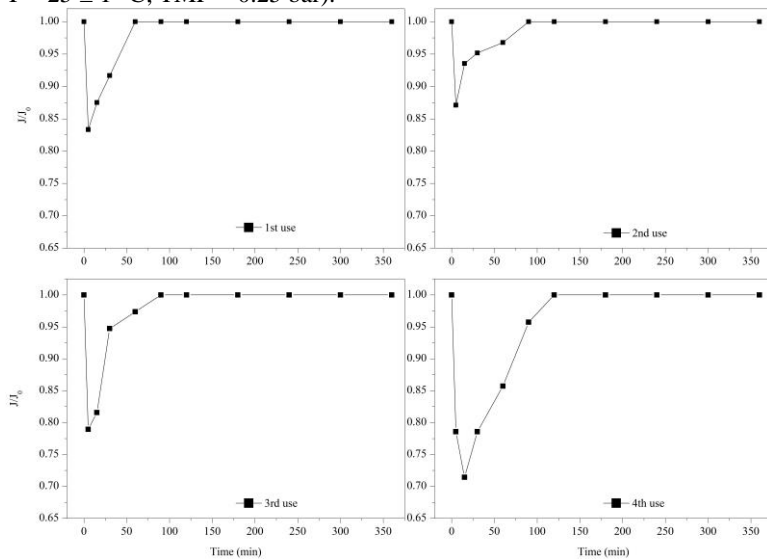
Source: Author's own elaboration

5.2.5 Toxicity evaluation

The toxicity of the water containing 1,4-dioxane before and after treatment using the CM and 0.9 mg cm^{-2} CuO-coated CM at times 0, 30, 60 and 360 min is shown in Figure 42. The acute toxicity observed after the treatment with the 0.9 mg cm^{-2} CuO-coated CM was significantly higher than in the CM. This is mainly due to the higher degradation rates obtained for the hybrid process with 0.9 mg cm^{-2} CuO-coated CM, which promoted the production of more intermediates, thus, increasing the acute toxicity before than the uncoated-hybrid process. It is known by the literature that 1,4-dioxane treatment by AOPs increase toxic intermediates in the solution, supporting the need of detailed toxicity studies before the implementation of AOPs. (SHEN et al., 2017; WANG et al., 2015). For catalytic ozonation of 1,4-dioxane using CuO in aqueous suspension the main intermediate compound is ethylene glycol (SCARATTI et al., 2019), which is readily biodegradable under both aerobic and anaerobic conditions (WORLD HEALTH ORGANIZATION, report 22, 2002).

Figure 41: Acute toxicity of 1,4-dioxane and by products after hybrid processes with 0.9 mg cm^{-2} CuO-coated CM and uncoated CM at 0, 30, 60 and 360 min of the reaction ([1,4-dioxane] = 200 ppm; ozone flow = 0.064 m³ h^{-1}; T = 25 ± 1 °C; TMP = 0.25 bar).
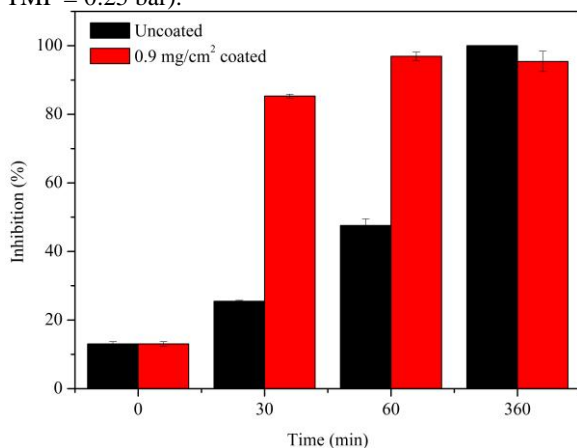
Source: Author's own elaboration

5.3 CONCLUSION

This study was conducted to assess the removal efficiency of 1,4-dioxane by catalytic ceramic membrane coupled to ozone. The catalyst

loading affects the removal of 1,4-dioxane and TOC. The proposed hybrid system effectively reduces membrane fouling and improves water quality in the permeate when used water from a Municipal Water Treatment Plant. A higher rate of 1,4-dioxane degradation was obtained with 0.9 mg cm^{-2} CuO-coated CM, in comparison to CM, contributing for acute toxicity increasing, since more intermediates compounds are being formed. Catalytic activity of the ceramic membrane kept the same for 1,4-dioxane and TOC removal during four consecutive cycles. The results obtained in this study shows that a unique process, coupling ceramic membrane modified with catalyst and ozonation, is a promising technology to treat small, carcinogenic and recalcitrant compounds that are not retained by membrane technology, as 1.4-dioxane.

6. FINAL CONCLUSION

CuO proved to be a suitable catalyst in comparison to FeOOH and CeO_2 to be applied to advanced oxidation process using ozone to degrade 1,4-dioxane. However, it did not promote 1,4-dioxane mineralization when applied as catalyst for peroxidation process. The catalytic activity in the presence of hydrogen peroxide is based on the non-radical mechanism, consequently, 1,4-dioxane degradation is negligible.

For catalytic ozonation, the reaction mechanism involves primarily superoxide radicals, with a high rate of mineralization in comparison to ozonation alone, reducing the acute toxicity of the treated water. The optimum pH value was found to be 7. 1,4-Dioxane degradation and mineralization depend on the amount of catalyst used. Therefore, there is a direct proportional relationship between catalyst loading and active sites available for ozone decomposition, which, consequently, enhance ROS production, leading to higher rates of mineralization. The catalyst exhibits weak copper leaching and high catalytic activity for five consecutive cycles.

The catalyst loading on the ceramic membrane surface affects 1,4-dioxane mineralization and ozone decomposition up to a limit, whereupon particles coating probably covered almost the entire ceramic membrane surface or the amount of coated particles were sufficient for catalytic ozonation process. Catalytic ceramic membrane coupled to ozonation is more efficient for reducing membrane fouling than the ceramic membrane coupled to ozonation. Catalytic activity of the hybrid process is stable during four successive cycles. A higher rate obtained for 1,4-dioxane removal with the 0.9 mg cm^{-2} CuO-coated ceramic membrane contributed for acute toxicity increasing. For this reason, more intermediates were formed and more than 6 h is necessary to reduce the acute toxicity.

Comparing catalytic ozonation ([CuO] = 3000 ppm = 3 mg cm^{-3}) and the hybrid process ultrafiltration coupled to catalytic ozonation (catalyst loading/membrane volume = 5.98 mg cm^{-3}), catalytic ozonation is more efficient in terms of rate constants and acute toxicity reduction. The pseudo-first order constants rates for catalytic ozonation were 6 and 2 times faster for TOC and 1,4-dioxane removal, respectively, when compared to the ultrafiltration plus catalytic ozonation process.

However, for large-scale application, the immobilization of the catalyst on membrane surface shows a series of advantages that overcome the loss of surface contact, such as no need of recovery of the catalyst in the end of the process and the production of free radicals that will react

with the organic matter retained on the membrane surface, consequently, reducing the fouling and increasing membrane lifetime.

Therefore, the results obtained in this study show that copper oxide presented a high catalytic activity for 1,4-dioxane mineralization. The hybrid process, ultrafiltration by ceramic membrane modified with copper oxide coupled to ozonation, is a promising technology to treat small and recalcitrant compounds that are not retained by membrane technology and to reduce fouling.

REFERENCES

ABE, A. Distribution of 1,4-dioxane in relation to possible sources in the water environment.**Science of the Total Environmental,** v. 277, n. 1, p. 41-47, 1999.

ADAMS, C. D.; SCANLAN, P. A.; SECRIST, N. D. Oxidation and biodegradability enhancement of 1,4-dioxane using hydrogen peroxide and ozone. **Environmental Science and Technology,** v. 28, n. 11, p. 1812-1818, 1994.

AGENCY FOR TOXIC SUBSTANCES AND DISEASES REGISTRY (ATSDR). **Toxicological profile for 1,4-dioxane.** Division of Toxicology and Environmental Medicine/Applied Toxicology Branch, Atlanta, 295 p., 2012.

AHMADI, M.; KAKAVANDI, B.; JAAFARZADEH, N.; BABAEI, A.A. Catalytic ozonation of high saline petrochemical wastewater using PAC@FeIIFeIIIO$_4$: Optimization, mechanisms and biodegradability studies. **Separation and Purification Technology,** v. 177, p. 293-303, 2017.

ALPATOVA, A.L.; DAVIES, S.H.; MASTEN, S.J. Hybrid ozonation-ceramic membrane filtration of surface waters: The effect of water characteristics on permeate flux and the removal of DBP precursors, dicloxacilin and ceftazidime. **Separation and Purification Technology,** v. 107, p. 179-186, 2013.

AMERICAN PUBLIC HEALTH ASSOCIATION..AMERICAN WATER WORKS ASSOCIATION.WATER ENVIRONMENT FEDERATION (APHA). **Standard methods for the examination of water and wastewater.** 19. ed. Washington, D.C.: APHA, c1995 1v.

ANANTH, A.; DHARANEEDHARAN, S.; HEO, M-S.; MOK, Y.S. Copper oxide nanomaterials: Synthesis, characterization and structure-specific antibacterial performance. **Chemical Engineering Journal,** v. 262, p. 179-188, 2015.

ANEGGI, E.; TROVARELLI, A.; GOI, D. Degradation of phenol in wastewaters via heterogeneous Fenton-like Ag/CeO$_2$ catalyst. **Journal of Environmental Chemical Engineering,** v. 5, p. 1159-1165, 2017.

ANGELIS, L.; CORTALEZZI, M. M. F.; Improved membrane flux recovery by Fenton-type reactions. **Journal of Membrane Science,** v. 500, p. 255-264, 2016.

ANGI, A.; SANLI, D.; ERKEY, C.; BIRER, Ö. Catalytic activity of copper (II) oxide prepared via ultrasound assisted Fenton-like reaction. **Ultrasonics Sonochemistry**, v. 21, n. 2, p. 854–859, 2014.

ASSÁLIN, Márcia Regina; DURÁN, Nelson. Novas tendências para aplicação de ozônio no tratamento de resíduos: ozonização catalítica. **Revista Analytica**, v. 26, p.76-85, 2007.

BAE, W.; WON, H.; HWANG, B.; TOLEDO, R.A. de; CHUNG, J.; KWON, K.; SHIM, H. Characterization of refractory matters in dyeing wastewater during a full-scale Fenton process following pure-oxygen activated sludge treatment. **Journal of Hazardous Materials**, v. 287, p. 421-428, 2015.

BAI, Z.; YANG, Q.; WANG, J. Catalytic ozonation of sulfamethazine using Ce$_{0.1}$Fe$_{0.9}$OOH as catalyst: Mineralization and catalytic mechanisms. **Chemical Engineering Journal,** v. 300, p. 169-176, 2016.

BARNDÕK, H.; BLANCO, L.; HERMOSILLA, D.; BLANCO, A. Heterogeneous photo-Fenton processes using zero valent iron microspheres for the treatment of wastewaters contaminated with 1,4-dioxane. **Chemical Engineering Journal,** v. 284, p. 112-121, 2016a.

BARNDÕK, H.; HERMOSILLA, D.; HAN, C.; DIONYSIOU, D.D.; NEGRO, C.; BLANCO, A. Degradation of 1,4-dioxane from industrial wastewater by solar photocatalysis using immobilized NF-TiO$_2$ composite with monodispere TiO$_2$ nanoparticles. **Applied Catalysis B: Environmental,** v, 180, p. 44-52, 2016b.

BARNDÕK, H.; CORTIJO, L.; HERMOSILLA, D.; NEGRO, A;. BLANCO, A. Removal of 1,4-dioxane from industrial wastewaters: Routes of decomposition under different operational conditions to

determine the ozone oxidation capacity. **Journal of Hazardous Materials,** v. 280, p. 340-347, 2014.

BARNDÕK, H.; HERMOSILLA, D.; NEGRO, C.; BLANCO, A. Comparison and Predesign Cost Assessment of Different Advanced Oxidation Processes for the Treatment of 1,4-dioxane-containing Wastewater from the Chemical Industry. **ACS Sustainable Chemistry & Engineering,** v. 6, n. 5, p. 5888-5894, 2018.

BARRETT, E. P.; JOYNER, L. G.; HALENDA, P. P. The Determination of Pore Volume and Area Distributions in Porous Substances. I. Computations from Nitrogen Isotherms. **Journal of the American Chemical Society**, v. 73, n. 1, p. 373-380, 1951.

BELTRÁN, Fernando J. **Ozone Reaction Kinetics for Water and Wastewater Systems.**1º ed. Badajoz, Spain, Lewis Publishers, 2004.

BELTRÁN, F. J.; RIVAS, F. J.; MONTERO-DE-ESPINOSA, R. Ozone-Enhanced Oxidation of Oxalic Acid in Water with Cobalt Catalysts. 2. Heterogeneous Catalytic Ozonation. **Industrial & Engineering Chemistry Research**, v. 42, n. 14, p. 3218-3224, 2003.

BHUVANESHWARI, S.; GOPALAKRISHNAN, N. Hydrothermally synthesized Copper Oxide (CuO) superstructures for ammonia sensing. **Journal of Colloid and Interface Science,** v. 480, p. 76-84, 2016.

BOKARE, A. D.; CHOI, W. Review of iton-free Fenton-like systems for activating H_2O_2 in advanced oxidation processes. **Journal of Hazardous Materials**, v. 275, p. 121-135, 2014.

BOLOVA, E.; GUNDUZ, G.; DUKKANCI, M. Heterogeneous Fenton-like degradation of Orange II in water using FeZSM-5 zeolite catalyst. **International Journal of Chemical Reactor,** v. 10, 2012.

BUETTNER, K.M.; RINCIOG, C.I.; MYLON, S.E. Aggregation kinetics of cerium oxide nanoparticles in monovalent and divalent electrolytes. **Colloids and Surfaces A: Physicochemical and Engineering Aspects,** v. 366, n. 1, p. 74-79, 2010.

BULANIN, K. M.; LAVALLEY, J.C.; TSYGANENKO, A.A. IR spectra of adsorbed ozone. **Colloids and Surfaces A: Physicochemical and Engineering Aspects**, v. 101, n. 2, p. 153-158, 1995.

BYUN, S.; DAVIES, S.H.; ALPATOVA, A.L.; CORNEAL, L.M.; BAUMANN, M;J.; TARABARA, V.V.; MASTEN, S.J. Mn oxide coated catalytic membranes for a hybrid ozonation-membrane filtration: comparison of Ti, Fe and Mn oxide coated membranes for water quality. **Water Research,** v. 45, n. 1, p. 163-170, 2011.

CAO, Y.; CASENAS, B.; PAN, W-P. Investigation of Chemical Looping Combustion by Solid Fuels. 2. Redox Reaction Kinetics and Product Characterization with Coal, Biomass, and Solid Waste as Solid Fuels and CuO as an Oxygen Carrier. **Energy & Fuels,** v. 20, p.1845-1854, 2006.

CENTURIÃO, A.P.S.L.; BALDISARELLI, V.; SCARATTI, G.; AMORIM, S.M. de.; MOREIRA, R.F.P.M. Enhanced ozonation degradation of petroleum refinery wastewater in the presence of oxide. **Environmental Technology,** doi: 10.1080/09593330.2017.1420103

CHEN, C.; CHEN, H.; GUO, X.; GUO, S.; YAN, G. Advanced ozone treatment of heavy oil refining wastewater by activated carbon supported iron oxide. **Journal of Industrial and Engineering Chemistry,** v. 20, n. 5, p. 2782-2791, 2014.

CHEN, C-J.; FANG, P-Y.; CHEN, K-C. Permeate flux recovery of ceramic membrane using TiO_2 with catalytic ozonation. **Ceramic International,** v. 43, p. S758-S764, 2017.

CHEN, S.; YU, J.; WANG, H.; YU, H.; QUAN, X. A pilot-scale coupling catalytic ozonation membrane filtration system for recirculating aquaculture wastewater treatment. **Desalination,** v. 363, p. 37-43, 2015.

CHEN, W.; LI, X.; PAN, Z.; MA, S.; LI, L. Effective mineralization of Diclofenac by catalytic ozonation using Fe-MCM-41 catalyst. **Chemical Engineering Journal,** v. 304, p. 594-601, 2016.

CHENG, X.; LIANG, H.; QU, F.; DING, A.; CHANG, H.; LIU, B.; TANG, X.; WU, D.; LI, G. Fabrication of Mn oxide incorporated

ceramic membranes for membrane fouling control and enhanced catalytic ozonation for p-chloronitrobenzene. **Chemical Engineering Journal,** v. 308, p. 1010-1020, 2017.

CHITRA, S.; PARAMASIVAN, K.; CHERALATHAN, M.; SINHA, P; K. Degradation of 1,4-dioxane using advanced oxidation processes. **Environmental Science Pollution Research,** v. 19, p. 871-878, 2012.

CHOI, P-G.; OHNO, T.; FUKUHARA, N.; MASUI, T.; IMANAKA, N. Catalytic liquid phase oxidation of 1,4-dioxane over a $Pt/CeO_2-ZrO_2-Bi_2O_3/SBA$-16 catalyst. **Journal of Advanced Ceramics,** v. 4, n.1, p. 71-75, 2015.

COLEMAN, H.M.; VIMONSES, V.; LESLIE, G.; AMAL, R. Degradation of 1,4-dioxane in water using TiO_2 based photocatalytic and H_2O_2/UV processes. **Journal of Hazardous Materials,** v. 146, n. 3, p. 496-501, 2007.

CORNEAL, L. M.; BAUMANN, M.J.; MASTEN, S. J.; DAVIES, S.H.R.; TARABARA, V.V.; BYUN, S. Mn oxide coated catalytic membranes for hybrid ozonation-membrane filtration: Membrane microstructural characterization. **Journal of Mmebrane Science,** v. 369, p. 182-187, 2011.

CORNELL, R. M.; SCHWERTMANN, U. **The Iron Oxides. Structure, Properties, Reactions, Occurences and Uses.** Second ed.: Wiley-VCI, 2003. p. 664.

CRITTENDEN, J.C.; TRUSSEL, R.R.; HAND, D.W.; HOWE, K.J.; TCHOBANOGLOUS, G. **MWH's Water Treatment: Principles and Design.** John Wiley & Sons, 2012.

CRUZ, P.; PÉREZ, Y.; DEL HIERRO, I.; FAJARDO, M. Copper, copper oxide nanoparticles and copper complexes supported on mesoporous SBA-15 as catalysts in the selective oxidation of benzyl alcohol in aqueous phase. **Microporous and Mesoporous Materials,** v. 220, n. 15, p. 136-147, 2016.

DEZOTTI, Márcia. **Processos e técnicas para o controle ambiental de efluentes líquidos.** Rio de Janeiro: E-papers, 2008. 360 p.

DIETRICH, M.; ANDALURI, G.; SMITH, R.C.; SURI, R. Combined Ozone and Ultrasound for the Removal of 1,4-dioxane from Drinking Water. **Ozone: Science & Engineering,** v. 39, n. 4, p. 244-254, 2017.

DU, J.; BAO, J.; FU. X.; LU, C.; KIM, S. H. Mesoporous sulfur-modified iron oxide as an effective Fenton-like catalyst for degradation of bisphenol A. **Applied Catalysis B: Environmental,** v. 184, p. 132-141, 2016.

DUBAL, D.P.; DHAWALE, D.S.; SALUNKHE, R.R.; JAMDADE, V.S. LOKHANDE, C.D. Fabrication of copper oxide multilayer nanosheets for supercapacitor application. **Journal of Alloys and Compounds,** v. 492, n. 1, p. 26-30, 2010.

EBERLE, D.; BALL, R.; ROVING, T.B. Peroxone activated persulfate treatment of 1,4-dioxane in the presence of chlorinated solvent co-contaminants. **Chemosphere,** v. 144, p. 728-735, 2016.

EUROPEAN CHEMICALS BUREAU (ECB). **E.U. risk assessment report: 1,4-dioxane**, **Second Priority List.** Office for Official Publications of the European Communities, Luxembourg, p. 1-129, 2002.

GABORIAUD, F.; EHRHARDT, J-J. Effects of different crystal faces on the surface charge of colloidal goethite (α-FeOOH) particles: an experimental and modeling study. **Geochimica et Cosmochimica Acta,** v. 67, n. 5, p. 967-983, 2003.

GAO, W.; LIANG, H.; MA, J.; HAN, M.; CHEN, Z-L. HAN, Z-S.; LI, G-B. Membrane fouling control in ultrafiltration technology for drinking water production: A review. **Desalination,** v. 272, p. 1-8, 2011.

GELUWE, S.V.; BRAEKEN, L.; BRUGGEN, B.V. Der. Ozone oxidation for the alleviation of membrane fouling by natural organic matter: A review. **Water Research,** v. 45, n.12, p. 3551-3570, 2011.

GHARBANI, P.; MEHRIZAD, A. Heterogeneous catalytic ozonation process for removal of 4-chloro-2-nitrophenol from aqueous solutions. **Journal of Saudi Chemical Society**, v. 18, n. 5, p. 601–605, 2012.

GUEDES, M.; FERREIRA, J.M.F.; FERRO, A.C. A study on the aqueous dispersion mechanism of CuO powders using Tiron. **Journal of Colloid and Interface Science,** v. 330, n. 1, p. 119-124, 2009.

GUO, Y.; SONG, Z.; XU, B.; LI, Y.; QI, F.; CROUE, J-P.; YUAN, D. A novel catalytic ceramic membrane fabricated with $CuMn_2O_4$ particles for emerging UV absorbers degradation from aqueous and membrane fouling elimination. **Journal of Hazardous Materials**, v. 344, p. 1229-1239, 2018.

GUO, Y.; XU, B.; QI, F. A novel ceramic membrane coated with MnO_2-Co_3O_4 nanoparticles catalytic ozonation for benzophenone-3 degradation in aqueous solution: Fabrication, characterization and performance. **Chemical Engineering Journal,** v. 287, p. 381-389, 2016.

HOIGNÉ, J.; BADER, H. Rate constants of reaction of ozone with organic and inorganic compounds in water II. **Water Research,** v. 17, n. 2, p,.185-194, 1983.

HU, E.; WU, X.; SHANG, S.; TAO, X.; JIANG, S.; GAN, L. Catalytic ozonation of simulated textile dyeing wastewater using mesoporous carbon aerogel supported copper oxide catalyst. **Journal of Cleaner Production**, v. 112, p. 4710–4718, 2016.

HUANG, L.; ZHENG, M.; YU, D.; YASEEN, M.; DUAN, L.; JIANG, W.; SHI, L. In-situ fabrication and catalytic performance of Co-Mn@CuO core-shell nanowires on copper meshes/foams. **Materials & Design,** v. 147, p. 182-190, 2018.

HUANG, Y.; CUI, C.; ZHANG, D.; LI, L.; PAN, D. Heterogeneous catalytic ozonation of dibutyl phtalate in aqueous solution in the presence of iron-loaded activated carbon. **Chemosphere,** v. 119, p. 295-301, 2015.

HUANG, Y.; SUN, Y.; XU, Z.; LUO, M.; ZHU, C.; LI, L. Removal of aqueous oxalic acid by heterogeneous catalytic ozonation with MnO_x/sewage sludge-derived activated carbon as catalysts. **Science of the Total Environment,** v. 575, p. 50-57, 2017.

IKHLAQ, A.; BROWN, D.R.; KASPRZYK-HORDERN, B.

Mechanisms of catalytic ozonation: an investigation into superoxide ion radical and hydrogen peroxide formation during catalytic ozonation on alumina and zeolites in water. **Applied Catalysis B: Environmental,** v. 129, p. 437-449, 2013.

ILLÉS, E.; TOMBÁCZ, E. The effect of humic acid adsorption on pH-dependent surface charging and aggregation of magnetite nanoparticles. **Journal of Colloid and Interface Science,** v. 295, n. 1, p. 115-123, 2006.

ISO 11348-3. Water quality – determination of the inhibitory effect of water samples on the light emission of *Vibrio fischeri* (Luminescent bacteria test), Part 3: Method using freeze-dried bacteria. Geneva: International Organization for Standardization, 2007.

JI, F.; LI, C.; DENG, L. Performance of CuO/Oxone system: Heterogeneous catalytic oxidation of phenol at ambient conditions. **Chemical Engineering Journal,** v. 178, p. 239-243, 2011.

KAMBHU, A.; GREN, M.; TANG, W.; COMFORT, S.; HARRIS, C.E. Remediating 1,4-dioxane-contaminated water with slow-release persulfate and zerovalent iron. **Chemosphere**, v. 175, p. 170-177, 2017.

KANG, Y-G.; YOON, H.; LEE, W.; KIM, E-J.; CHANG, Y-S. Comparative study of peroxide oxidants activated by nZVI: Removal of 1,4-dioxane and arsenic(III) in contaminated waters. **Chemical Engineering Journal,** v. 334, p. 2511-2519, 2018.

KARCI, A. Degradation of chlorophenols and alkylphenol ethoxylates, two representative textile chemicals, in water by advanced oxidation processes: The state of the art on transformation products and toxicity. **Chemosphere**, v. 99, p. 1-18, 2014.

KARNIK, B.S.; DAVIES, S.H.; BAUMANN, M.J.; MASTEN, S.J. Fabrication of catalytic membranes for the treatment of drinking water using combined ozonation and ultrafiltration. **Environmental Science and Technology,** v. 39, p. 7656-7661, 2005.

KASPRZYK-HORDERN, B.; ZIÓŁEK, M.; NAWROCKI, J. Catalytic ozonation and methods of enhancing molecular ozone reactions in water

treatment. **Applied Catalysis B: Environmental**, v. 46, n. 4, p. 639-669, 2003.

KIKER, J.H.; CONNOLY, J.B.; MURRAY, W.A.; PEARSON, S.C.P.; REED, S.T.E.R. Ex-situ wellhead treatment of 1,4-dioxane using Fenton's reagent. **Proceedings of the Annual International Conference on Soilds, Sediments, Water and Energy,** v. 15, p. 210-226, 2010.

KIM, E-J.; OH, D.; LEE, C-S.; GONG, J.; KIM, J.; CHANG, Y-S. Manganese oxide nanorods as a robust Fenton-like catalyst at neutral pH: Crystal phase-dependent behavior. **Catalysis Today,** v. 282, n. 1, p. 71-76, 2017.

KIM, H-S.; KWON, B-H.; YOA, S-J.; KIM, I-K. Degradation of 1,4-dioxane by photo-Fenton processes. **Journal of Chemical Engineering of Japan,** v. 41, p. 829-835, 2008.

KIM, J.; DAVIES, S.H.R.; BAUMANN, M.J.; TARABARA, V.V.; MASTEN, S.J. Effect of ozone dosage and hydrodynamic conditions on the permeate flux in a hybrid ozonation-ceramic ultrafiltration system treating natural waters. **Journal of Membrane Science,** v. 311, p. 165-172, 2008.

KISHIMOTO, N. Dependeny of Advanced Oxidation Performance on the Contaminated Water Feed Mode for Ozonation Combined with Electrolysis Using a Two-compartment Electrolytic Flow-Cell. **Journal of Advanced Oxidation Technologies,** v. 10, p. 241-246, 2016.

KOSMULSKI, M. pH-dependent surface charging and points of zero charge II. Update. **Journal of Colloid and Interface Science,** v. 275, n. 1, p. 214-224, 2004.

KWON, S.C.; KIM, J.Y.; YOON, S.M.; BAE, W.; KANG, S.K.; RHEE, Y.W. Treatment characteristic of 1,4-dioxane by ozone-based advanced oxidation processes. **Journal of Industrial and Engineering Chemistry,** v. 18, n. 6, p. 1951-1955, 2012.

LA PLATA, G. B. O. de; ALFANO, O. M.; CASSANO, A. E. Decomposition of 2-chlorophenol employing goethite as Fenton catalyst. I. Proposal of a feasible, combined reaction scheme of

heterogeneous and homogeneous reactions. **Applied Catalysis B: Environmental,** v.95, n. 1–2, p. 1-13, 2010.

LAN, B.Y.; NIGMATULLIN, R.; LI PUMA, G.; Ozonation kinetic of cork-processing water in a bubble column reactor. **Water Research,** v. 42, p. 2473-2482, 2008.

LEE, K-C.; BEAK, H-J.; CHOO, K-H. Membrane photoreactor treatment of 1,4-dioxane containing textile wastewater effluent: Performance, modeling and fouling control. **Water Research,** v. 86, p. 58-65, 2015.

LEE, K-C.; CHOO, K-H. Hybrization of TiO_2 photocatalysis and coagulation and flocculation for 1,4-dioxane removal in drinking water treatment. **Chemical Engineering Journal,** v. 231, p. 227-235, 2013.

LEE, I. S.; SIM, W. J.; KIM, C.W; CHANG, Y. S.; OH, J. E. Characteristic occurrence patterns of micropollutants and their removal efficiencies in industrial wastewater treatment plants. **Journal of Environmental Monitoring,** v. 13, n. 2, p. 391-397, 2011.

LI, C-C.; CHANG, M-H. Colloidal stability of CuO nanoparticles in alkanes via oleate modifications. **Materials Letters,** v. 58, n. 30, p. 3903-3907, 2004.

LI, M.; CONLON, P.; FIORENZA, S.; VITALE, R.J.; ALVAREZ, P.J.J. Rapid analysis of 1,4-dioxane in Groundwater by Frozen Micro-Extraction with Gas Chromatography/Mass Spectrometry. **Groundwater Monitoring and Remediation,** v. 31, n. 4, p. 70-76, 2011.

LI, M.; MATHIEU, J.; LIU, Y.; VAN ORDEN, E.T.; YANG, Y.; FIORENZA, S.; ALVAREZ, P.J.J. The Abundance of Tetrahydrofuran/Dioxane Monooxygenase Genes (thmA/dxmA) and 1,4-Dioxane Degradation Activity Are Significantly Correlated at Various Impacted Aquifers. **Environmental Science and Technology Letters,** v. 1, p. 122-127, 2014.

LI, W.; PATTON, S.; GLEASON, J.M.; MEZYK, S.P.; ISHIDA, K.P.; LIU, H. UV Photoholysis of Chloramine and Persulfate for 1,4-Dioxane Removal in Reverse-Osmosis Permeate for Potable Water Reuse.

Environmental Science & Technology, v. 52, n. 11, p. 6417-6425, 2018.

LIN, S-S.; GUROL, M.D. Catalytic decomposition of hydrogen peroxide on iron oxide: kinetics, mechanism and implications. **Environmental Science & Technology,** v. 32, n. 10, p. 1417-1423, 1998.

LIU, H.; CHEN, T.; ZOU, X.; QING, C.; FROST, R. L. Thermal treatment of natural goethite: Thermal transformation and physical properties. **Thermochimica Acta**, v. 568, p. 115-121, 2013.

LVOV, Y.; MUNGE, B.; GIRALDO, O.; ICHINOSE, I.; SUIB, S.L.; RUSLING, J.F. Films os manganese oxide nanoparticles with polycations or myoglobin from alternate-layer adsorption. **Langmuir,** v. 16, p. 8850-8857, 2000.

LU, M-C. Oxidation of chlorophenols with hydrogen peroxide in the presence of goethite. **Chemosphere,** v. 40, n. 2, p. 125-130, 2000.

LUPAN, O.; CRETU, V.; POSTICA, V.; ABABII, N.; POLONSKYI, O.; KAIDAS, V.; SCHÜTT, F.; MISHRA, Y. K.; MONAICO, E.; TIGINYANU, I.; SONTEA, V.; STRUNSKUS, T.; FAUPEL, F.; ADELUNG, R. Enhanced ethanol vapour sensing performances of copper oxide nanocrystals with mixed phases. **Sensor and Actuators B-Chemical,** v. 224, p. 434-448, 2016.

LV, A.; HU, C.; NIE, Y.; QU, J. Catalytic ozonation of toxic pollutants over magnetic cobalt-doped Fe_3O_4 suspensions. **Applied Catalysis B: Environmental**, v. 117–118, p. 246-252, 2012.

MA, Z.; REN, L.; XING, S.; WU, Y.; GAO, Y. Sodium Dodecyl Sulfate Modified $FeCo_2O_4$ with Enhanced Fenton-Like Activity at Neutral pH. **The Journal of Physical Chemistry C,** v. 119, n. 40, p. 23068-23074, 2015.

MA, Z.; ZHU, L.; LU, X.; XING, S.; WU, Y.; GAO, Y. Catalytic ozonation of p-nitrophenol over mesoporous Mn-Co-Fe oxide. **Separation and Purification Technology,** v. 133, p. 357-364, 2014.

MAMONTOV, E.; EGAMI, T.; BREZNY, R.; KORANNE, M.; TYAGI, S. Lattice defects and oxygen storage capacity of nanocrystalline ceria and ceria-zirconia. **The Journal of Physical Chemistry B,** v. 104, n. 47, p. 11110-11116, 2000.

MASHAYEKH-SALEHI, A.; MOUSSAVI, G.; YAGHMAEIAN, K. Preparation, characterization and catalytic activity of a novel mesoporous nanocrystalline MgO of a novel mesoporous nanocrystalline MgO nanoparticle for ozonation of acetaminophen as an emerging water contaminant. **Chemical Engineering Journal,** v. 310, n. 1, p. 157-169, 2017.

MELERO, J.A.; MARTÍNEZ, F.; BOTAS, J.A.; MOLINA, R.; PARIENTE, M.I.. Heterogeneous catalytic wet peroxide oxidation systems for the treatment of an industrial pharmaceutical wastewater. **Water Research,** v. 43, n. 16, p. 4010-4018, 2009.

MERAYO, N.; HERMOSILLA, D.; CORTIJO, L.; BLANCO, A. Optimization of the Fenton treatment of 1,4-dioxane and on-line FTIR monitoring of the reaction. **Journal of Hazardous Materials,** V. 268, P. 102-109, 2014.

MESQUITA, I.; MATOS, L.C.; DUARTE, F.; MALDONADO-HÓDAR, F.J.; MENDES, A., MADEIRA, L.M. Treatment of azo dye-containing wastewater by a Fenton-like process in a continuous packed-bed reactor filled with activated carbon. **Journal of Hazardous Materials,** v. 237-238, p. 30-37. 2012.

MIRZAEI, A.; CHEN, Z.; HAGHIGHAT, F.; YERUSHALMI, L. Removal of pharmaceuticals from water by homo/heterogeneous Fenton-type processes – A review. **Chemosphere,** v. 174, p. 665-668, 2017.

MOHR, T.K.G. **Environmental Investigation and Remediation: 1,4-dioxane and Other Solvent Stabilizers.** CRC Press, Boca Raton, 2010.

NAWAZ, F.; XIE, Y.; CAO, H.; XIAO, J.; WANG, Y.; ZHANG, X.; LI, M.; DUAN, F. Catalytic ozonation of 4-nitrophenol over an mesoporous α-MnO_2 with resistance to leaching. **Catalysis Today,** v. 258, n. 2, p. 595-601, 2015.

NABAVI, M.; SPALLA, O.; CABANE, B. Surface Chemistry of Nanometric Ceria Particles in Aqueous Dispersions. **Journal of Colloid and Interface Science,** v. 160, n. 2, p.459-471, 1993.

NAWROCKI, J. Catalytic ozonation in water: controversis and questions. **Applied Catalysis B: Environmental,** v. 142-143, p. 465-471, 2013.

NAWROCKI, J.; KASPRZYK-HORDERN. The efficiency and mechanisms of catalytic ozonation. **Applied Catalysis B: Environmental,** v. 99, n. 1-2, p. 27-42, 2010.

OLIVEIRA, Josiane Silva de. **Tratamento da Água Produzida Utilizando a Eletroflotação e o Processo Combinado Eletroflotação/Fenton em Reator de Reciclo Fechado.** 2012. 113 f.

OPUTU, O.; CHOWDHURY, M.; NYAMAYARO, K.; FATOKI, O.; FESTER, V. Catalytic activities of ultra-small β-FeOOH nanorods in ozonation of 4-chlorophenol. **Journal of Environmental Sciences,** v. 35, p. 83-90, 2015.

PARK, H.; MAMEDA, N.; CHOO, K-H. Catalytic metal oxide nanopowder composite Ti mesh for eletrochemical oxidation of 1,4-dioxane and dyes. **Chemical Engineering Journal,** v. 345, p. 233-241, 2018.

PARK, J-S.; CHOI, H.; CHO, J. Kinetic decomposition of ozone and para-chlorobenzoic acid (pCBA) during catalytic ozonation. **Water Research,** v. 38, n. 9, p. 2285-2292, 2004.

PATNAIK, Pradyot. **Hanbook of inorganic chemicals.** New York: McGraw-Hill, 2003.

PIERA, E.; CORONAS, J.; MENENDEZ, M.; SANTAMARIA, J. High separation selectivity with imperfect zeolite membranes. **Chemical Communications,** v. 12, p. 1309-1310, 1999.

POBINER, H. Determination of Hydroperoxides in Hydrocarbon by Conversion to Hydrogen Peroxide and Measurement by Titanium Complexing. **Analytical Chemistry,** v. 33, n. 10, p. 1423-1426, 1961.

QI, F.; CHU, W.; XU, B. Ozonation of phenacetin in associated with a magnetic catalyst CuFe2O4: The reaction and transformation. **Chemical Engineering Journal,** v. 262, p. 552-562, 2015.

RAJ, A.S.A.; BIJU, V. Nanostructured CuO: Facile synthesis, optical absorption and defect dependent electrical conductivity. **Nanomaterials Science in Semiconductor Processing,** v. 68, p. 38-47, 2017.

RODRÍGUEZ, J.L.; POZNYAK, T.; VALENZUELA, M. A.; TIZNADO, H.; CHAIREZ, I. Surface interactions and mechanistic studies of 2,4-dichlorophenoxyacetic acid degradation by catalytic ozonation in presence of Ni/TiO$_2$. **Chemical Engineering Journal,** v. 222, p. 426-434, 2013.

ROSMAN, N.; SALLEH, W.N.W.; MOHAMED, M.A.; JAAFAR, J.; ISMAIL, A.F.; HARUN, Z. Hybrid membrane filtration-advanced oxidation processes for removal of pharmaceutical residue. **Journal of Colloid and Interface Science,** v. 532, p. 236-260, 2018.

ROUT, K.; DASH, A.; MOHAPATRA, M.; ANAND, S. Manganese doped goethite: Structural, optical and adsorption properties. **Journal of Environmental Chemical Engineering,** v. 2, p. 434-443, 2014.

SABLE S. S.; GHUTE, P.P.; FAKHRNASOVA D.; MANE R.B.; RODE C.V.; MEDINA F.; CONTRERAS S. Catalytic ozonation of clofibric acid over copper-based catalysts: In situ ATR-IR studies. **Applied Catalysis B: Environmental**, v. 209, n. 15, p. 523-529, 2017.

SADANA, A.; KATZER, J.R. Involvement of free radicals in the aqueous-phase catalytic oxidation of phenol over copper oxide. **Journal of Catalysis,** v. 35, p. 140-152, 1974.

SCARATTI, G. **Óxidos de metais de transição aplicados como catalisadores da ozonização de efluente simulado de refinaria de petróleo.** 2015. 107 f. Dissertação (Mestrado). Programa de Pós Graduação em Engenharia Química, Universidade Federal de Santa Catarina, 2015.

SCARATTI, G. **Removal of 1,4-dioxane from industrial wastewaters: Routes of decomposition using catalytic ozonation or peroxidation coupled to membrane filtration.** 2017, 117 f.

(Qualifying exam – Dissertation). Graduation in Chemical Engineering, Federal University of Santa Catarina, 2017.

SCARATTI, G.; BASSO, A.; LANDERS, R.; ALVAREZ, P.J.J.; PUMA, G.L. Treatment of aqueous solutions of 1,4-dioxane by ozonation and catalytic ozonation with copper oxide (CuO). **Environmental Technology.** **h**ttps://doi.org/10.1080/09593330.2018.1538259

SEHATI, S.; ENTEZARI, M. H. Sono-incorporation of CuO nanoparticles on the surface and into the mesoporous hexatitanate layers: Enhanced Fenton-like activity in degradation of orange-G at its neutral pH. **Applied Surface Science,** v. 339, p. 732-741, 2017.

SHEN, W.; WANG, Y.; ZHAN, J.; WANG, B.; HUANG, J.; DENG, S.; YU, G. Kinetics and operational parameters of 1,4-dioxane degradation by the photoelectron-peroxone process. **Chemical Engineering Journal,** v. 310, p. 249-258, 2017.

SHEN, Y.; GUO, M.; XIA, X.; SHAO, G. Role of materials chemistry on the electrical/electronic properties of CuO thin films. **Acta Materialia,** v.85, p. 122-131, 2015.

SO, M.H.; HAN, J.S.; HAN, T.H.; SEO, J.W.; KIM, C.G. Decomposition of 1,4-dioxane by photo-Fenton oxidation coupled with activated sludge in a polyester manufacturing process. **Water Science and Technology,** v. 59, p. 1003-1009, 2009.

STEPIEN, D.K.; DIEHL, P.; HELM, J. THOMS, A.; PÜTTMANN, W. Fate of 1,4-dioxane in the aquatic environment: From sewage to drinking water. **Water Research,** v. 48, p. 406-419, 2014.

SULLIVAN, D. E.; ROTH, J. A. Kinetics of ozone self-decomposition in aqueous solution. **AlChe Symposium**. Series.79, p. 142-149, 1979.

SUSHMA; KUMARI, M.; SAROHA, A.K. Performance of various catalysts on treatment of refractory pollutants in industrial wastewater by catalytic wet air oxidation: A review. **Journal of Environmental Management,** v. 228, p. 169-188, 2018.

SUH, J. H.; MOHSENI, M. A study on the relationship between

biodegradability enhancement and oxidation of 1,4-dioxane using ozone and hydrogen peroxide. **Water Research**, v. 38, n. 10, p. 2596–2604, 2004.

THOMAS, J.K. Rates of reaction of the hydroxyk radical. **Transactions of the Faraday Society,** v. 61, p. 702-707, 1965.

THOMMES, M.; KANEKO, K.; NEIMARK, A.V.; OLIVIER, J.P.; RODRIGUEZ-REINOSO, F.; ROUQUEROL, J.; SING, K.S.W. Physisorption of gases, with special reference to the evalaution of surface area and pore size distribution (IUPAC Technical Report). **Pure Applied Chemistry,** v. 87, p. 9-10, 2015.

TIAN, G-P.; WU, Q-Y.; LI, A.; WANG, W-L.; HU, H-Y. Promoted ozonation for the decomposition of 1,4-dioxane by activated carbon. **Water Science and Technology: Water Supply,** IWA Publishing, 2016.

ULLMANN, Fritz. **Encyclopedia of Industrial Chemistry.** 5th edition, Wiley-VCH, 200

U.S. Environmental Protection Agency (USEPA). **Treatment Technologies for 1,4-Dioxane: Fundamentals and Field Applications**, EPA-542-R-06-009, USEPA, Office of Solid Waste and Emergency Response, Washington, DC, 2006.

U.S. Environmental Protection Agency (USEPA). **Toxicological review of 1,4-dioxane (CAS N° 123-91-1), EPA/635/R-09/005-F.** USEPA, Office of Solid Waste and Emergency Response, Washington, DC, 2010.

U.S. Environmental Protection Agency (USEPA). **Integrated risk information system (IRIS) on 1,4-dioxane.** National Center for Environemntal Assesment. Office of Research and Development, Washington, DC, 2013.

VAKILABADI, D.R.; HASSANI, A.H.; OMRANI, G.; RAMAVANDI, B. Catalytic potential of Cu/Mg/Al-chitosan for ozonation of real landfill leachate. **Process Safety and Environmental Protection,** v. 107, p. 227-237, 2017.

VESCOVI, T.; COLEMAN, H. M.; AMAL, R. The effect of pH on UV-based advanced oxidation technologies – 1,4-Dioxane degradation. **Journal of Hazardous Materials,** v. 182, n. 1-3, p. 75-79, 2010.

VOLLHARDT, K.P.C.; SCHORE, N.E. Organic Chemistry: Structure and Function, sixth ed., W.H. Freeman and Co., Reston, VA, 2011.

VORONTSOV, A.V. advancing Fenton and photo-Fenton water treatment through the catalyst design. **Journal of Hazardous Materials**, 2018, doi.org/10.1016/j.jhazmat.2018.04.033.

VON, G.U. Ozonation of drinking water: Part I. Oxidation kinetics and product formation. **Water Research,** v. 37, p. 1443-1467, 2003.

WANG, H.; BAKHEET, B.; YUAN, S.; LI, X.; YU, G.; MURAIAMA, S.; WANG, Y. Kinetics and energy efficiency for the degradation of 1,4-dioxane by electro-peroxone process. **Journal of Hazardous Materials,** v. 294, p. 90-98, 2015.

WAN, Z.; WANG, J. Degradation of sulfamethazine using Fe_3O_4-Mn_3O_4/reduced graphene oxide hybrid as Fenton-like catalyst. **Journal of Hazardous Materials,** v. 324, n. B, p. 653-664, 2017.

WANG, X.; DAVIES, S.H.; MASTEN, S.J. Analysis of energy costs for catalytic ozone membrane filtration. **Separation and Purification Technologies,** v. 186, p. 182-187, 2017.

WEIMAR, R. Prevent groundwater contamination before it's too late. **Water Wastes Engineering,** v. 17, p. 30-33, 1980.

WEISS, J. J. Electron transfer processes in the mechanism of chemical reactions in solution. **Berichte der Bunsengesellschaft für physikalische Chemie,** v. 73, n. 2, p.131-135, 1969.

WORLD HEALTH ORGANIZATION (WHO). **Ethylene glycol: environmental aspects.** Concise international chemical assessment document; 22, Geneva, 2002.

XIONG, Z.; LAI, B.; YUAN, Y.; CAO, J.; YANG, P.; ZHOU, Y. Degradation of p-nitrophenol (PNP) in aqueous solution by a micro-size

Fe^0/O$_3$ process (mFe^0/O$_3$): Optimization, kinetic, performance and mechanism. **Chemical Engineering Journal,** v. 302, p. 137-145, 2016.

XU, L.; SRINIVASAKANNAN, C.; PENG, J.; ZHANG, L.; ZHANG, D. Synthesis of Cu-CuO nanocomposite in microreactor and its application to photocatalic degradation. **Journal of Alloys and photocatalytic,** v. 695, p. 263-269, 2017.

XU, L.; WANG, J. Magnetic Nanoscaled Fe$_3$O$_4$/CeO$_2$ Composite as an Efficient Fenton-Like Heterogeneous Catalyst for Degradation of 4-Chlorophenol. *Environmental Science & Technology,* v. 46, n. 18, p. 10145-10153, 2012.

YANG, M-Q.; ZHANG, Y.; ZHANG, N.; TANG, Z-R.; XU, Y-J. Visible-light-driven oxidation of primary C-H bonds over CdS with dual co-catalysts grapheme and TiO$_2$. **Scientific reports 3,** número do artigo: 3314, 2013.

ZBILJIC, J.; GUZSVÁNY, V.; VAJDLE, O.; PRLINA, B.; AGBABA, J.; DALMACIJA, B.; KÓNYA, Z.; KALCHER, K. Determination of H$_2$O$_2$ by MnO$_2$ modified screen printed carbon electrode during Fenton and visible light-assisted photo-Fenton based removal of acetamiprid from water. **Journal of Electroanalytical Chemistry**, v. 755, p. 77–86, 2015.

ZENG, Q.; DONG, H.; WANG, X.; YU, T.; CUI, W. Degradation of 1,4-dioxane by hydroxyl radicals produced from clay minerals. **Journal of Hazardous Materials,** v. 331, p. 88-98, 2017.

ZENKER, M. J.; BORDEN, R. C.; BARLAZ, M. A. Occurrence and Treatment of 1,4-Dioxane in Aqueous Environments. **Environmental Engineering Science**, v. 20, n. 5, p. 423–432, 2003.

ZHANG, J.S.; STANFORTH, R.; PEHKONEN, S.O. Photo-arsenic adsorption ratios and zeta potential measurements: Implications for pronotation of hydroxyl on the goethite surface. **Journal of Colloid and Interface,** v. 315, n. 1, p. 13-20, 2007.

ZHANG, J.; YU, H.; QUAN, X.; CHEN, S.; ZHANG, Y. Ceramic membrane separation coupled with catalytic ozonation for tertiary treatment of dyestuff wastewater in a pilot-scale study. **Chemical Engineering Journal,** v. 301, p. 19-26, 2016.

ZHANG, S.; GEDALANG, P.B.; MAHENDRA, S. Advances in bioremediation of 1,4-dioxane contaminated waters. **Journal of Environmental Management,** v. 204, p. 765-774, 2017.

ZHANG, T.; LI, W.; COUÉ, J-P. Catalytic ozonation of oxalate with a cerium supported palladium oxide: an efficient degradation not relying on hydroxyl radical oxidation. **Environmental Science & Tecnology,** v. 45, n. 21, p. 9339-9346, 2011.

ZHANG, T.; LI, C.; MA, J.; TIAN, H.; QIANG, Z. Surface hydroxyl groups of synthetic α-FeOOH in promoting OH generation from aqueous ozone: Property and activity relationship. **Applied Catalysis B: Environmental,** v. 82, n. 1, p. 131-137, 2008.

ZHAO, L.; MA, J.; SUN, Z.; ZHAI, X. Preliminary kinetic study on the degradation of nitrobenzene by modified ceramic honeycomb-catalytic ozonation in aqueous solution. **Journal of Hazardous Materials,** v. 161, p. 988-994, 2009.

ZHAO, H.; DONG, Y.; JIANG, P.; WANG, G.; ZHANG, J.; ZHANG, C. $ZnAl_2O_4$ as a novel high-surface-area ozonation catalyst: One-step green synthesis, catalytic performance and mechanism. **Chemical Engineering Journal,** v. 260, p. 623-630, 2015.

ZHUANG, H.; HAN, H.;JIA,S.; HOU, B.; ZHAO, Q. Advanced treatment of biologically pretreated coal gasification wastewater by a novel integration of heterogeneous catalytic ozonation and biological processes. **Bioresource Technology,** v. 166, p. 592-595, 2014.

SHEN, W.; WANG, Y.; ZHAN, J.; WANG, B.; HUANG, J.; DENG, S.; YU, G. Kinetics and operational parameters of 1,4-dioxane degradation by the photoelectron-peroxone process. **Chemical Engineering Journal,** v. 310, p. 249-258, 2017.

ZHOU, L-J.; ZOU, Y-C.; ZHAO, J.; WANG, P-P.; FENG, L-L.; SUN, L-W. WANG, D-J.; LI, G-D. Facile synthesis of highly stable and porous CuO/CuO cubes with enhanced gas sensing properties. **Sensors and Sctuators B-Chemical,** v.188, p. 533-539, 2013.

ZIYLAN-YAVAŞ A.; INCE N. H. Catalytic ozonation of paracetamol using commercial and Pt-supported nanocomposites of Al_2O_3: The

impact of ultrasound. **Ultrasonics Sonochemistry**, Available online 16 February 2017.